Aus der Poliklinik für Kieferorthopädie
Klinik der Ludwig-Maximilians-Universität München
Direktorin: Prof. Dr. Andrea Wichelhaus

In-vitro investigation of frictional behavior and influence of normal forces on orthodontic materials in wet and dry states

Dissertation
zum Erwerb des Doktorgrades der Zahnmedizin
an der Medizinischen Fakultät der
Ludwig-Maximilians-Universität zu München

vorgelegt von
Haoyan Li
aus
Hebei, China
2021

Mit Genehmigung der Medizinischen Fakultät
der Universität München

Berichterstatterin:	Prof. Dr. med. dent. Andrea Wichelhaus
Mitberichterstatter:	Prof. Dr. Bogna Stawarczyk
	Prof. Dr. Dr. Matthias Folwaczny
Mitbetreuung druch den promovierten Mitarbeiter:	Dipl.-Phys. Dr. rer. nat. Sebastian Stapfner
	Dipl.-Ing. Thomas Stocker
	Dipl.-Biol. Dr. rer. nat. Uwe Baumert
Dekan:	Prof. Dr. med. dent. Reinhard Hickel
Tag der mündlichen Prüfung:	13.08.2021

CONTENT

SUMMARY

This present in-vitro study investigates static and kinetic frictional forces between brackets and orthodontic archwires. To cover a wide field of parameters, which influence sliding, different environmental states and characteristics of orthodontic materials are taken into account. The study is divided into two parts: a) material study and b) simulation of the clinical situation. The material study focuses on the evaluation of the influence of the different environments as well as various orthodontic materials on frictional forces. The second part of the study targets at comparing the effect of various normal forces and ligation mechanisms on friction during the orthodontic tooth movement.

The material study is conducted under (36±1) ℃and a constant normal force *(F_N)* of 1N in four different environmental states: 1) dry state; 2) whole human saliva; 3) deionized water and 4) artificial saliva. The fluids 2)-4) are applied to the bracket-wire combination at a rate of about 3ml/min. The study part concerning the simulation of the clinical situation is performed using artificial saliva at (36±1) ℃and different normal forces (F_N) of 1N, 1.5N, 2N, 2.5N. All other parameters are the same as in the material tests. The experimental setup consists of an Instron® 4444 universal testing machine (Instron® Corp. Norwood, MA, USA), which is used to pull the archwire through the slot of the bracket and a FTD-Nano-17 - SI-25-0.25 six-axis force-torque sensor (ATI, Industrial Automation, Apex, NC, USA). This sensor records the forces opposing sliding, which are equivalent to the frictional forces.

The results show that (human) saliva acts in most cases as adhesive and increases frictional forces. Active self-ligating brackets produce higher frictional forces compared to conventional and passive self-ligating brackets, especially when combined with large size wires. The measured values of stainless steel archwires present higher frictional forces compared to NiTi wires for all bracket types. The static and kinetic frictional forces increase as the archwire size and normal force increase. Thus, using the correct archwire size and moderately normal forces is important to generate appropriate friction forces during sliding therapy.

Based on the results of the current in-vitro study, further investigations are needed to focus on, such as the comparison of different compositions of artificial saliva and the evaluation on which component in saliva affects friction. Also, other factors, which can have an effect on the resistance to sliding, like angulation, binding, various wire length and inter-bracket span, should be precisely compared and investigated.

ZUSAMMENFASSUNG

Die vorliegende in-vitro-Studie untersucht die statische und kinetische Friktion zwischen Brackets und kieferorthopädischen Bögen. Um ein breites Feld von Parametern abzudecken, die das Gleiten beeinflussen, werden verschiedene Umgebungsbedingungen und Eigenschaften kieferorthopädischer Materialien berücksichtigt. Die Studie gliedert sich in zwei Teile: a) Materialstudie und b) Simulation der klinischen Situation. Die Materialstudie konzentriert sich auf die Bewertung des Einflusses verschiedene Umgebungen sowie verschiedener kieferorthopädischer Materialien auf die Reibungskräfte. Der zweite Teil der Studie zielt darauf ab, den Einfluss verschiedener Normalkräfte und Ligationsmechanismen auf die Reibung während der kieferorthopädischen Zahnbewegung zu vergleichen.

Die Materialstudie wird unter (36±1) ℃und einer konstanten Normalkraft *(F_N)* von 1N bei vier verschiedenen Umgebungbedingungen durchgeführt: 1) trocken 2) menschlicher Speichel; 3) entionisiertes Wasser und 4) künstlicher Speichel. Die Flüssigkeiten 2)-4) werden auf die Bracket-Draht-Kombination mit einer Geschwindigkeit von etwa 3 ml/min aufgebracht. Der Studienteil, der die Simulation der klinischen Situation betrifft, wird mit künstlichem Speichel bei (36±1) ℃und verschiedenen Normalkräften (FN) von 1N, 1,5N, 2N, 2,5N durchgeführt. Alle anderen Parameter sind dieselben wie in den Materialtests. Der Versuchsaufbau besteht aus einer Instron®-Universalprüfmaschine 4444 (Instron® Corp. Norwood, MA, USA), mit der der Bogen durch den Slot des Brackets gezogen wird, und einem Sechs-Achs Kraft-Momenten-Sensor FTD-Nano-17 - SI-25-0,25 (ATI, Industrial Automation, Apex, NC, USA). Dieser Sensor erfasst die dem Gleiten entgegenwirkenden Kräfte, die den Friktionskräften entsprechen.

Die Ergebnisse zeigen, dass (menschlicher) Speichel in den meisten Fällen als Adhäsiv wirkt und die Reibungskräfte erhöht. Aktiv selbstligierende Brackets erzeugen im Vergleich zu konventionellen und passiv selbstligierenden Brackets höhere Friktion, insbesondere in Kombination mit großen Drähten. Die Messwerte von Edelstahlbögen zeigen für alle Brackettypen höhere Reibungskräfte im Vergleich zu NiTi-Drähten. Die statische und kinetische Friktion nimmt mit zunehmenden Abmessungen des Drahts und der Normalkraft zu. Daher ist die Verwendung der richtigen Bogenabmessung und mäßiger Normalkräfte wichtig um bei der Gleitbogentherapie geeignete Reibungskräfte erzeugen.

Basierend auf den Ergebnissen der aktuellen in-vitro-Studie sind weitere Untersuchungen erforderlich, wie z.B. der Vergleich verschiedener Zusammensetzungen künstlichen Speichels

und die Beurteilung, welche Komponente im Speichel Friktion beeinflusst. Auch andere Faktoren, die einen Einfluss auf den Gleitwiderstand haben können, wie Angulation, Binding, verschiedene Drahtlängen und die Interbracketabstände, sollten genau verglichen und untersucht werden.

LIST OF ABBREVIATIONS

μ_k	Kinetic Frictional Coefficient
μ_s	Static Frictional Coefficient
ANOVA	Analysis of Variance
AS	Artificial Saliva
BI	Binding
CI	Confidence Intervals for the Mean
CMC	Carboxymethyl cellulose
Dz	Length from the bottom of bracket's slot to the top part of the sensor
F_f	Friction/Frictional force
F_N	Normal Force
F_x	Initial "x-axis" force
F_y	Initial "y-axis" force
NiTi	Nickel-Titanium
NO	Notching
RS	Resistance to Sliding
R_z	Rotate Angulation around z-axis
SD	Standard Deviations
TMA	Titanium-Molybdenum Alloy

1. INTRODUCTION

Orthodontics is defined as the field of dentistry concerned with the supervision, guidance and correction of growing and malformations of dentofacial structures by application of functional forces within the craniofacial complex (William et al. 2007). Therefore, when the functional forces are correcting malocclusions using different orthodontic techniques, the corresponding frictional force and its effect on tooth movement are the most crucial part of the orthodontic treatment.

As one of the most commonly used orthodontic techniques, the straight archwire technique, introduced in the 1970s, plays an important role in orthodontics. Based on the edgewise technique, the straight archwire technique has been designed to achieve three-dimensional control of orthodontic tooth movement without the need for bends in the wire (Lombardo et al. 2012).

However, the tooth movement during orthodontic treatment is not a continuous process, but a sequence of slow and consistent steps (Wichelhaus et al. 2017). A previous research divides this process into four phases (Drescher et al. 1989). In Phase 1, after the alignment of the dental arch and before the exertion of the mesiodistal force, the archwire states no friction in the slot of the bracket. In phase 2, friction is produced at the contact points of the archwire or ligature with the bracket, respectively. When an initial mesiodistal force is applied, the tooth rotates around the occlusal and the sagittal plane. This is due to the fact that the point of application of the mesiodistal force lies away from the centre of resistance. In phase 3, the rotation of the tooth and the continuous mesiodistal force increase the load and the frictional force of the contact area between the archwire and the bracket, and the elastic deformation of the archwire occurs. Meanwhile, the mesiodistal force is decreased due to the rising of the frictional force, and the anti-deformation force of the archwire makes the tooth stand upright. This force system then guides the tooth in a series of alternating movements consisting from tilting and uprighting along the archwire. In phase 4, a permanent deformity of the archwire can occur within an unbalanced system, which should be avoided (Drescher et al. 1989).

With the wide application of the edgewise technique and sliding mechanics, the influence of friction as well as the efficiency of the orthodontic treatment process have become the focus of many studies (Frank and Nikolai 1980; Tidy 1989).

1.1 FRICTIONAL FORCE AND ITS PROPERTIES

From the perspective of physics, frictional force is a force occurring between contacting surfaces and opposes motion. Actually, the force necessary to surmount friction and to move an object over another is a function of the normal force between the two surfaces in contact. The frictional force is proportional to this normal force, linked by the frictional coefficient μ. It is described physically by means of the frictional equation:

$$F_f = \mu \cdot F_N \qquad \textit{Eq. 1}$$

F_f represents the frictional force tested in the present study, F_N represents the normal force, which is perpendicular to the contacting surfaces, and μ is the coefficient of friction.

In general, friction consists of two phases: static and kinetic friction (Figure 1). Static friction occurs until the force is high enough to overcome the initial resistance of movement of an object. This resistance is caused by the two surfaces in contact interacting with each other due to their adhesion. When the object starts moving after overcoming the point of static friction, kinetic friction takes place, which opposes the continuation of the movement. Kinetic friction remains constant between the contacting surfaces, regardless of the relative speed of their movement. Generally, the force to overcome static friction is higher than that of kinetic friction. That means the extent of frictional force is usually less than the force necessary to overcome the initial resistance to movement. Both static and kinetic friction have a corresponding frictional coefficient (Burrow 2009; Omana et al. 1992).

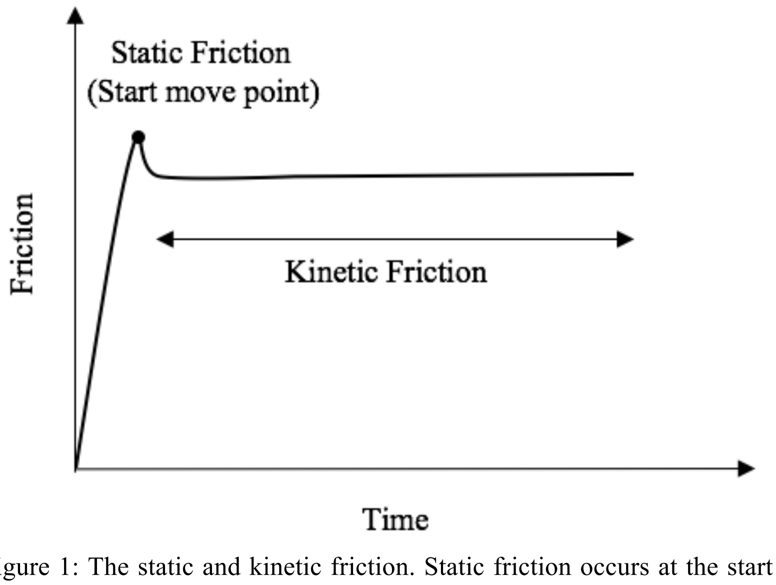

Figure 1: The static and kinetic friction. Static friction occurs at the start point that overcomes the initial resistance (the highest point). Kinetic friction is usually opposite to the direction of the continuous movement (modified after Burrow (2009) and Williams and Khalaf (2013)).

1.2 FRICTIONAL FORCE AND RELATED VARIABLES IN ORTHODONTICS

Friction is receiving much attention in clinical orthodontics, because it affects the functional force transmitted to the tooth and therefore greatly influences the efficiency of the orthodontic treatment process. Thus, studying the frictional force is of great interest with regard to orthodontics and its appliances. During the process of orthodontic tooth movement, friction results from the interaction of the archwires with the surfaces of the brackets' slots or the ligatures. When the applied functional forces are sufficiently to overcome the friction between the bracket-wire combination, tooth movement occurs (Monteiro et al. 2014; Wichelhaus et al. 2017).

After induced at the interface of the bracket-wire combination, the friction will be influenced by many factors occurring during sliding:

a) The type, slot size, surface roughness and design of the bracket (Mezeg and Primozic 2017; Omana et al. 1992; Williams and Khalaf 2013)

b) The size, shape, alloy, surface roughness and physical properties of the archwire (Huffman and Way 1983; Kapila et al. 1990; Tecco et al. 2009)

c) Method of ligation and the angulation between the bracket's slot and orthodontic wire (Hain et al. 2006; Monteiro et al. 2014)

d) Some intraoral variables such as variation of saliva (Fidalgo et al. 2011; Kusy and Schafer 1995; Kusy and Whitley 2003; Leal et al. 2014; Pimentel et al. 2013)

In addition to friction (FR), considering the overall resistance to sliding (RS) that impedes orthodontic tooth movement, binding (BI) and notching (NO) are also important for the movement of an orthodontic archwire through a bracket slot and therefore for the overall biomechanics. Binding appears if forces are exerted to brackets in order to induce tooth movement. It means that flexing of the wire or tooth tipping happens due to the applied force until the wire contacts the corners of the bracket. When permanent deformation of the wire appears at the bracket-wire corner interface, the notched wire is clamped to the corner of the bracket and the tooth stops moving, which is notching (Burrow 2009; Frank and Nikolai 1980; Kusy and Whitley 1999).

Additionally, BI and NO have close relationship with the contact angle (θ) between the wire and bracket slot when a tooth tips or a wire flexes (Figure 2). In addition, these two parameters are only created at the condition of an active configuration ($\theta \geq \theta_c$), which can be divided into four situations (Burrow 2009; Kusy and Whitley 1997, 1999).

a) θ is less than the critical contact angle ($\theta_c \approx 4°$), RS=FR. FR is important, as BI and NO are non-existent (Figure 2a).
b) θ is equal or just exceeds θ_c, RS=FR+BI. Sliding is somewhat blocked because of FR and BI, NO is negligible (Figure 2b).
c) θ is clearly greater than θ_c, RS $\approx$ BI. Mainly BI restricts sliding (Figure 2c).
d) θ is much greater than θ_c, RS $\approx$ NO. FR and BI are both negligible relative to NO, sliding is impossible (Figure 2c).

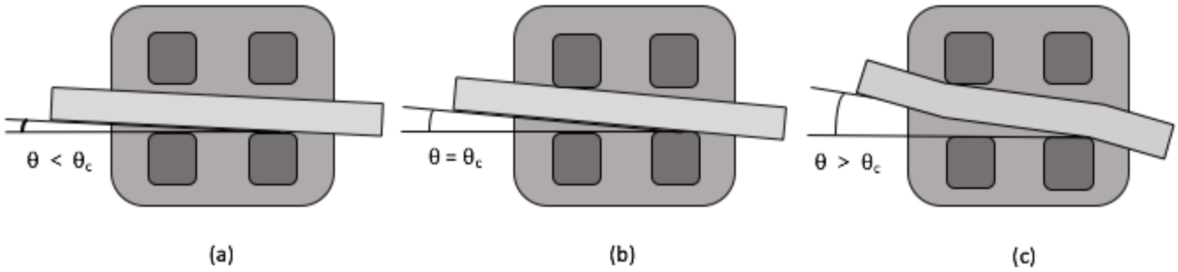

Figure 2: Schematic drawing of a bracket-wire combination. When the contact angle θ is less than the critical contact angle θ_c, BI and NO are non-existent (a). FR is important when θ is equal or just exceeds θ_c (b). BI occurs, resistance to sliding includes FR and BI; when θ is greater than θ_c (c). NO is produced, tooth movement stops and sliding is impossible (modified after Burrow (2009) and Kusy and Whitley (1999)).

Apart from that, the frictional coefficient μ of an orthodontic material is also an important factor for evaluating the characteristic of an orthodontic appliance. The coefficient is a constant for a particular combination of materials and their properties, namely roughness, texture, and/or hardness of the contacting surfaces (Loftus et al. 1999) as well as the testing environment (Kusy and Whitley 2003). Additionally, the variety of materials also has an influence on the coefficient's performance under different sliding velocities (Kusy and Whitley 1989). But all of this should be premised on the law of friction, which is only valid for moderate drawing speeds, because of the generation of excessive heat if the speed gets too high (Feynman et al. 2006).

During orthodontic tooth movement, the friction may exhaust about half of the total force that contributes to the tooth movement and the magnitude of friction will cause different effects on various phases of the treatment (Brauchli et al. 2011; Kusy and Whitley 1997). For the initial phase of the orthodontic treatment, low friction is extremely important, while high levels of frictional force are undesirable, as the purpose of this stage is to align or level the teeth and retract canines. Therefore, high levels of friction will cause unwanted deformation of the wire and even unwanted side effects on the tooth. Moreover, higher friction may lead to pain for the patients, tissue damage or it causes difficulties to move teeth smoothly and continuously or even to prevent extraction space closure or anchorage loss (Begg and Kesling 1977; Kapila et al. 1990; Kim et al. 2008). As a result, methods to lower friction are receiving more and more attention to obtain desired tooth movement in orthodontic treatment (Redlich et al. 2003). On the contrary, as recent critical studies concluded, later phases of treatment need a higher frictional force to acquire a three-dimensional control of the archwires and teeth positions (Brauchli et al. 2011; Brauchli et al. 2012; Monteiro et al. 2014).

1.3 EFFECT OF ORTHODONTIC MATERIALS AND ENVIRONMENT ON FRICTION

Self-ligating brackets, exhibiting low friction and high effectivity as its biggest advantages, have become widely used (Brauchli et al. 2011; Burrow 2009; Kim et al. 2008; Monteiro et al. 2014). The decreased friction compared to that of elastomeric rings with conventional brackets is also an inherent characteristic of the self-ligating mechanism (Harradine 2003). This kind of brackets, by definition without an elastic ring or wire ligature but an inbuilt "ligature" mechanism, was first mentioned by Stolzenberg (1935) in the mid-1930s of the Russell Attachment (Stolzenberg 1935). The purpose of the self-ligating mechanism was to increase treatment efficiency by saving the time spent for ligation, since elastic ligatures were not available at that time (Brauchli et al. 2012). According to the statement of Harradine (2017), different from the ligation methods of conventional brackets, elastomeric ligation produces unreliable archwire control and high friction. Due to the roughness of the elastomeric ligation surface, it is more likely to accumulate food residuals and may have a negative effect on oral hygiene. On the other hand, wire ligation can be applied tightly or loosely to the archwire, which leads to highly inconsistent force application, and there is a latent risk that the wire may cause trauma to patients (Harradine 2017). However, self-ligating brackets have an inbuilt mechanical "ligature" which can be opened and closed to fix the archwire. Thus, the use of additional ligatures for attachment becomes obsolete. In this way, with the wide acceptance of self-ligating brackets, the advantages of reducing chair time, faster archwire removal and ligation, as well as relieving the discomfort for patients caused by ligature wires are beneficial to orthodontists and patients (Harradine 2003).

In addition, some studies comparing self-ligating brackets with conventional brackets using different contact angulations of the archwire show, that the resistances to sliding of the self-ligating brackets is lower than those of the conventional brackets (Monteiro et al. 2014; Thorstenson and Kusy 2001). Some other studies give evidence that there is no difference between self-ligating and conventional brackets (Francisconi et al. 2016; Szczupakowski et al. 2016), while part of authors even find increased friction in the self-ligating brackets (Redlich et al. 2003). A systematic review concludes, that self-ligating brackets produce lower friction only when coupled with small round archwires if compared to conventional brackets (Ehsani et al. 2009).

Depending on the systems of ligature mechanisms of self-ligating brackets, two main groups can be distinguished: active and passive self-ligating brackets (Figure 3).

(a)

(b)

Figure 3: The difference between passive and active self-ligating brackets lies in the clip mechanism. The clip of active self-ligating bracket (a) exerts pressure on archwire with larger cross sections, while the clip of a passive self-ligating bracket (b) makes the slot appear like a tube and does not cause active pressure against the surface of the archwire.

Active self-ligating brackets, such as the Speed System™ (Strite Industries Limited, Canada), In–Ovation C® (Dentsply Sirona®, Islandia, NY, USA), and BioQuick® (Forestadent®, Pforzheim, Germany) have a slot-closure system, similar to a clip that closes the slot from the top (labial-buccal). The active spring clip applies an additional force and pressure on the archwire, therefore the additional forces can be stored in the deflection of the spring clip.

In contrast, passive self-ligating brackets, such as Damon™ (Ormco™, Glendora, Calif, USA) and SmartClip™ (SL3 Self-Ligating Appliance System, 3M Unitek, USA) have a closure system that acts like a door and turns the slot into a tube. This kind of slide can be opened and closed up and down (vertical to the surface of occlusion), which does not lead to active pressure on the archwire and creates a rigid or passive labial-buccal closure of the slot. Moreover, this passive slide can "store" some of the forces by deflection of a metal clip (Brauchli et al. 2012; Ehsani et al. 2009; Harradine 2003). Thus, it is worth to consider the difference between active and passive self-ligating brackets in detail. Harradine (2003) evaluated the performance of passive slides and active clips of self-ligating mechanisms from the aspects of alignment, friction and ease of using. For example, the initial alignment can be more complete using an active clip for a particular wire size. When using a hard wire with an active self-ligating bracket, the possible drawbacks of an active clip are higher friction and lower capability for applying torque in one direction. The active clip will generate additional forces on the archwire during tooth movement. In contrast, the increased clearance between the wire and the passive slide could produce lower forces and may release the constraining force caused by adjacent tilted tooth (Harradine 2003).

Apart from the ligation mechanism, metallic brackets hold a dominant position in the field of orthodontics for both conventional and self-ligating brackets. Even though they are in the market since a long time, metallic brackets are still the most commonly used types of brackets in the orthodontic treatment process due to their superior working efficiency (Arash et al. 2015). As the number of adult patients seeking orthodontic treatment is continuously growing, the request for aesthetic aspects of the treatment system is becoming increasingly important which is the inherent drawback of metallic brackets. Ceramic brackets in tooth-like colours became more and more popular since the 1980s because of their improved colour aesthetics closer to the colour of nature teeth (William et al. 2007).

Although this kind of brackets have reduced the aesthetic issues, they also have drawbacks. The ceramic brackets fracture more easily, cause enamel abrasion, have a higher coefficient of friction, and increase the RS (Arash et al. 2015). Nishio et al. (2004) concluded that the traditional ceramic bracket presented the greatest frictional force in all tested combinations, when comparing with stainless steel brackets and ceramic brackets with metal reinforced slot (Nishio et al. 2004). Fidalgo et al. (2011) also give the consistent conclusion, the use of ceramic brackets with TMA (titanium-molybdenum alloy) wire was observed to have a higher friction coefficient and should be judiciously used as this system (Fidalgo et al. 2011). Nevertheless, this characteristic of friction does not affect the potential use of ceramic brackets.

Furthermore, wire materials, as one of the most important factors, affect the frictional force at the same time. Previous investigation report that NiTi wires produced higher frictional forces than stainless steel wire (Ireland et al. 1991; Kapila et al. 1990; Mezeg and Primozic 2017; Nishio et al. 2004; Thomas et al. 1998; Tidy 1989). Other researchers are finding that there is no significant difference between stainless steel and NiTi wires in terms of friction (Cacciafesta et al. 2003; Downing et al. 1994; Peterson et al. 1982). In addition, another author suggests the inconsistent results could be attributed to the forces of ligation applied in the different investigations and the archwires used being provided by different manufactures and combined with different bracket materials (Thorstenson and Kusy 2003). Considering these contradictory findings, Nishio et al (2004) mentions that flexible orthodontic wires could present a slight decrease of frictional force, and rigid wires could cause higher friction. This is, because rigid wires lack flexibility, could therefor create shaper angles and increase the resistance to sliding. Therefore, the frictional forces are probably influenced by the texture and stiffness of orthodontic archwires (Nishio et al. 2004).

Apart from that, the environment of a treatment process also acts as an important factor affecting friction. Saliva, as an inevitable part of the environment in orthodontics, has been studied by numerous authors so far. Some studies use artificial saliva to evaluate orthodontic appliances in sliding (Kusy and Whitley 2003; Leal et al. 2014) because artificial saliva is also frequently used as substitute of natural saliva for people suffering a systemic disease such as Sjoegren syndrome or oral cancer. The long term radiotherapy of these cancer patients destroys the secretion function of the salivary glands (Fann and Shannon 1978).

However, the use of artificial saliva in investigations of orthodontic frictional systems has always been discussed controversially. Some studies comparing the dry state and artificial saliva as environmental states report that the dry state exhibits a significantly lower frictional force (Alfonso et al. 2013; Chang et al. 2013; Kusy and Whitley 2003), while some other studies show that artificial saliva produces lower friction (Baker et al. 1987; Fidalgo et al. 2011; Saunders and Kusy 1994). Furthermore, there is an evidence that the evaluated mucin- and CMC-based artificial saliva compared to human saliva show no differences amongst each other. They can therefore provide a reliable alternative to human natural saliva (Leal et al. 2014).

Considering the different results above, some studies give reasons for the discrepancies. Pratten et al. (1990) concludes that, saliva acting as lubricant or adhesive might be due to the different loading forces that are exerted on the bracket-wire combinations. In some cases, saliva is forced out of the contact surface of bracket and wire in the high load situation, which may increase friction, while for lower loads it acts as a lubricant (Pratten et al. 1990). Another statement of Kusy and Whitley (2003) claims that the reason for the discrepancies may lie in the subtle difference of the components of artificial saliva, therefore leading to different performances of frictional force and coefficient (Kusy and Whitley 2003). Tselepis et al. (1994) shares the same point of view with Kusy and Whitley (2003). They mentioned that these contradictory findings may result from the different artificial saliva solution formulations and the technique used in various investigations (Tselepis et al. 1994). An interesting explanation of saliva lubricating effects is that saliva can perform a boundary layer on the contact surface of bracket and archwire to reduce the interaction of them, and thus, decrease the friction (Christersson et al. 2000; Saunders and Kusy 1994). To conclude, saliva composition, viscosity and even minor differences in experimental techniques, are extremely important in explaining divergences in the frictional force found in different studies.

1.4 RESEARCH PURPOSE AND SIGNIFICANCE

The present study mainly focuses on the effect of material interactions with surrounding media and the influence of normal forces of different magnitude on the frictional force during tooth movement. This takes into consideration that the properties of materials are crucial for the study of friction, which are the basis of the research on the other additional factors such as angulations and wire-coatings. The investigation of material properties with respect to friction can be used to identify additional parameters for further research. Thus, the current study concentrates on the evaluation of the frictional properties of orthodontic materials in simulated clinical applications.

a) The aim of the material related study part is to investigate the influence of different testing conditions on frictional forces between various brackets in combination with stainless steel archwires.

b) The aim of the clinical simulation study part is to evaluate the influence of normal forces on conventional and self-ligating brackets with NiTi and stainless steel archwire in artificial saliva.

2. MATERIALS AND METHODS

This present research consists of two parts: a) material study and b) simulation of clinical situation study. Both are conducted by the same experimental setup and testing program. The material study focuses on comparing different testing environments and orthodontic materials characteristics, while the simulation of the clinical situation study targets at evaluating the influence of various normal forces and ligation mechanisms on the clinical tooth movement.

2.1 ORTHODONTIC MATERIALS

The samples used for the in vitro experiments consist of 60 ceramic active self-ligating brackets (In-Ovation® C, Dentsply Sirona®, Islandia, NY, USA), 60 metal active self-ligating brackets (BioQuick®, Forestadent®, Pforzheim Germany), 24 metal passive self-ligating brackets (Damon™ 3MX, Ormco™, Glendora, CA, USA), and 60 conventional metal twin brackets (Mini Sprint®, Forestadent®, Pforzheim Germany) (Table 1). The slot size of all brackets used in test is 0.022” (≈ 0.56 mm). Prescriptions of the brackets with torque and angulation are compensated by the use of manually adjustable platforms in the testing machine (Figure 7). 156 stainless steel archwires and 48 Nickel-Titanium (NiTi) archwires with the dimensions of 0.016”x0.022”, 0.018”x0.025”, 0.019”x0.025” (Table 1) are chosen for the frictional experiment.

Table 1: Orthodontic bracket and wire materials investigated. Involving product name, manufacturer, material, ligation method, dimension and sample numbers.

Product	***Manufacturer***	***Material***	***Dimension***	***Ligation***	***N***
Mini Sprint®	Forestadent®	Stainless steel	.022”	Ligature wire	60
In-Ovation® C	Dentsply Sirona®	Ceramic	.022”	Active self-ligating	60
BioQuick®	Forestadent®	Stainless steel	.022”	Active self-ligating	60
Damon™ 3MX	Ormco™	Stainless steel	.022”	Passive self-ligating	24
			0.016”x0.022”	——	52
Steel arch wires	Forestadent®	Stainless steel	0.018”x0.025”	——	52
			0.019”x0.025”	——	52
			0.016”x0.022”	——	16
BioTorque® Arches	Forestadent®	Nickel-Titanium	0.018”x0.025”	——	16
			0.019”x0.025”	——	16

2.2 EXPERIMENTAL CONDITIONS – ENVIRONMENTS

Dry and wet states are investigated and compared to each other. The wet conditions are deionized water, human saliva and artificial saliva. The dry condition serves as a control group.

2.2.1 WHOLE HUMAN SALIVA

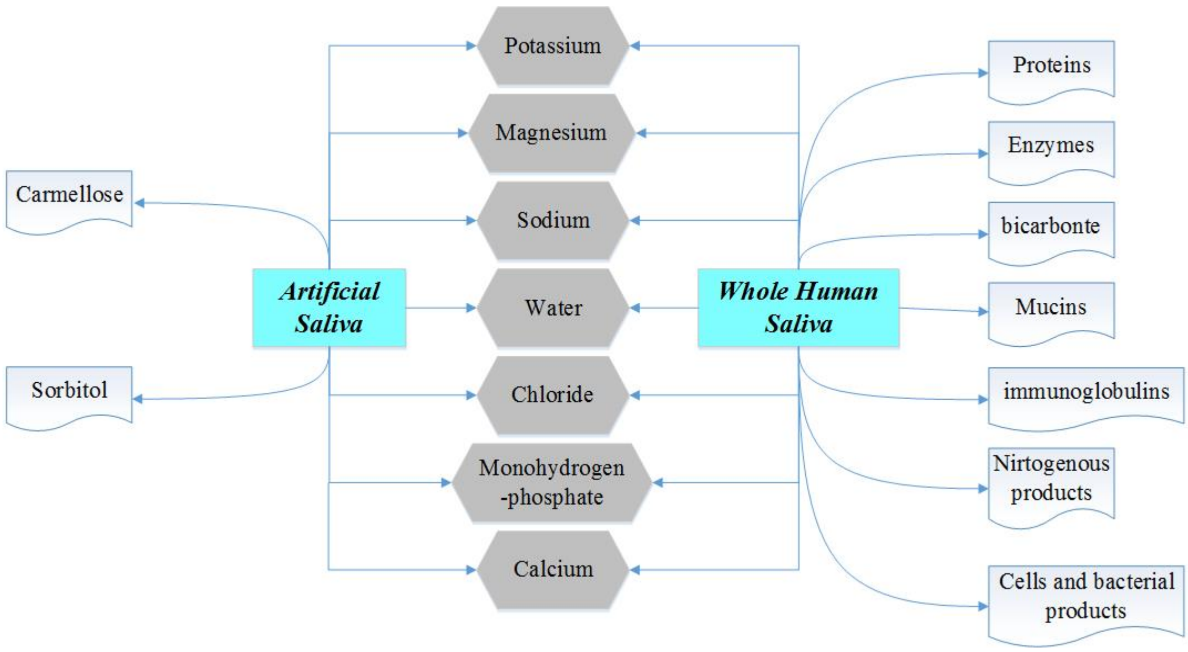

Figure 4: Composition of artificial saliva and human saliva in comparison. Artificial saliva has only water and electrolytes in common with human saliva. Except water and electrolytes, human saliva owns proteins, enzymes, mucins and different products from cells (according to (Humphrey and Williamson 2001)).

Human saliva is a clear, slightly acidic fluid, which is produced and secreted by oral salivary glands. It is a mixture of electrolytes (sodium, potassium, calcium, magnesium, phosphates and bicarbonate), immunoglobulins, proteins, enzymes, mucins, nitrogenous products and oral bacteria (Humphrey and Williamson 2001) (Figure 4).

For this current experiment, human fresh saliva is used. Based on the inclusion and exclusion criteria of Leal et al. (2014) the donator of the human saliva must be not smoking, nor having any systemic or dental disease. During human saliva collection, the donator is reminded not to drink and to rinse the mouth, with head tilted forward one side, to allow saliva flowing naturally into a sterile container (Leal et al. 2014). Whole human saliva is obtained immediately before the friction tests and without additional stimulation.

2.2.2 ARTIFICIAL SALIVA IN TEST

Glandosane Neutral® (Cell Pharm GmbH, Bad Villbel, Germany) is used as artificial saliva (AS) test. The composition and weight of ingredients of AS is listed below (Table 2).

Table 2: The contents of Glandosane Neutral® in accordance with the list of ingredients on the packaging in 50ml of aqueous solution.

Ingredients	*Weight (g)*
Carmellose-Sodium	0.5075
Sorbitol (Ph.Eur.)	1.5225
Potassium chloride	0.0609
Sodium chloride	0.0428
Magnesium chloride hexahydrate	0.0026
Calcium chloride dihydrade	0.0074
Potassium monohydrogen phosphate	0.0174

It almost fully consists just from water and electrolyte but not of proteins, enzymes, mucins, cells and bacterial products like human saliva does. The difference regarding the components of human saliva and artificial saliva may lead to different performance in friction force during tooth movement (Winkeljann et al. 2018).

2.3 MATERIAL PREPARATION

The orthodontic wire is placed and subjected to sliding in each bracket in both, fluids as well as dry condition. All archwires and brackets are cleaned with 95% ethanol and air dried before testing.

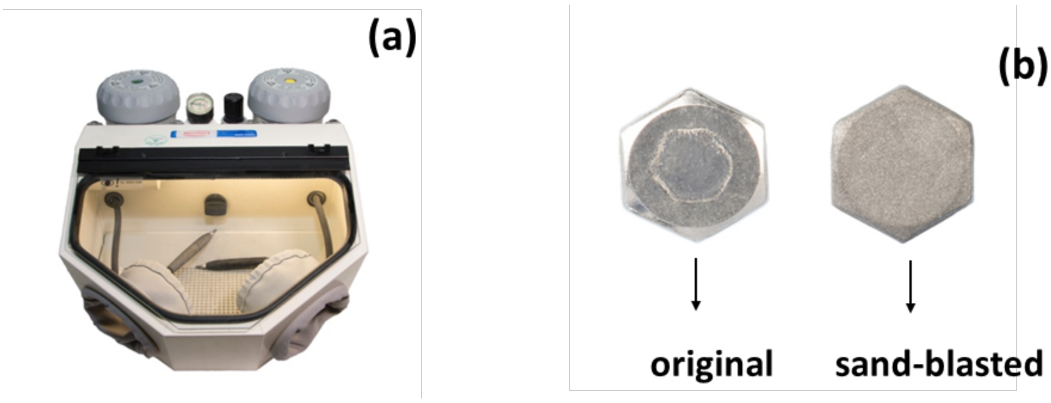

Figure 5: The sandblast machine (a) spray with 50 µm alumina particles on the top of the bracket holder screw (b). Comparing with the original screw (b left) before sandblasting, the surface of the screw head (b right) is rougher and therefore easier to bond with brackets after sandblasted.

All brackets used in this study are bonded on the top of a metal hex flat head screw (M5 x 4.97mm) with UHU® PLUS (UHU® GmbH&Co.KG, D-77815, Bühl, Germany) adhesive by the same person. Before bonding, the surface of the screw's top is sandblasted with 50 µm alumina particles (Figure 5).

Rectangular orthodontic wires, measuring 0.016"x0.022", 0.018"x0.025", 0.019"x0.025", are sectioned using cutting pliers in 7-cm segments starting from the end of the straight part of the archwire to obtain wire samples. The wire samples are then inserted into a special wire-holder, using a rectangular module to align the segments of the wires within the wire-holder. To make sure they are aligned, the segments of wires are fixed within the wire-holder using 8 fixing screws at 4 places (Figure 6).

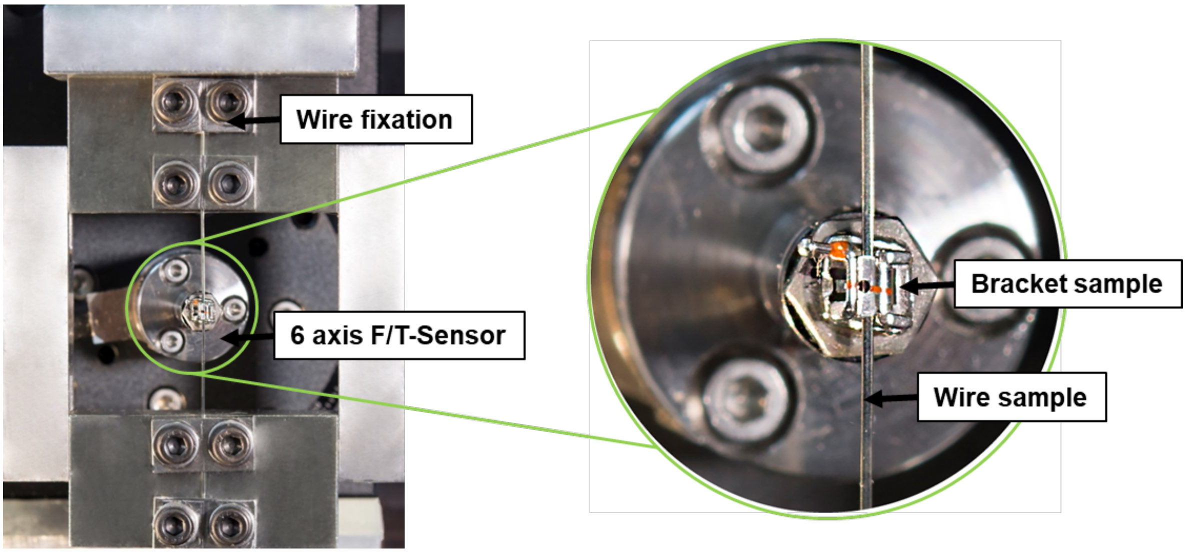

Figure 6: The close view of the test device and bracket-wire test combination. The wire sample is fixed in the wire-holder by 8 fixing screws at 4 places. Perpendicular to the wire holder, a 6-axis force-torque sensor is fixed in the testing machine. The bracket-bonded metal screw is inserted and fixed in the sensor of the friction-testing machine. The wire is fixed into the wire-holder and aligned straight and parallel with the slot of the brackets.

Afterwards, the wire-holder is mounted into a holder to couple it with the loading cell of the Instron universal testing machine. Perpendicular to the wire holder, a FTD-Nano-17-SI-25-0.25 6-axis force-torque sensor (ATI, Industrial Automation, Apex, NC, USA) is attached to the testing machine. The metal screw with the bonded bracket is fixed on the extension rod at the front of the sensor. After this, using an 8x magnifying lens (Tech-line, Schweizer, Munich, Germany) the angulation between slot and wire, is adjusted to make sure that the wire fixed into the wire-holder is straight and parallel with the slot of the brackets. This adjustment is possible by means of three movable platforms, which are aligned using the sub-millimeter scales of the platforms (Figure 7).

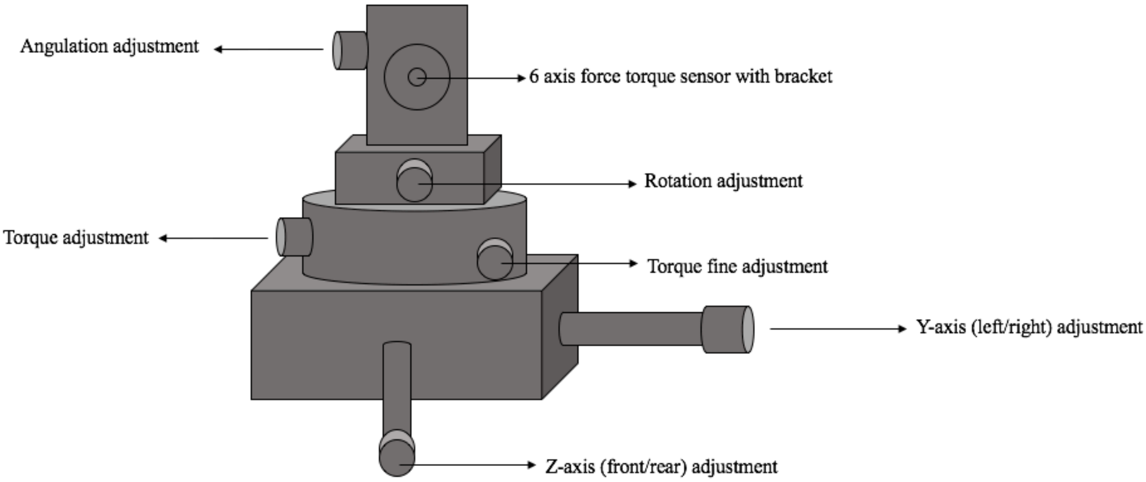

Figure 7: Schematic drawing of movable stages with adjustment spindles. The bracket can be adjusted in angulation, rotation, torque, vertical and horizontal direction.

2.4 TESTING PROCEDURE

After preparing the experimental set-up, the parameters of the sample combination are entered into the operation panel of the measurement program developed in Labview 2012® (National Instruments™, Austin, Texas, USA) (Figure 8). First of all, the parameters of brackets (manufacturer, type, slot), wires (manufacturer, type, dimension), testing conditions (rotation, angulation, torque, number of cycle, temperature), sensor (channel, timing and GPIB parameters), Instron universal testing machine (extension limit, load limit and x-head speed) and D_z (length from the bottom of bracket's slot to the top part of the sensor) are entered into the measurement program and a folder to record the test data is chosen (Figure 9). Following the above-mentioned steps, the position of the brackets is adjusted to offset the pre-torque parameter of the used bracket type.

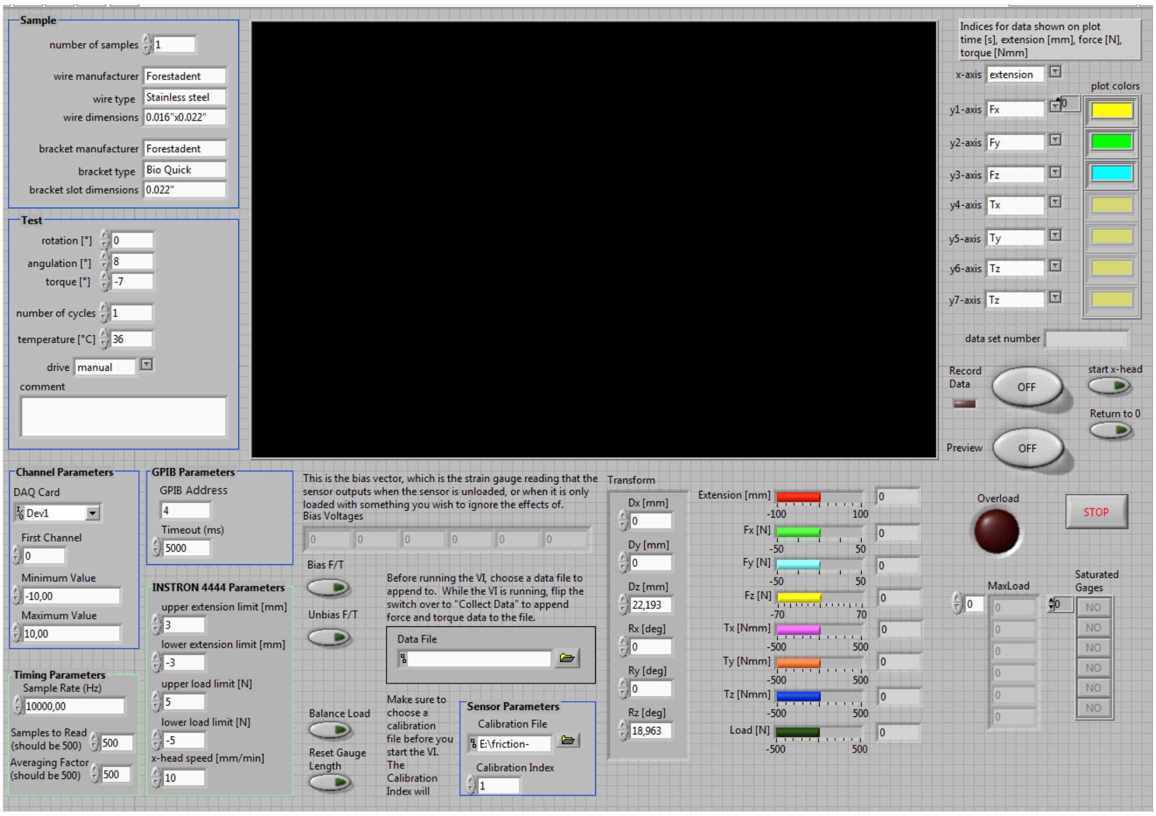

Figure 8: Operation panel of measurement program in Labview 2012. The parameter of materials and testing results are shown on the operation panel of the measurement program.

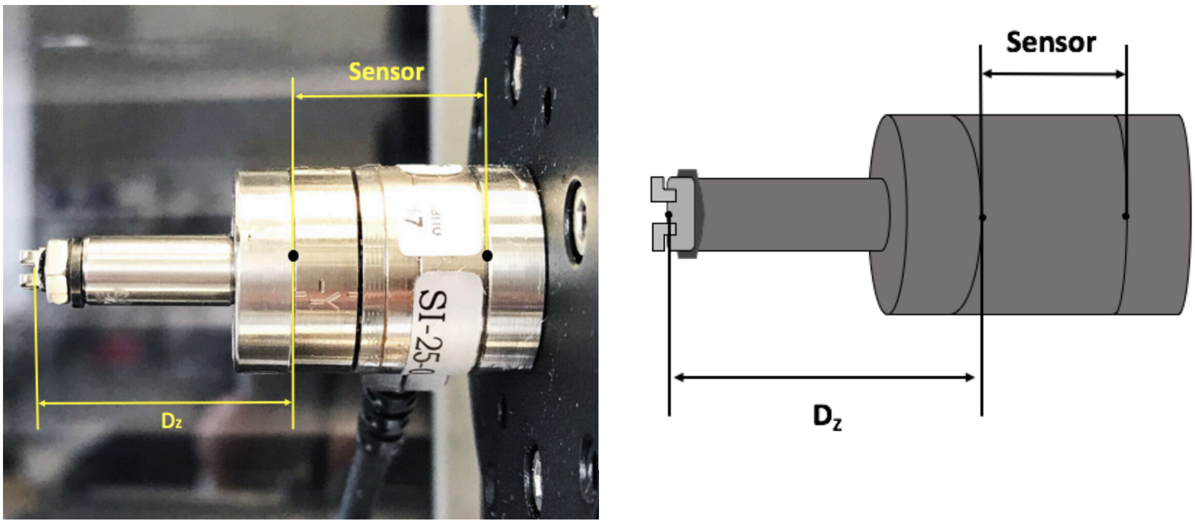

Figure 9: Close view (a) and schematic drawing (b) show the sensor and how D_z is calculated. The sensor is the part behind the rod with the bonded bracket. D_z is the length from the slot of each kind of bracket to the top part of the sensor. Different brackets own different D_z. D_z (Mini Sprint®) is 22.42 mm, D_z (In-Ovation® C) is 22.27 mm, D_z (BioQuick®) is 22.19 mm and D_z (Damon™ 3MX) is 23.06 mm.

The position of the bracket-wire combination is set to zero and double-checked before the test. Before starting the measurement, the angle "R_z" between the x- or y-axis of the coordinate system of the F/T sensor and the direction of wire movement respectively has to be calculated. Assuming that both planes (x-/y-axes of sensor and direction of movement) are parallel "R_z" can be calculated by the following simple trigonometric equation:

$$R_z = tan^{-1}(F_x/F_y) \qquad \textit{Eq. 2}$$

with R_z = Rotate angulation, F_x = Initial "x-axis" force and F_y = Initial "y-axis" force.

The force components needed for the calculation can be determined by pressing the wire perpendicular to the direction of movement against the bracket mounted on the sensor. This way, the sensor shows the components of the force in the coordinate system of the sensor. The x and y components of the force are F_x or F_y respectively in *Eq. 2*. This is also visible from Figure 10. Using *Eq. 2* and the recorded force component values "R_z" can be calculated. When setting up the parameter of R_z, the forces in x- and y-direction of the sensor's coordinate system are transformed by means of a rotational matrix following the roll-pitch-yaw convention, to the forces F'_x or F'_y in the coordinate system of the bracket-wire system. Therefore, the frictional force resisting the sliding of the wire in the slot of the bracket is focused on vertical direction F'_x during the study (Figure 10).

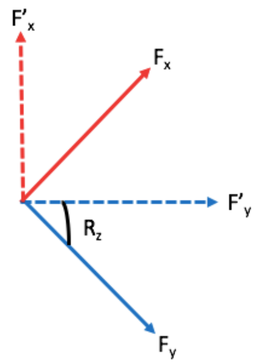

Figure 10: The initial orientation of F_x and F_y at the sensor can be at any direction. R_z is the angulation that the sensor must be rotated if changed to the direction of F'_x (vertical) and F'_y (horizontal). The panel of the measurement program displayed the initial value of F_x and F_y. When the wire pressed against the screw-head at the direction of F_y, there is an associated measured value of F_x showing on the panel, then using *Eq*. 2 to calculate the angulation R_z.

After the steps mentioned above, the screw-head and the wire are separated, placing the wire with the wire-holder in the middle of the bracket, using again the 8x magnifying lens to make sure that the wire is still parallel to the slot of the bracket. Then the measured force is set to zero again within the measurement program, to make sure the sensor provides correct measurement values. After that, the archwire is ligated in the brackets using a standard steel wire ligature. Finally, a certain amount of normal force (1N, 1.5N, 2N, 2.5N) is applied by controlled "z"-axis adjustment (Figure 7), pushing the sensor with the mounted bracket in a well-defined way against the wire. The direction of this normal force points in the "z-axis" positive direction that points against archwire and measured as F_z. After these preparatory procedures, the machine is able to draw the wire through the fixed bracket slot to measure the frictional forces.

2.5 DESCRIPTION OF FRICTIONAL TEST

All experiments are performed at 36±1℃ in an air chamber, and the temperature is controlled by a PID thermostat (REX-C100, Tokyo, Japan). An Instron® 4444 universal testing machine (Instron® Corp. Norwood, MA, USA) with a static loading cell 2530-427 of 100 N (Instron® Corp. Norwood, MA, USA) is used for all samples (Figure 11).

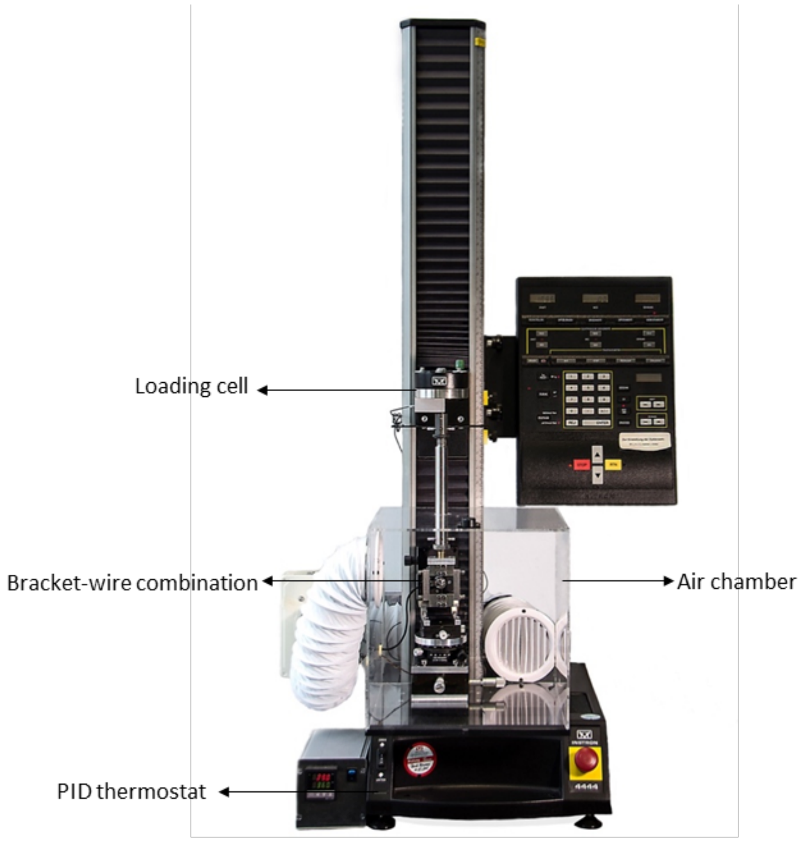

Figure 11: Experimental setup used in this study. It consists of the loading cell of 100N with a precision of ±0.25%, and the bracket-wire combination with the sensor that is installed in the Instron® 4444 Universal testing machine. All tests are performed at 36±1℃ in a chamber where the temperature was controlled by a PID thermostat.

After putting the wire into the bracket, the wire is moved a distance of 6 mm (-3 mm to +3mm) at the speed of 10 mm/min through the slot of the bracket.
For the ligation of the conventional bracket (Mini Sprint®), a 0.010” stainless steel ligature wire is used. The ligature wire is first twisted until it is taut against the archwire and then untwisted by one quarter turn (Tidy 1989). For the self-ligating bracket, it is enough to open or close the latch or slide to fix the wire. Five consecutive tests are performed for each wire-bracket combination.
The force values in the 6 directions in space (x, y, z, -x, -y, -z) measured by the sensor are recorded by the measurement program. F_x directs at the way that the wires move up and down (x, -x), F_y directs at the force exerting from left and right (y, -y), while F_z directs at the force inducing the direction inside and outside (z, -z) (Figure 12).

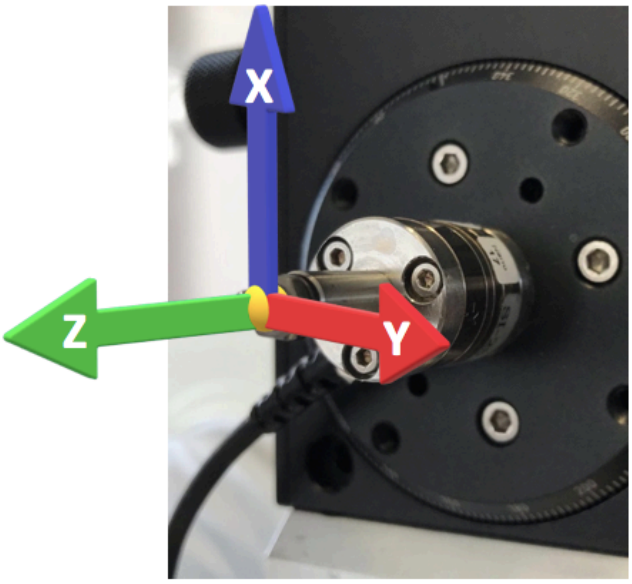

Figure 12: Diagrammatic general view of the 6-axis (x, y, z, -x, -y, -z) force torque sensor used in this study. F_x directs at up and down (x, -x), F_y directs at left and right (y, -y), while F_z directs at in and outside (z, -z). When the universal testing machine moved the wire up and down through the slot of the bracket, the loading cell connected with the wire-holder recorded the force at “x” direction (F_x). “z” is the direction of the normal force (F_z), which is produced by the slot of the bracket pushed against the wire.

When the frictional testing machine made the wire to move up and down through the slot of the bracket, the loading cell at recorded the force in x-direction (F_x) that resisted to sliding, which is defined as the frictional force. Out of the measured values of F_x versus distance, static and kinetic friction are calculated. The initial peak value is recorded as static frictional force. The kinetic friction is calculated out of the average value of the first 1 mm after the static frictional force peak. Moreover, the coefficient of friction can be calculated from *Eq.1*.

2.6 FRICTIONAL TEST PROCEDURE

This present material study is conducted under (36±1) ℃ and constant normal force F_N of 1N in four different environmental conditions: 1) dry state; 2) whole human saliva; 3) deionized water and 4) artificial saliva. The fluids groups 2)-4) are applied to the bracket-wire combination by means of a flexible tube attached to a syringe which dripped the fluid at about a rate of 3ml/min. 36 ceramic active self-ligating brackets (In-Ovation® C, Dentsply Sirona®, Islandia, NY, USA), 36 metal active self-ligating brackets (BioQuick®, Forestadent®, Pforzheim Germany) and 36 conventional metal brackets (Mini Sprint®, Forestadent®, Pforzheim Germany) with a 0.022" slot size are used and combined with 108 rectangular stainless steel archwires measuring 0.016"x0.022", 0.018"x0.025", 0.019"x0.025". Material tests of this current research are focused on observing the influence produced by different environments on frictional forces and the various performances and characteristics of different orthodontic materials.
The study for simulation of the clinical situation is performed using artificial saliva at a temperature of (36±1) ℃, which simulates oral environment during orthodontic treatment. Sliding efficiency and reproducibility were evaluated with the universal testing machine. The test is concluded using different amounts of normal force F_N of 1N, 1.5N, 2N, 2.5N, and proceeded under the same parameters as in the material tests.

2.7 STATISTICAL ANALYSIS

Descriptive statistics including mean values, standard deviations (SD), maximum, minimum and median values together with the confidence intervals for the mean (CI) are calculated for each testing groups of frictional data of material and simulation clinical situation tests. Box plots are used to visualize the analyses graphically. Normal distribution of the data is tested using the Kolmogorov-Smirnov test. Two-way analysis of variance (ANOVA) and Tukey *post hoc* test are used to compare and indicate significant differences in the material study and simulation clinical situation study. Calculations are carried out using SPSS 25 (IBM Corp., Armonk, NY, USA), with a significance level of P=5%.

For the purpose of minimizing the influence of experiment error, all samples are tested in random order. Each sample is repeated 4-5 times. According to the Kolmogorov-Smirnov test, almost all testing groups were normally distributed; the means and standard deviations are calculated.

3. RESULTS

3.1. MATERIAL STUDY

The descriptive parameters of static and kinetic frictional force for each bracket-wire combination in various states are analysed and summarized in Tables 3 and 4. All measurements of the present material study are conducted with a clinically relevant normal force of 1N. The frictional coefficients are calculated using the results from the frictional force measurements by means of *Eq. 1*. Following the descriptive tables, the statistical analysis' results are presented in Tables 5 to 8. The data are visualized by means of box plots, showing the distribution and median of the frictional values in the material study (Figures 14 to 19).

3.1.1. TYPICAL MEASRUREMENT CURVE OF "FRICTIONAL FORCE VERSUS DISTANCE"

Typical graph patterns obtained in friction measurements are shown in Figure 13, which shows frictional force versus the motion distance of a 0.016"x0.022" stainless steel archwire against the slot of In-Ovation® C bracket in four different environments.

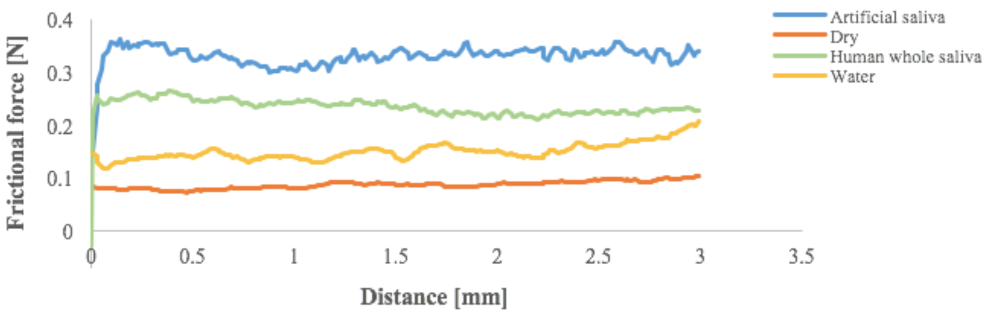

Figure 13: Exemplary trace plots obtained from the frictional force against distance at 1N normal force in four different environments.

3.1.2. DESCRIPTIVE ANALYSIS

3.1.2.1. STATIC FRICTION

The following subchapter includes the recorded initial peak value as static frictional force summarized in Table 3. It is obvious that saliva leads to higher static friction than dry state. The highest static frictional force 1.640±0.257 N is recorded with the 0.019”x0.025” stainless steel wires combined with BioQuick® in artificial saliva, followed by In-Ovation® C brackets combined with 0.018”x0.025” wires which reaches up to 0.565±0.055 N in whole human saliva. Compared to the other two brackets, Mini Sprint® with 0.019”x0.025” wires showed the lowest static friction (0.446±0.052 N) in artificial saliva.

Among all test environments, dry state produces the lowest static friction for all brackets if combined with 0.016”x0.022” stainless steel wires. The static friction caused by In-Ovation® C shows the lowest values (0.083±0.015 N), followed by Mini Sprint® (0.121±0.012 N) and BioQuick® (0.231±0.039 N).

Comparing the median of box-whisker plots of different bracket-wire combinations in each environment, saliva shows higher static frictional values, while dry conditions produce the lowest values. For almost all brackets in the material study, the variance of the dry state is much narrower than in other environments, but when In-Ovation® C and BioQuick® brackets are combined with 0.019”x0.025” wires, the variance of water was the narrowest (Figures 14 to 16).

Table 3: Descriptive statistics for static frictional force in different environments. N-count; SD-Standard deviation; Min-Minimum; Max-Maximum; CI-confidence interval for the mean.

Static Frictional Force [N]								
Bracket	**Environment**	**Wire size [inch]**	**N**	**Mean (SD)**	**Min**	**Max**	**Median**	**95% CI**
In-Ovation® C	Artificial Saliva	0.016x0.022	13	0.335 (0.033)	0.297	0.414	0.324	0.365 to 0.414
		0.018x0.025	13	0.336 (0.052)	0.228	0.383	0.363	0.373 to 0.384
		0.019x0.025	13	0.334 (0.039)	0.265	0.394	0.327	0.377 to 0.394
	Dry	0.016x0.022	13	0.083 (0.015)	0.060	0.118	0.081	0.086 to 0.118
		0.018x0.025	14	0.176 (0.013)	0.155	0.200	0.177	0.185 to 0.200
		0.019x0.025	13	0.209 (0.072)	0.116	0.308	0.232	0.281 to 0.308
	Whole human saliva	0.016x0.022	14	0.264 (0.026)	0.223	0.314	0.262	0.291 to 0.314
		0.018x0.025	12	0.562 (0.055)	0.430	0.616	0.574	0.606 to 0.616
		0.019x0.025	12	0.552 (0.059)	0.409	0.655	0.565	0.573 to 0.655
	Water	0.016x0.022	14	0.169 (0.032)	0.136	0.244	0.162	0.203 to 0.244
		0.018x0.025	14	0.207 (0.033)	0.156	0.264	0.208	0.235 to 0.264
		0.019x0.025	14	0.237 (0.050)	0.192	0.340	0.219	0.313 to 0.340
Mini Sprint®	Artificial Saliva	0.016x0.022	13	0.315 (0.038)	0.216	0.360	0.324	0.340 to 0.360
		0.018x0.025	15	0.434 (0.058)	0.319	0.516	0.438	0.498 to 0.516
		0.019x0.025	13	0.446 (0.052)	0.296	0.490	0.464	0.477 to 0.490
	Dry	0.016x0.022	15	0.121 (0.012)	0.101	0.141	0.124	0.131 to 0.141
		0.018x0.025	15	0.131 (0.016)	0.107	0.156	0.131	0.148 to 0.156
		0.019x0.025	15	0.133 (0.026)	0.100	0.187	0.128	0.151 to 0.187
	Whole human saliva	0.016x0.022	13	0.276 (0.086)	0.150	0.416	0.264	0.349 to 0.416
		0.018x0.025	15	0.336 (0.046)	0.279	0.412	0.329	0.396 to 0.412
		0.019x0.025	15	0.311 (0.054)	0.240	0.416	0.293	0.388 to 0.416
	Water	0.016x0.022	12	0.252 (0.072)	0.153	0.363	0.265	0.310 to 0363
		0.018x0.025	13	0.361 (0.078)	0.222	0.464	0.375	0.433 to 0.464
		0.019x0.025	14	0.373 (0.067)	0.252	0.442	0.394	0.429 to 0.442
BioQuick®	Artificial Saliva	0.016x0.022	14	0.359 (0.101)	0.196	0.505	0.367	0.462 to 0.505
		0.018x0.025	15	0.988 (0.149)	0.589	1.180	1.026	1.103 to 1.180
		0.019x0.025	14	1.640 (0.257)	1.163	1.922	1.778	1.878 to 1.922
	Dry	0.016x0.022	13	0.231 (0.039)	0.145	0.309	0.236	0.253 to 0.309
		0.018x0.025	12	0.857 (0.052)	0.784	0.944	0.847	0.908 to 0.944
		0.019x0.025	14	0.939 (0.132)	0.682	1.169	0.970	1.040 to 1.169
	Whole human saliva	0.016x0.022	15	0.579 (0.052)	0.479	0.647	0.579	0.640 to 0.647
		0.018x0.025	15	0.925 (0.132)	0.706	1.170	0.914	1.062 to 1.170
		0.019x0.025	14	1.032 (0.136)	0.837	1.370	1.000	1.075 to 1.370
	Water	0.016x0.022	15	0.262 (0.047)	0.196	0.335	0.274	0.303 to 0.335
		0.018x0.025	15	0.685 (0.066)	0.565	0.782	0.689	0.752 to 0.782
		0.019x0.025	14	1.042 (0.086)	0.903	1.207	1.042	1.119 to 1.207

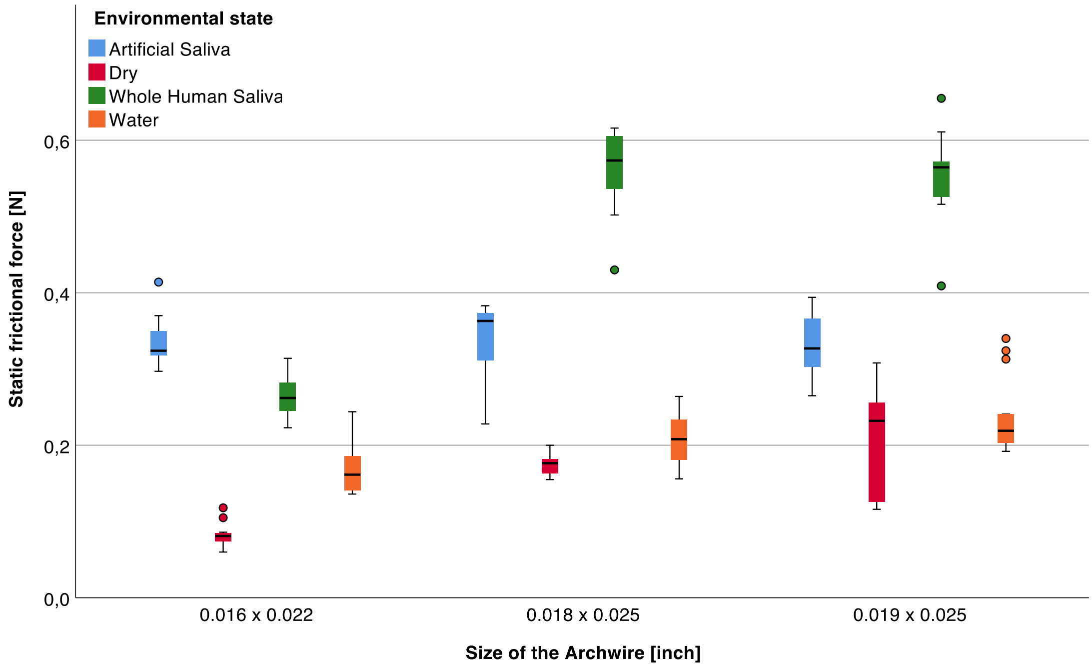

Figure 14: Box-Whisker plots of the static frictional force of In-Ovation® C bracket.

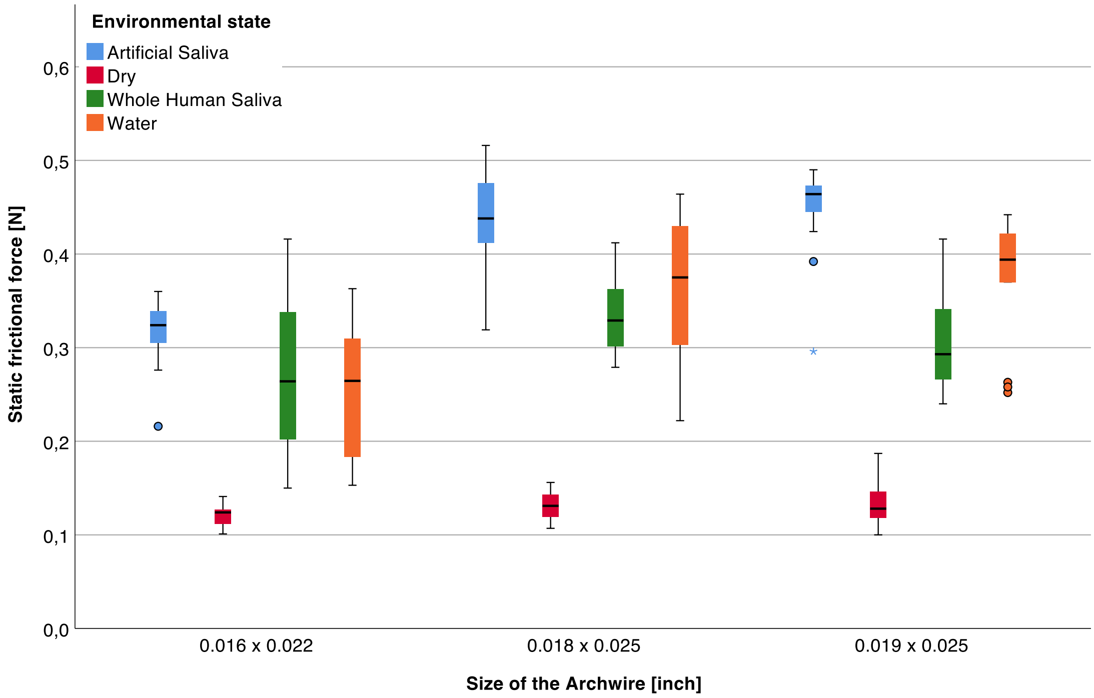

Figure 15: Box-Whisker plots of the static frictional force of Mini Sprint® bracket.

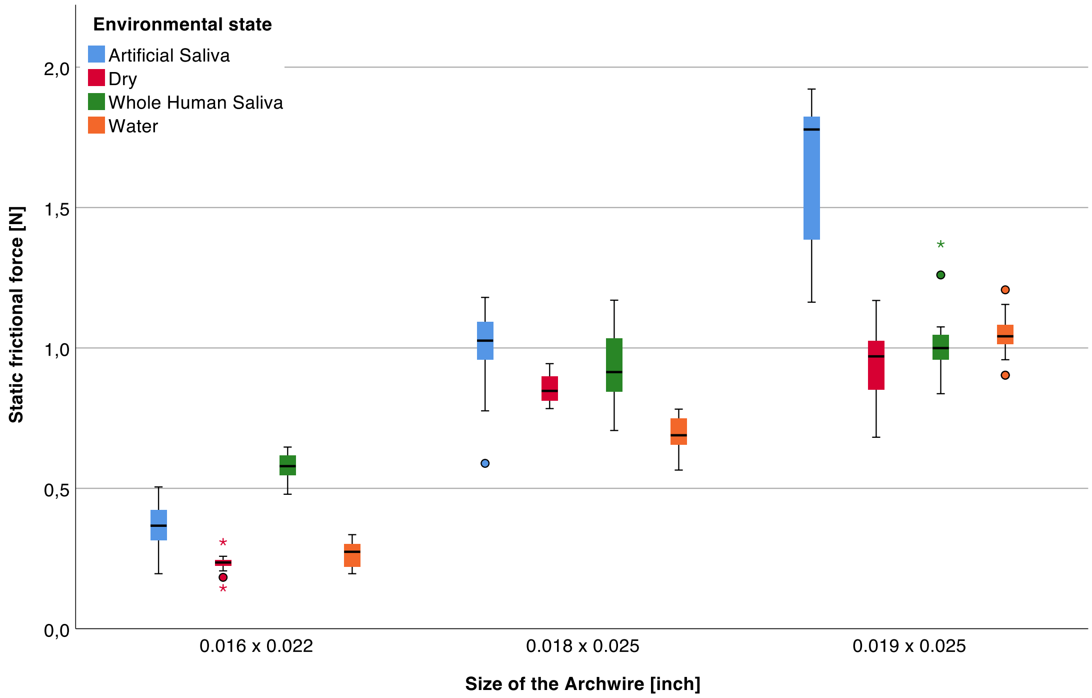

Figure 16: Box-Whisker plots of the static frictional force of BioQuick® bracket.

3.1.2.2. KINETIC FRICTION

The following subchapter contains the recorded kinetic frictional force, which is calculated from the average value of the first 1 mm after the static friction. The results of kinetic friction are summarized and presented below in Table 4 and Figures 17 to19.

The descriptive analysis of kinetic friction is displayed in Table 4. All brackets perform highest kinetic friction if they are combined with 0.019”x0.025” stainless steel wires in saliva. The highest kinetic frictional force (1.862±0.336 N) is shown by BioQuick® brackets in artificial saliva, followed by In-Ovation® C brackets (0.682±0.063 N) in whole human saliva. Mini Sprint® show the lowest kinetic friction in artificial saliva (0.460±0.048 N).

Comparing the four environments, dry state produces the lowest kinetic friction for all brackets combined with 0.016”x0.022” stainless steel wires. The kinetic friction caused by In-Ovation® C (0.086±0.016 N) is the lowest, followed by Mini Sprint® (0.126±0.011 N) and BioQuick® (0.235±0.040 N). Assessing the median and the variance visible in the box plots, it demonstrates that saliva produced the highest kinetic frictional values, while dry state produces lowest ones, which was similar to Figures 14 to 16. For almost all brackets in the material study, the variance of the dry state is the narrowest. However, if 0.019”x0.025” stainless steel wires are combined with In-Ovation® C and BioQuick® bracket, the variance of artificial saliva and water is narrower (Figure 17 to 19).

Table 4: Descriptive statistics for kinetic frictional force caused in different environments. N-count; SD-Standard deviation; Min-Minimum; Max-Maximum; CI-confidence interval for the mean.

Kinetic Frictional Force [N]								
Bracket	**Environment**	**Wire size [inch]**	**N**	**Mean (SD)**	**Min**	**Max**	**Median**	**95% CI**
In-Ovation® C	Artificial Saliva	0.016x0.022	13	0.401 (0.051)	0.326	0.489	0.387	0.461 to 0.489
		0.018x0.025	13	0.380 (0.067)	0.244	0.474	0.388	0.441 to 0.474
		0.019x0.025	13	0.418 (0.067)	0.279	0.526	0.408	0.486 to 0.526
	Dry	0.016x0.022	13	0.086 (0.016)	0.061	0.108	0.087	0.102 to 0.108
		0.018x0.025	14	0.201 (0.022)	0.161	0.244	0.200	0.220 to 0.244
		0.019x0.025	13	0.235 (0.065)	0.142	0.338	0.241	0.308 to 0.338
	Whole Human Saliva	0.016x0.022	14	0.280 (0.019)	0.249	0.306	0.279	0.301 to 0.306
		0.018x0.025	12	0.634 (0.052)	0.511	0.680	0.652	0.672 to 0.680
		0.019x0.025	12	0.682 (0.063)	0.535	0.770	0.698	0.731 to 0.770
	Water	0.016x0.022	14	0.212 (0.057)	0.138	0.298	0.195	0.284 to 0.298
		0.018x0.025	14	0.245 (0.031)	0.180	0.295	0.247	0.273 to 0.295
		0.019x0.025	14	0.298 (0.079)	0.210	0.458	0.281	0.401 to 0.458
Mini Sprint®	Artificial Saliva	0.016x0.022	13	0.333 (0.044)	0.262	0.428	0.328	0.366 to 0.428
		0.018x0.025	15	0.432 (0.042)	0.372	0.495	0.429	0.488 to 0.495
		0.019x0.025	13	0.460 (0.048)	0.358	0.524	0.463	0.508 to 0.524
	Dry	0.016x0.022	15	0.126 (0.011)	0.106	0.142	0.126	0.138 to 0.142
		0.018x0.025	15	0.148 (0.018)	0.117	0.189	0.142	0.165 to 0.189
		0.019x0.025	15	0.144 (0.022)	0.119	0.202	0.137	0.159 to 0.202
	Whole Human Saliva	0.016x0.022	13	0.258 (0.056)	0.154	0.349	0.247	0.295 to 0.349
		0.018x0.025	15	0.342 (0.050)	0.275	0.428	0.343	0.402 to 0.428
		0.019x0.025	15	0.336 (0.066)	0.248	0.422	0.357	0.402 to 0.422
	Water	0.016x0.022	12	0.290 (0.094)	0.170	0.423	0.279	0.382 to 0.423
		0.018x0.025	13	0.389 (0.064)	0.218	0.488	0.391	0.427 to 0.488
		0.019x0.025	14	0.407 (0.056)	0.287	0.490	0.418	0.435 to 0.490
BioQuick®	Artificial Saliva	0.016x0.022	14	0.366 (0.094)	0.210	0.523	0.374	0.443 to 0.523
		0.018x0.025	15	1.150 (0.156)	0.744	1.349	1.221	1.241 to 1.349
		0.019x0.025	14	1.862 (0.336)	1.338	2.278	2.023	2.162 to 2.278
	Dry	0.016x0.022	13	0.235 (0.040)	0.146	0.303	0.243	0.262 to 0.303
		0.018x0.025	12	0.870 (0.066)	0.768	0.969	0.865	0.938 to 0.969
		0.019x0.025	14	0.982 (0.141)	0.706	1.202	1.000	1.101 to 1.202
	Whole Human Saliva	0.016x0.022	15	0.556 (0.054)	0.455	0.622	0.560	0.612 to 0.622
		0.018x0.025	15	0.983 (0.185)	0.699	1.345	0.925	1.192 to 1.345
		0.019x0.025	14	1.127 (0.113)	0.928	1.295	1.156	1.199 to 1.295
	Water	0.016x0.022	15	0.265 (0.042)	0.170	0.329	0.263	0.306 to 0.329
		0.018x0.025	15	0.739 (0.084)	0.602	0.871	0.761	0.822 to 0.871
		0.019x0.025	14	1.102 (0.086)	0.956	1.221	1.126	1.176 to 1.221

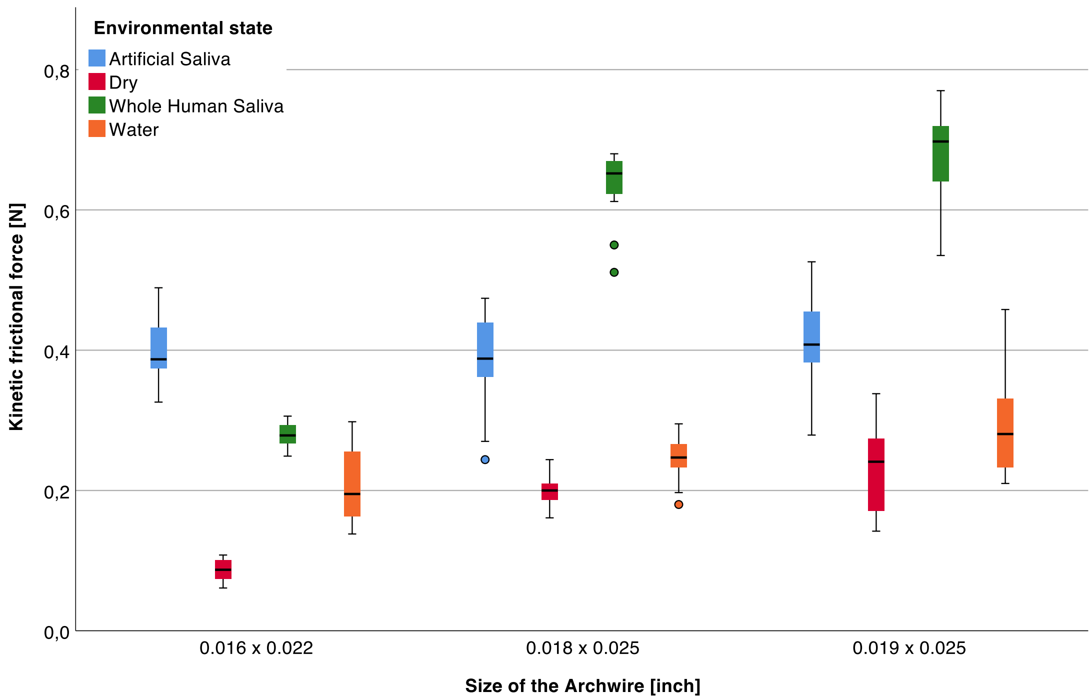

Figure 17: Box-Whisker plots of the kinetic frictional force of In-Ovation® C bracket.

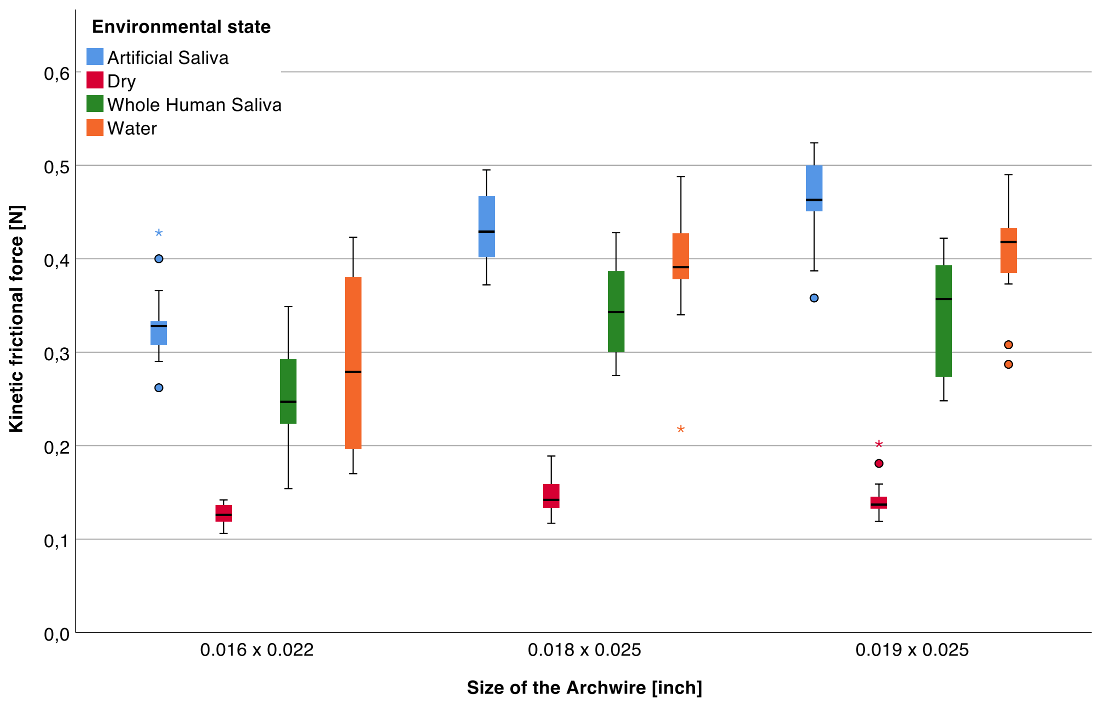

Figure 18: Box-Whisker plots of the kinetic frictional force of Mini Sprint® bracket.

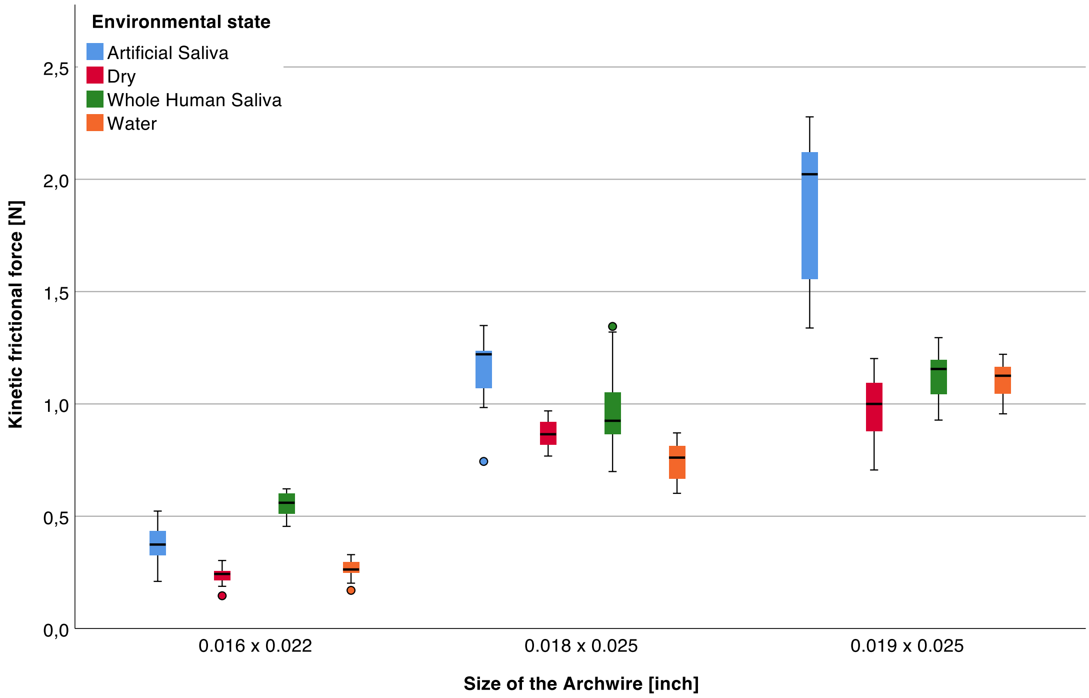

Figure 19: Box-Whisker plots of the kinetic frictional force of BioQuick® bracket.

3.1.3. INFERENTIAL STATISTICS

3.1.3.1. INFLUENCE OF WIRE DIMENSION

Pairwise comparisons between various wire sizes combined with three kinds of brackets are evaluated using two-way ANOVA combined with Tukey post-hoc test to determine whether they have significant difference with $P < 0.05^*$ (Tables 5 and 6).

3.1.3.1.1. STATIC FRICTION

This subchapter contains the data of static frictional force of each bracket-wire combination among different wire size. Table 5 summarizes that almost all static frictional force values show significant difference ($P < 0.05^*$) between different archwire dimensions, except 0.018”x0.025” and 0.019”x0.025” wires combined with In-ovation® C and Mini Sprint® brackets ($P > 0.05$). However, a comparison of static friction indicates that all brackets showed a significant difference when they were used with small sized wires ($P < 0.05^*$).

Table 5: Results of two-way ANOVA combined with Tukey *post hoc test*, comparing static frictional force for different wire sizes. Mean Difference (I-J) - The absolute difference between the mean values in two different groups; Std. Error - Standard Deviation Error; CI - confidence intervals for the mean. *present $P < 0.05$.

Static Frictional Force [N] (Tukey HSD)						
Bracket	**(I) Wire size [inch]**	**(J) Wire size [inch]**	**Mean Difference (I-J)**	**Std. Error**	***P***	**95% CI**
In-Ovation® C	0.016x0.022	0.018x0.025	-0.098*	0.008	<0.001	-0.118 to -0.078
		0.019x0.025	-0.114*	0.008	<0.001	-0.134 to -0.094
	0.018x0.025	0.016x0.022	0.098*	0.008	<0.001	0.078 to 0.118
		0.019x0.025	-0.016	0.008	0.141	-0.036 to 0.004
	0.019x0.025	0.016x0.022	0.114*	0.008	<0.001	0.094 to 0.134
		0.018x0.025	0.016	0.008	0.141	-0.004 to 0.036
Mini Sprint®	0.016x0.022	0.018x0.025	-0.078*	0.010	<0.001	-0.102 to -0.053
		0.019x0.025	-0.074*	0.010	<0.001	-0.099 to -0.050
	0.018x0.025	0.016x0.022	0.078*	0.010	<0.001	0.053 to 0.102
		0.019x0.025	0.003	0.010	0.938	-0.021 to 0.027
	0.019x0.025	0.016x0.022	0.074*	0.010	<0.001	0.050 to 0.099
		0.018x0.025	-0.003	0.010	0.938	-0.028 to 0.021
BioQuick®	0.016x0.022	0.018x0.025	-0.502*	0.023	<0.001	-0.555 to -0.448
		0.019x0.025	-0.801*	0.023	<0.001	-0.855 to -0.748
	0.018x0.025	0.016x0.022	0.502*	0.023	<0.001	0.448 to 0.555
		0.019x0.025	-0.299*	0.023	<0.001	-0.353 to -0.246
	0.019x0.025	0.016x0.022	0.801*	0.023	<0.001	0.748 to 0.855
		0.018x0.025	0.299*	0.023	<0.001	0.246 to 0.353

3.1.3.1.2. KINETIC FRICTION

The kinetic friction of each bracket with various wire dimensions is presented in Table 6. The exceptions are Mini Sprint® brackets with 0.018”x0.025” and 0.019”x0.025” wires ($P > 0.05$). Different from the static friction, the kinetic one of large size wires combined with In-Ovation® C presented significant difference ($P < 0.05$*).

Table 6: Results of two-way ANOVA combined with Tukey post hoc test, comparing kinetic frictional force in different wire size. Mean Difference (I-J) - The absolute difference between the mean values in two different groups; Std. Error - Standard Deviation Error; CI - confidence intervals for the mean. *present $P < 0.05$.

Kinetic Frictional Force [N] (Tukey HSD)						
Bracket	**(I) Wire size [inch]**	**(J) Wire size [inch]**	**Mean Difference (I-J)**	**Std. Error**	***P***	**95% CI**
In-Ovation® C	0.016x0.022	0.018x0.025	-0.110*	0.010	<0.001	-0.134 to -0.086
		0.019x0.025	-0.156*	0.010	<0.001	-0.181 to -0.132
	0.018x0.025	0.016x0.022	0.110*	0.010	<0.001	0.086 to 0.134
		0.019x0.025	-0.047*	0.010	<0.001	-0.071 to -0.022
	0.019x0.025	0.016x0.022	0.156*	0.010	<0.001	0.132 to 0.181
		0.018x0.025	0.047*	0.010	<0.001	0.022 to 0.071
Mini Sprint®	0.016x0.022	0.018x0.025	-0.079*	0.010	<0.001	-0.102 to -0.056
		0.019x0.025	-0.085*	0.010	<0.001	-0.108 to -0.062
	0.018x0.025	0.016x0.022	0.079*	0.010	<0.001	0.056 to 0.102
		0.019x0.025	-0.006	0.010	0.831	-0.028 to 0.017
	0.019x0.025	0.016x0.022	0.085*	0.010	<0.001	0.062 to 0.108
		0.018x0.025	0.006	0.010	0.831	-0.017 to 0.028
BioQuick®	0.016x0.022	0.018x0.025	-0.579*	0.026	<0.001	-0.642 to -0.517
		0.019x0.025	-0.909*	0.027	<0.001	-0.972 to -0.846
	0.018x0.025	0.016x0.022	0.579*	0.026	<0.001	0.517 to 0.642
		0.019x0.025	-0.329*	0.027	<0.001	-0.392 to -0.266
	0.019x0.025	0.016x0.022	0.909*	0.027	<0.001	0.846 to 0.972
		0.018x0.025	0.329*	0.027	<0.001	0.266 to 0.392

3.1.3.2. INFLUENCE OF ENVIRONMENTAL MEDIA

The two-way ANOVA combined with Tukey *post-hoc* test is used to evaluate the significant differences of frictional values between each environment and all other states (Tables 7 and 8).

3.1.3.2.1. STATIC FRICTION

The results of Table 7 show the static frictional values, which compare the friction parameters among each test condition. Table 7 indicates that static frictional force shows a highly significant difference ($P < 0.05$*) in comparison between the various environments. The exceptions are static friction of BioQuick® bracket in comparison between dry condition and water ($P > 0.05$) and Mini Sprint® bracket with whole human saliva and water ($P > 0.05$).

Table 7: Results of two-way ANOVA combined with Tukey *post hoc test*, comparing static frictional force in different environment. Mean Difference (I-J) - The absolute difference between the mean values in two different groups; Std. Error - Standard Deviation Error; CI - confidence intervals for the mean. *present $P < 0.05$.

Static Frictional Force [N] (Tukey HSD)						
Bracket	**(I) Environment**	**(J) Environment**	**Mean Difference (I-J)**	**Std. Error**	***P***	**95% CI**
In-Ovation® C	Artificial Saliva	Dry	0.178*	0.010	<0.001	0.153 to 0.204
		Whole human saliva	-0.114*	0.010	<0.001	-0.140 to -0.089
		Water	0.130*	0.010	<0.001	0.105 to 0.155
	Dry	Artificial Saliva	-0.178*	0.010	<0.001	-0.204 to -0.153
		Whole human saliva	-0.293*	0.010	<0.001	-0.318 to -0.267
		Water	-0.048*	0.010	<0.001	-0.073 to -0.023
	Whole human saliva	Artificial Saliva	0.114*	0.010	<0.001	0.089 to 0.140
		Dry	0.293*	0.010	<0.001	0.267 to 0.318
		Water	0.244*	0.010	<0.001	0.219 to 0.270
	Water	Artificial Saliva	-0.130*	0.010	<0.001	-0.155 to -0.105
		Dry	0.048*	0.010	<0.001	0.023 to 0.073
		Whole human saliva	-0.244*	0.010	<0.001	-0.270 to -0.219
Mini Sprint®	Artificial Saliva	Dry	0.272*	0.012	<0.001	0.241 to 0.302
		Whole human saliva	0.091*	0.012	<0.001	0.060 to 0.122
		Water	0.068*	0.012	<0.001	0.037 to 0.100
	Dry	Artificial Saliva	-0.272*	0.012	<0.001	-0.302 to -0.241
		Whole human saliva	-0.181*	0.012	<0.001	-0.211 to -0.151
		Water	-0.203*	0.012	<0.001	-0.234 to -0.173
	Whole human saliva	Artificial Saliva	-0.091*	0.012	<0.001	-0.122 to -0.060
		Dry	0.181*	0.012	<0.001	0.151 to 0.211
		Water	-0.023	0.012	0.239	-0.054 to 0.009
	Water	Artificial Saliva	-0.068*	0.012	<0.001	-0.100 to -0.037
		Dry	0.203*	0.012	<0.001	0.173 to 0.234
		Whole human saliva	0.023	0.012	0.239	-0.009 to 0.054
BioQuick®	Artificial Saliva	Dry	0.317*	0.027	<0.001	0.248 to 0.386
		Whole human saliva	0.154*	0.026	<0.001	0.087 to 0.221
		Water	0.341*	0.026	<0.001	0.274 to 0.408
	Dry	Artificial Saliva	-0.317*	0.027	<0.001	-0.386 to -0.248
		Whole human saliva	-0.163*	0.026	<0.001	-0.232 to -0.095
		Water	0.024	0.026	0.809	-0.045 to 0.092
	Whole human saliva	Artificial Saliva	-0.154*	0.026	<0.001	-0.221 to -0.087
		Dry	0.163*	0.026	<0.001	0.095 to 0.232
		Water	0.187*	0.026	<0.001	0.120 to 0.253
	Water	Artificial Saliva	-0.341*	0.026	<0.001	-0.408 to -0.274
		Dry	-0.024	0.026	0.809	-0.092 to 0.045
		Whole human saliva	-0.187*	0.026	<0.001	-0.253 to -0.120

3.1.3.2.2. KINETIC FRICTION

In the following subchapter, the kinetic frictional forces are compared pairwise among the four different environments (Table 8).

The kinetic friction also shows a highly significant differences ($P < 0.05$*) in each comparison of environment similar to static friction values in Table 7, with the exception of BioQuick® brackets in comparison between dry condition and water ($P > 0.05$).

Table 8: Results of two-way ANOVA combined with Tukey post hoc test, comparing Kinetic frictional force in different environment. Mean Difference (I-J) - The absolute difference between the mean values in two different groups; Std. Error - Standard Deviation Error; CI - confidence intervals for the mean. *present $P < 0.05$.

Kinetic Frictional Force [N] (Tukey HSD)						
Bracket	**(I) Environment**	**(J) Environment**	**Mean Difference (I-J)**	**Std. Error**	***P***	**95% CI**
In-Ovation® C	Artificial Saliva	Dry	0.225*	0.012	<0.001	0.194 to 0.257
		Whole human saliva	-0.119*	0.012	<0.001	-0.150 to -0.087
		Water	0.148*	0.012	<0.001	0.118 to 0.179
	Dry	Artificial Saliva	-0.225*	0.012	<0.001	-0.257 to -0.194
		Whole human saliva	-0.344*	0.012	<0.001	-0.375 to -0.313
		Water	-0.077*	0.012	<0.001	-0.108 to-0.047
	Whole human saliva	Artificial Saliva	0.119*	0.012	<0.001	0.087 to 0.150
		Dry	0.344*	0.012	<0.001	0.313 to 0.375
		Water	0.267*	0.012	<0.001	0.236 to 0.298
	Water	Artificial Saliva	-0.148*	0.012	<0.001	-0.179 to -0.118
		Dry	0.077*	0.012	<0.001	0.047 to 0.108
		Whole human saliva	-0.267*	0.012	<0.001	-0.298 to -0.236
Mini Sprint®	Artificial Saliva	Dry	0.270*	0.011	<0.001	0.241 to 0.299
		Whole human saliva	0.095*	0.011	<0.001	0.066 to 0.124
		Water	0.044*	0.011	<0.001	0.014 to 0.074
	Dry	Artificial Saliva	-0.270*	0.011	<0.001	-0.299 to -0.241
		Whole human saliva	-0.175*	0.011	<0.001	-0.204 to -0.147
		Water	-0.226*	0.011	<0.001	-0.255 to -0.196
	Whole human saliva	Artificial Saliva	-0.095*	0.011	<0.001	-0.124 to -0.066
		Dry	0.175*	0.011	<0.001	0.147 to 0.204
		Water	-0.050*	0.011	<0.001	-0.080 to -0.021
	Water	Artificial Saliva	-0.044*	0.011	<0.001	-0.074 to -0.014
		Dry	0.226*	0.011	<0.001	0.196 to 0.255
		Whole human saliva	0.050*	0.011	<0.001	0.021 to 0.080
BioQuick®	Artificial Saliva	Dry	0.428*	0.031	<0.001	0.347 to 0.509
		Whole human saliva	0.243*	0.030	<0.001	0.164 to 0.322
		Water	0.433*	0.030	<0.001	0.354 to 0.512
	Dry	Artificial Saliva	-0.428*	0.031	<0.001	-0.509 to -0.347
		Whole human saliva	-0.185*	0.031	<0.001	-0.266 to -0.104
		Water	0.005	0.031	0.998	-0.075 to 0.086
	Whole human saliva	Artificial Saliva	-0.243*	0.030	<0.001	-0.322 to -0.164
		Dry	0.185*	0.031	<0.001	0.104 to 0.266
		Water	0.190*	0.030	<0.001	0.112 to 0.269
	Water	Artificial Saliva	-0.433*	0.030	<0.001	-0.512 to -0.354
		Dry	-0.005	0.031	0.998	-0.086 to 0.075
		Whole human saliva	-0.190*	0.030	<0.001	-0.269 to -0.112

3.2. SIMULATION OF CLINICAL SITUATION

The data from the simulation of the clinical situation are presented graphically in order to compare the material characteristics of each bracket-wire combination (Figure 20 to 31). The mean frictional values and the corresponding descriptive parameters for each bracket with NiTi and stainless steel wires tested under artificial saliva and different normal forces are summarized in Tables 9 to 14.

3.2.1. STATIC FRICTION

It can be derived from Tables 9 to 11 for almost all bracket-wire combinations that the static frictional force increases if the normal force raises. This is visualized in the rise of the median of the box-plots of different bracket-wire combinations. When combined with 0.018”x0.025”, 0.019”x0.025” NiTi and stainless-steel wires, Damon™ 3MX and Mini Sprint® produced lower static frictional values than In-Ovation® C and BioQuick® brackets. In other words, the static friction of active self-ligating brackets is higher than that of passive self-ligating and conventional brackets. Moreover, as assessed from active self-ligating brackets, the metal active self-ligating brackets’ friction is much higher than that of ceramic ones. However, when combined with 0.016”x0.022” archwires, the difference between the evaluated brackets is not so obvious (Figure 20 to 25). Additionally, for all bracket-wires combinations, the static friction produced by the NiTi wire was lower than that of stainless-steel wire.

Table 9: Descriptive statistics for static frictional force of different bracket-wire combined with 0.016”x0.022” NiTi and stainless steel wires at various normal forces. N-count; SD-Standard deviation; Min-Minimum; Max-Maximum; CI-confidence interval for the mean.

		Static Frictional Force [N]						
Normal Force [N]	**Archwire Material**	**Bracket**	**N**	**Mean (SD)**	**Min**	**Max**	**Median**	**95% CI**
1	NiTi	Damon™ 3MX	5	0.195 (0.028)	0.151	0.221	0.192	0.218 to 0.221
		In-Ovation® C	5	0.174 (0.033)	0.148	0.225	0.156	0.189 to 0.225
		Mini Sprint®	5	0.233 (0.052)	0.184	0.303	0.210	0.271 to 0.303
		BioQuick®	5	0.152 (0.012)	0.133	0.163	0.155	0.162 to 0.163
	Stainless steel	Damon™ 3MX	5	0.286 (0.041)	0.254	0.357	0.272	0.282 to 0.357
		In-Ovation® C	5	0.354 (0.022)	0.319	0.377	0.358	0.366 to 0.377
		Mini Sprint®	5	0.319 (0.052)	0.256	0.381	0.338	0.345 to 0.381
		BioQuick®	5	0.441 (0.046)	0.371	0.482	0.466	0.468 to 0.482
1.5	NiTi	Damon™ 3MX	5	0.324 (0.091)	0.230	0.440	0.313	0.348 to 0.440
		In-Ovation® C	5	0.242 (0.037)	0.190	0.294	0.242	0.249 to 0.294
		Mini Sprint®	4	0.381 (0.067)	0.292	0.443	0.395	0.422 to 0.443
		BioQuick®	5	0.228 (0.028)	0.194	0.264	0.233	0.242 to 0.264
	Stainless steel	Damon™ 3MX	5	0.481 (0.050)	0.426	0.522	0.511	0.521 to 0.522
		In-Ovation® C	5	0.589 (0.033)	0.551	0.627	0.574	0.621 to 0.627
		Mini Sprint®	5	0.617 (0.017)	0.589	0.631	0.622	0.626 to 0.631
		BioQuick®	5	0.655 (0.019)	0.639	0.679	0.644	0.671 to 0.679
2	NiTi	Damon™ 3MX	5	0.300 (0.044)	0.250	0.349	0.296	0.340 to 0.349
		In-Ovation® C	5	0.288 (0.041)	0.241	0.334	0.307	0.312 to 0.334
		Mini Sprint®	5	0.428 (0.075)	0.311	0.497	0.450	0.482 to 0.497
		BioQuick®	5	0.336 (0.047)	0.275	0.384	0.320	0.384 to 0.384
	Stainless steel	Damon™ 3MX	5	0.792 (0.150)	0.548	0.909	0.862	0.892 to 0.909
		In-Ovation® C	5	0.684 (0.032)	0.642	0.716	0.697	0.704 to 0.716
		Mini Sprint®	5	0.845 (0.013)	0.832	0.864	0.845	0.849 to 0.864
		BioQuick®	5	0.840 (0.040)	0.803	0.899	0.829	0.858 to 0.899
2.5	NiTi	Damon™ 3MX	5	0.457 (0.057)	0.413	0.540	0.438	0.444 to 0.540
		In-Ovation® C	5	0.518 (0.136)	0.371	0.689	0.461	0.632 to 0.689
		Mini Sprint®	5	0.443 (0.062)	0.373	0.519	0.415	0.496 to 0.519
		BioQuick®	5	0.651 (0.141)	0.502	0.825	0.682	0.736 to 0.825
	Stainless steel	Damon™ 3MX	5	0.701 (0.141)	0.522	0.865	0.703	0.808 to 0.865
		In-Ovation® C	5	0.802 (0.059)	0.708	0.869	0.804	0.825 to 0.869
		Mini Sprint®	5	0.913 (0.034)	0.858	0.942	0.929	0.931 to 0.942
		BioQuick®	5	0.962 (0.022)	0.929	0.990	0.965	0.970 to 0.990

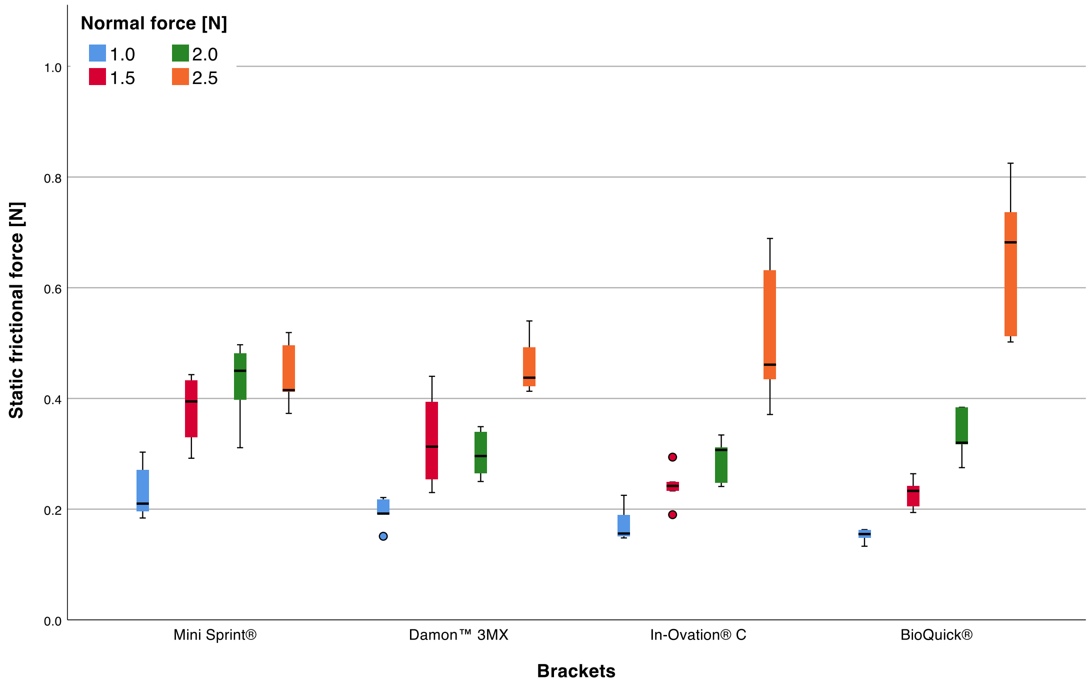

Figure 20: Box-Whisker plots of the static frictional force of different bracket-wire combined with 0.016”x0.022” NiTi wires.

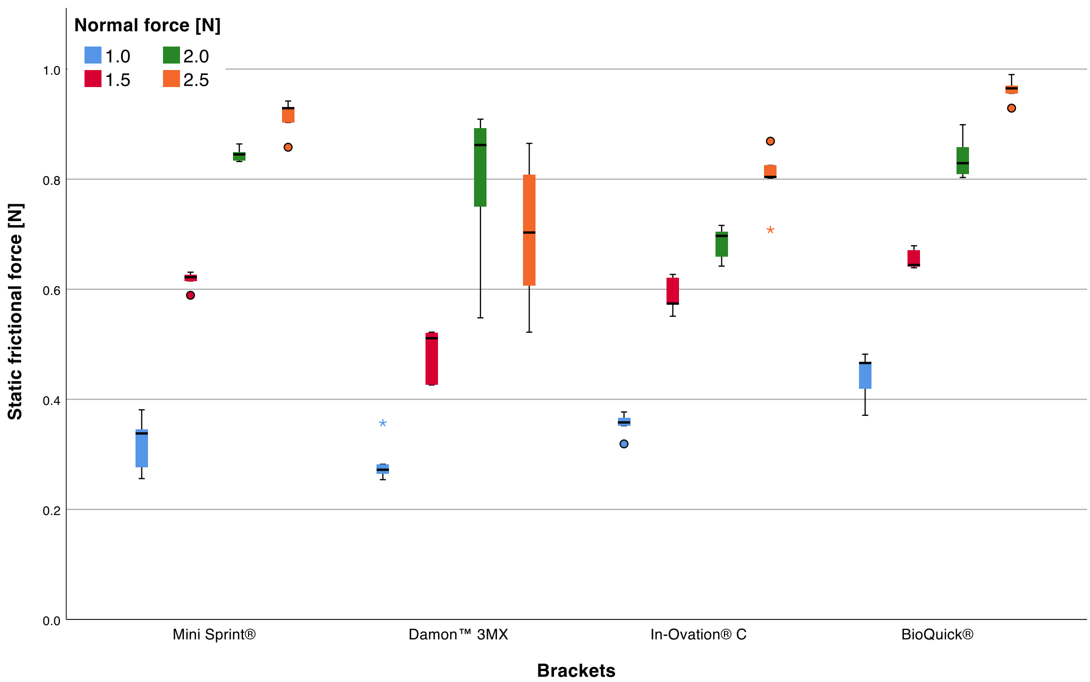

Figure 21: Box-Whisker plots of the static frictional force of different bracket-wire combined with 0.016”x0.022” stainless steel wires.

Table 10: Descriptive statistics for static frictional force of different bracket-wire combined with 0.018"x0.025" NiTi and stainless steel wires at various normal forces. N-count; SD-Standard deviation; Min-Minimum; Max-Maximum; CI-confidence interval for the mean.

Static Frictional Force [N]

Normal Force [N]	**Archwire Material**	**Bracket**	**N**	**Mean (SD)**	**Min**	**Max**	**Median**	**95% CI**
1	NiTi	Damon™ 3MX	5	0.213 (0.053)	0.141	0.267	0.223	0.223 to 0.267
		In-Ovation® C	5	0.382 (0.023)	0.356	0.418	0.377	0.386 to 0.418
		Mini Sprint®	5	0.296 (0.008)	0.284	0.303	0.297	0.302 to 0.303
		BioQuick®	5	0.500 (0.075)	0.418	0.618	0.473	0.520 to 0.618
	Stainless steel	Damon™ 3MX	5	0.243 (0.036)	0.215	0.301	0.223	0.254 to 0.301
		In-Ovation® C	5	0.565 (0.029)	0.532	0.611	0.561	0.572 to 0.611
		Mini Sprint®	5	0.432 (0.005)	0.424	0.436	0.433	0.435 to 0.436
		BioQuick®	5	1.078 (0.043)	1.033	1.131	1.088	1.103 to 1.131
1.5	NiTi	Damon™ 3MX	5	0.332 (0.055)	0.286	0.424	0.311	0.336 to 0.424
		In-Ovation® C	5	0.505 (0.030)	0.480	0.546	0.489	0.528 to 0.546
		Mini Sprint®	5	0.344 (0.057)	0.275	0.413	0.342	0.386 to 0.413
		BioQuick®	5	0.929 (0.087)	0.785	0.991	0.971	0.990 to 0.991
	Stainless steel	Damon™ 3MX	5	0.454 (0.095)	0.336	0.559	0.488	0.514 to 0.559
		In-Ovation® C	5	0.704 (0.021)	0.692	0.742	0.695	0.699 to 0.742
		Mini Sprint®	5	0.622 (0.029)	0.590	0.662	0.612	0.641 to 0.662
		BioQuick®	5	1.176 (0.124)	0.982	1.292	1.222	1.254 to 1.292
2	NiTi	Damon™ 3MX	5	0.422 (0.096)	0.319	0.565	0.420	0.451 to 0.565
		In-Ovation® C	5	0.551 (0.043)	0.516	0.621	0.542	0.560 to 0.621
		Mini Sprint®	5	0.379 (0.051)	0.311	0.432	0.403	0.410 to 0.432
		BioQuick®	4	0.884 (0.211)	0.683	1.156	0.849	0.942 to 1.156
	Stainless steel	Damon™ 3MX	5	0.649 (0.108)	0.499	0.782	0.621	0.721 to 0.782
		In-Ovation® C	5	0.894 (0.032)	0.851	0.936	0.890	0.912 to 0.936
		Mini Sprint®	5	0.808 (0.085)	0.663	0.878	0.824	0.860 to 0.878
		BioQuick®	5	1.362 (0.223)	1.110	1.674	1.368	1.462 to 1.674
2.5	NiTi	Damon™ 3MX	4	0.537 (0.113)	0.374	0.657	0.556	0.617 to 0.657
		In-Ovation® C	4	0.800 (0.036)	0.751	0.838	0.806	0.808 to 0.838
		Mini Sprint®	5	0.496 (0.118)	0.374	0.657	0.455	0.580 to 0.657
		BioQuick®	5	1.186 (0.201)	0.957	1.438	1.200	1.319 to 1.438
	Stainless steel	Damon™ 3MX	5	0.960 (0.086)	0.862	1.044	1.011	1.012 to 1.044
		In-Ovation® C	5	1.031 (0.013)	1.014	1.047	1.028	1.041 to 1.047
		Mini Sprint®	5	1.021 (0.034)	0.978	1.064	1.012	1.045 to 1.064
		BioQuick®	5	1.853 (0.161)	1.686	2.029	1.831	2.008 to 2.029

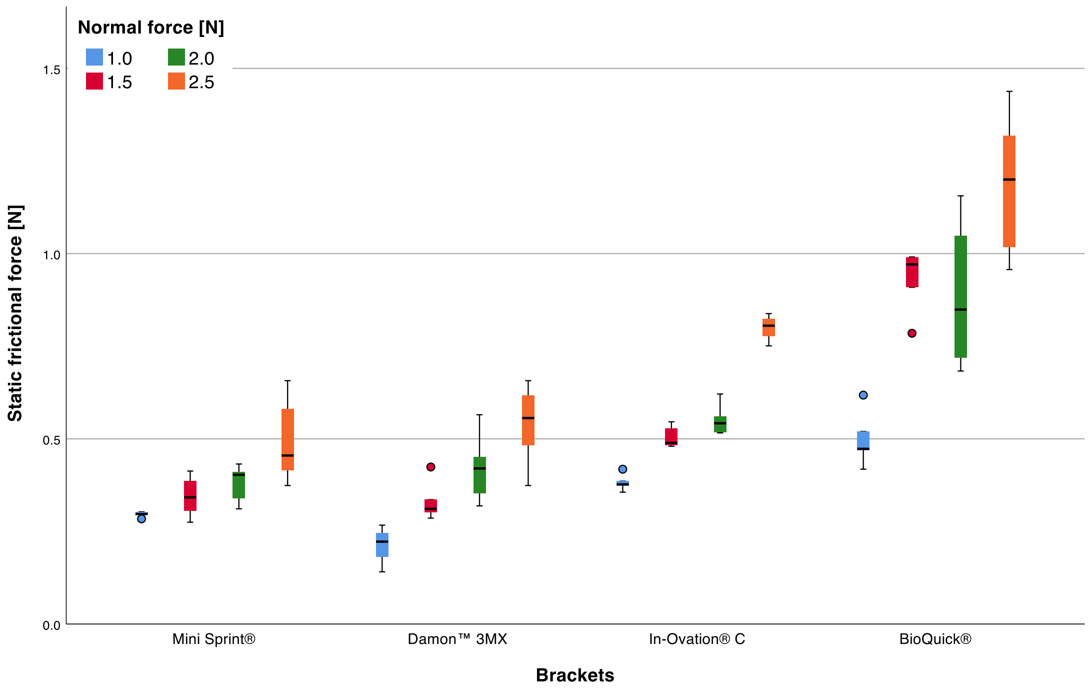

Figure 22: Box-Whisker plots of the static frictional force of different bracket-wire combined with 0.018"x0.025" NiTi wires.

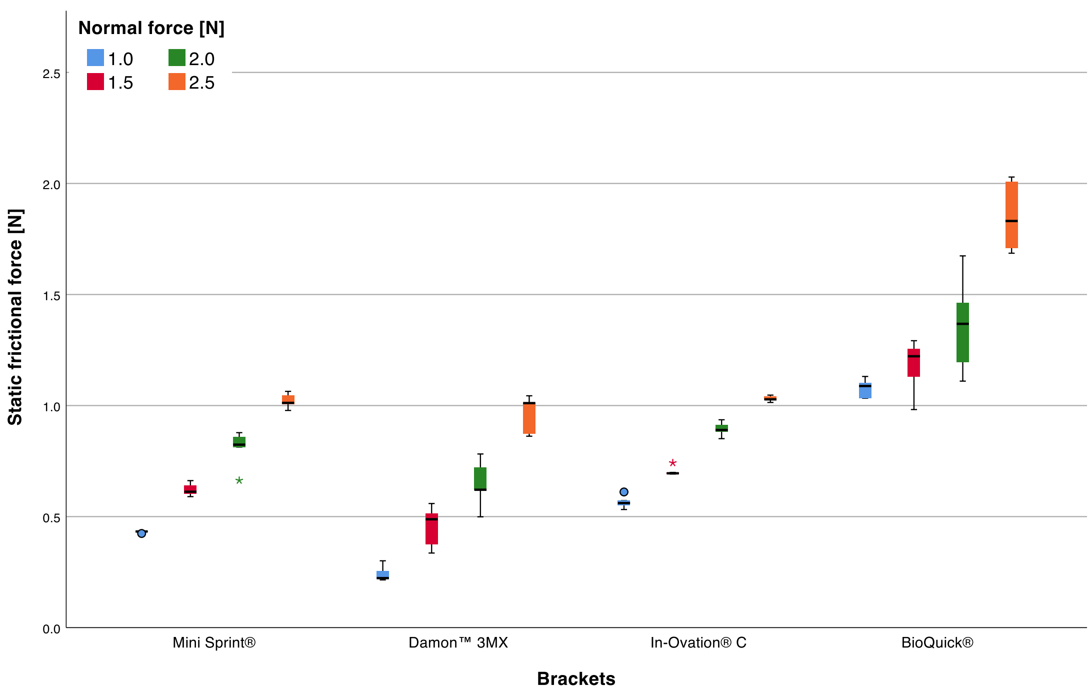

Figure 23: Box-Whisker plots of the static frictional force of different bracket-wire combined with 0.018"x0.025" stainless steel wires.

Table 11: Descriptive statistics for static frictional force of different bracket-wire combined with 0.019"x0.025" NiTi and stainless steel wires at various normal forces. N-count; SD-Standard deviation; Min-Minimum; Max-Maximum; CI-confidence interval for the mean.

		Static Frictional Force [N]						
Normal Force [N]	**Archwire Material**	**Bracket**	**N**	**Mean (SD)**	**Min**	**Max**	**Median**	**95% CI**
1	NiTi	Damon™ 3MX	5	0.176 (0.020)	0.155	0.206	0.168	0.188 to 0.206
		In-Ovation® C	5	0.398 (0.044)	0.338	0.458	0.389	0.417 to 0.458
		Mini Sprint®	4	0.174 (0.054)	0.133	0.248	0.157	0.181 to 0.248
		BioQuick®	5	0.832 (0.099)	0.671	0.914	0.832	0.912 to 0.914
	Stainless steel	Damon™ 3MX	5	0.229 (0.069)	0.153	0.326	0.200	0.274 to 0.326
		In-Ovation® C	5	0.360 (0.069)	0.275	0.455	0.367	0.386 to 0.455
		Mini Sprint®	5	0.312 (0.034)	0.273	0.360	0.297	0.333 to 0.360
		BioQuick®	5	1.160 (0.081)	1.072	1.246	1.183	1.221 to 1.246
1.5	NiTi	Damon™ 3MX	5	0.250 (0.021)	0.231	0.282	0.244	0.256 to 0.282
		In-Ovation® C	5	0.475 (0.053)	0.408	0.530	0.461	0.528 to 0.530
		Mini Sprint®	5	0.315 (0.035)	0.282	0.360	0.299	0.344 to 0.360
		BioQuick®	5	0.924 (0.128)	0.770	1.033	0.989	1.026 to 1.033
	Stainless steel	Damon™ 3MX	5	0.509 (0.064)	0.413	0.563	0.530	0.563 to 0.563
		In-Ovation® C	5	0.686 (0.178)	0.471	0.896	0.732	0.794 to 0.896
		Mini Sprint®	5	0.499 (0.052)	0.442	0.555	0.505	0.543 to 0.555
		BioQuick®	5	1.488 (0.024)	1.463	1.523	1.477	1.502 to 1.523
2	NiTi	Damon™ 3MX	5	0.354 (0.108)	0.267	0.524	0.291	0.397 to 0.524
		In-Ovation® C	5	0.521 (0.064)	0.454	0.587	0.513	0.586 to 0.587
		Mini Sprint®	4	0.395 (0.055)	0.346	0.471	0.382	0.400 to 0.471
		BioQuick®	5	0.714 (0.041)	0.668	0.781	0.712	0.712 to 0.781
	Stainless steel	Damon™ 3MX	5	0.594 (0.154)	0.427	0.811	0.583	0.670 to 0.811
		In-Ovation® C	5	1.212 (0.046)	1.154	1.253	1.235	1.248 to 1.253
		Mini Sprint®	5	0.713 (0.018)	0.694	0.739	0.715	0.717 to 0.739
		BioQuick®	5	2.400 (0.056)	2.325	2.470	2.407	2.431 to 2.470
2.5	NiTi	Damon™ 3MX	4	0.587 (0.182)	0.388	0.784	0.566	0.761 to 0.784
		In-Ovation® C	4	0.756 (0.060)	0.676	0.815	0.766	0.786 to 0.815
		Mini Sprint®	4	0.395 (0.055)	0.346	0.471	0.382	0.400 to 0.471
		BioQuick®	5	1.025 (0.072)	0.947	1.095	1.039	1.091 to 1.095
	Stainless steel	Damon™ 3MX	5	0.814 (0.172)	0.596	1.032	0.862	0.890 to 1.032
		In-Ovation® C	5	1.156 (0.237)	0.819	1.423	1.113	1.338 to 1.423
		Mini Sprint®	5	0.713 (0.018)	0.694	0.739	0.715	0.717 to 0.739
		BioQuick®	5	2.654 (0.064)	2.589	2.757	2.635	2.665 to 2.757

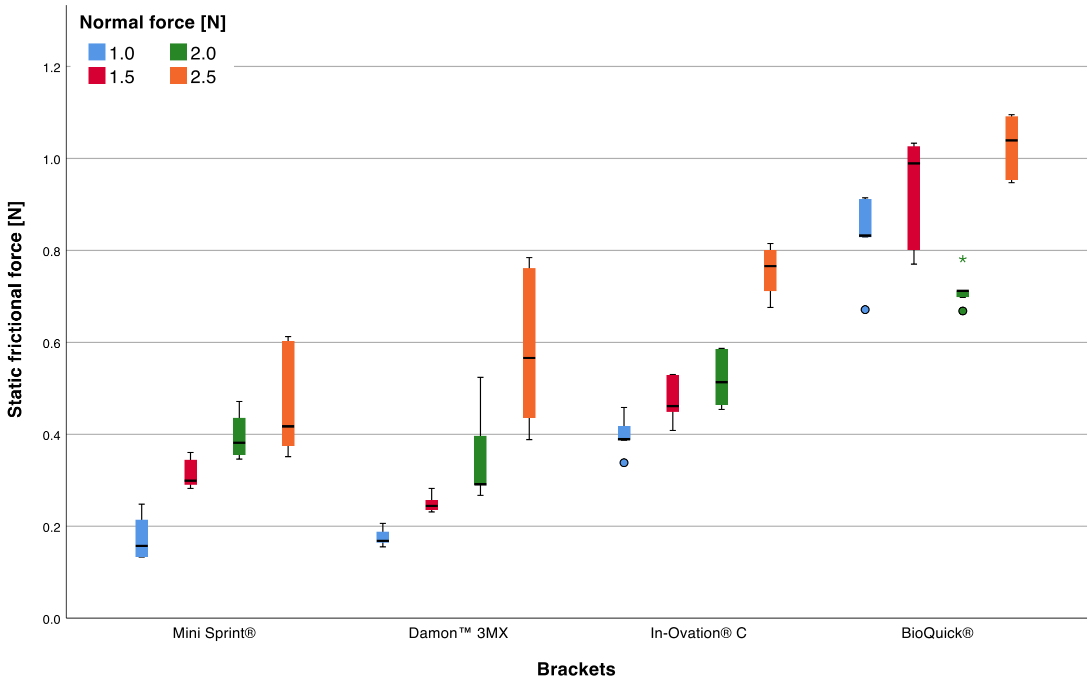

Figure 24: Box-Whisker plots of the static frictional force of different bracket-wire combined with 0.019”x0.025” NiTi wires.

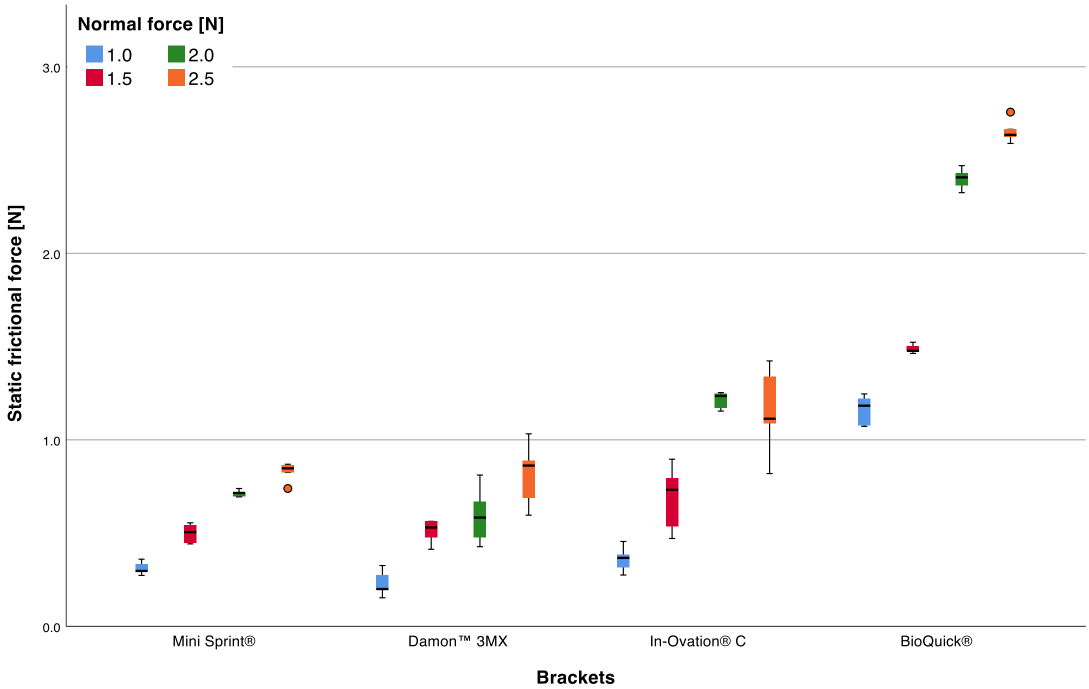

Figure 25: Box-Whisker plots of the static frictional force of different bracket-wire combined with 0.019”x0.025” stainless steel wires.

3.2.2. KINETIC FRICTION

The kinetic frictional forces of each bracket-wire combination were similar to the static ones, which increased as the normal force raised. As viewing from the Tables 12 to 14, the kinetic friction produced by stainless steel wires are higher than the ones of NiTi wires. When combined with large dimension archwires, the kinetic friction of active self-ligating brackets was higher than that of passive self-ligating and conventional brackets. The metal active self-ligating brackets also performed higher kinetic friction than that of ceramic ones, which consisted with the results of static frictions. In addition, almost no differences between the tested brackets were visible when coupled with 0.016”x0.022” archwires (Figure 26 to 31).

Table 12: Descriptive statistics for kinetic frictional force of different bracket-wire combined with 0.016"x0.022" NiTi and stainless steel wires at various normal forces. N-count; SD-Standard deviation; Min-Minimum; Max-Maximum; CI-confidence interval for the mean.

Kinetic Frictional Force [N]								
Normal Force [N]	**Archwire Material**	**Bracket**	**N**	**Mean (SD)**	**Min**	**Max**	**Median**	**95% CI**
1	NiTi	Damon™ 3MX	5	0.199 (0.020)	0.164	0.217	0.207	0.207 to 0.217
		In-Ovation® C	5	0.142 (0.025)	0.118	0.174	0.132	0.162 to 0.174
		Mini Sprint®	5	0.183 (0.035)	0.149	0.228	0.178	0.209 to 0.228
		BioQuick®	5	0.148 (0.020)	0.124	0.175	0.151	0.158 to 0.175
	Stainless steel	Damon™ 3MX	5	0.296 (0.035)	0.252	0.348	0.290	0.304 to 0.348
		In-Ovation® C	5	0.358 (0.029)	0.327	0.389	0.357	0.384 to 0.389
		Mini Sprint®	5	0.359 (0.043)	0.310	0.401	0.365	0.401 to 0.401
		BioQuick®	5	0.447 (0.045)	0.384	0.492	0.471	0.472 to 0.492
1.5	NiTi	Damon™ 3MX	5	0.315 (0.088)	0.229	0.436	0.297	0.312 to 0.436
		In-Ovation® C	5	0.230 (0.039)	0.164	0.264	0.244	0.247 to 0.264
		Mini Sprint®	5	0.370 (0.082)	0.272	0.469	0.370	0.389 to 0.469
		BioQuick®	5	0.207 (0.027)	0.179	0.235	0.210	0.232 to 0.235
	Stainless steel	Damon™ 3MX	5	0.500 (0.035)	0.458	0.538	0.501	0.530 to 0.538
		In-Ovation® C	5	0.625 (0.029)	0.583	0.655	0.627	0.648 to 0.655
		Mini Sprint®	5	0.578 (0.019)	0.556	0.594	0.587	0.593 to 0.594
		BioQuick®	5	0.753 (0.054)	0.669	0.816	0.761	0.778 to 0.816
2	NiTi	Damon™ 3MX	5	0.333 (0.060)	0.275	0.426	0.330	0.350 to 0.426
		In-Ovation® C	5	0.276 (0.062)	0.179	0.335	0.288	0.320 to 0.335
		Mini Sprint®	5	0.476 (0.088)	0.356	0.596	0.479	0.508 to 0.596
		BioQuick®	5	0.342 (0.042)	0.306	0.405	0.326	0.361 to 0.405
	Stainless steel	Damon™ 3MX	5	0.806 (0.123)	0.591	0.889	0.861	0.875 to 0.889
		In-Ovation® C	5	0.726 (0.023)	0.705	0.765	0.719	0.723 to 0.765
		Mini Sprint®	5	0.790 (0.018)	0.770	0.813	0.785	0.805 to 0.813
		BioQuick®	5	0.818 (0.015)	0.801	0.835	0.821	0.828 to 0.835
2.5	NiTi	Damon™ 3MX	5	0.439 (0.092)	0.368	0.563	0.413	0.454 to 0.563
		In-Ovation® C	5	0.591 (0.158)	0.373	0.765	0.580	0.718 to 0.765
		Mini Sprint®	5	0.505 (0.089)	0.394	0.622	0.499	0.557 to 0.622
		BioQuick®	5	0.616 (0.118)	0.451	0.734	0.669	0.689 to 0.734
	Stainless steel	Damon™ 3MX	5	0.715 (0.108)	0.570	0.831	0.724	0.802 to 0.831
		In-Ovation® C	5	1.084 (0.239)	0.730	1.352	1.088	1.243 to 1.352
		Mini Sprint®	5	0.782 (0.045)	0.704	0.818	0.794	0.805 to 0.818
		BioQuick®	5	0.960 (0.014)	0.940	0.975	0.964	0.969 to 0.975

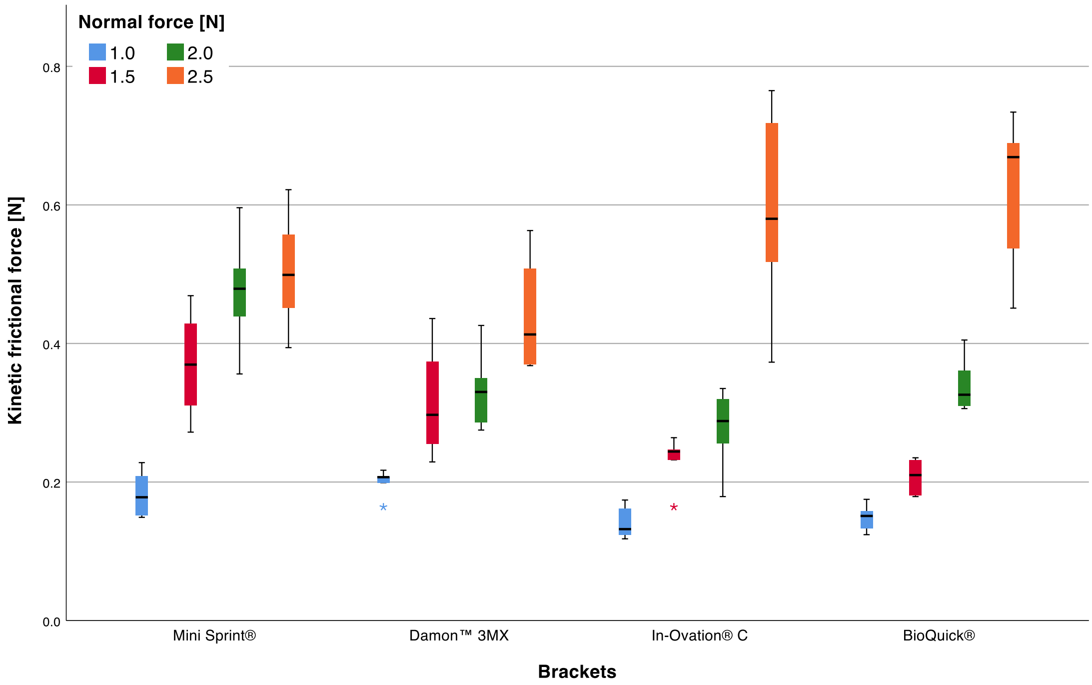

Figure 26: Box-Whisker plots of the kinetic frictional force of different bracket-wire combined with 0.016”x0.022” NiTi wires.

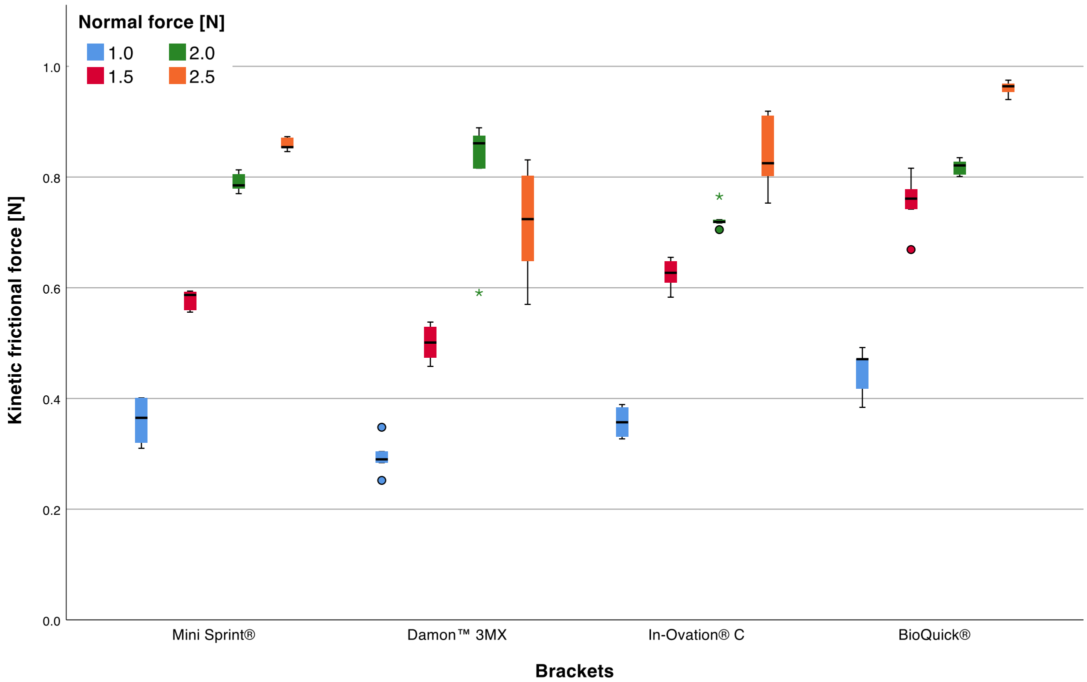

Figure 27: Box-Whisker plots of the kinetic frictional force of different bracket-wire combined with 0.016”x0.022” Stainless steel wires.

Table 13: Descriptive statistics for kinetic frictional force of different bracket-wire combined with 0.018"x0.025" NiTi and stainless steel wires at various normal forces. N-count; SD-Standard deviation; Min-Minimum; Max-Maximum; CI-confidence interval for the mean.

Kinetic Frictional Force [N]								
Normal Force [N]	**Archwire Material**	**Bracket**	**N**	**Mean (SD)**	**Min**	**Max**	**Median**	**95% CI**
1	NiTi	Damon™ 3MX	5	0.212 (0.035)	0.161	0.239	0.225	0.225 to 0.239
		In-Ovation® C	5	0.367 (0.021)	0.339	0.396	0.364	0.375 to 0.396
		Mini Sprint®	5	0.300 (0.019)	0.278	0.325	0.292	0.316 to 0.325
		BioQuick®	5	0.616 (0.113)	0.468	0.764	0.623	0.675 to 0.764
	Stainless steel	Damon™ 3MX	5	0.222 (0.026)	0.198	0.252	0.213	0.247 to 0.252
		In-Ovation® C	5	0.592 (0.020)	0.565	0.621	0.594	0.597 to 0.621
		Mini Sprint®	5	0.423 (0.012)	0.409	0.435	0.421	0.435 to 0.435
		BioQuick®	5	1.228 (0.019)	1.199	1.252	1.232	1.233 to 1.252
1.5	NiTi	Damon™ 3MX	5	0.333 (0.049)	0.288	0.413	0.313	0.345 to 0.413
		In-Ovation® C	5	0.484 (0.039)	0.443	0.526	0.469	0.524 to 0.526
		Mini Sprint®	5	0.340 (0.064)	0.264	0.424	0.354	0.369 to 0.424
		BioQuick®	5	1.061 (0.051)	0.996	1.114	1.065	1.105 to 1.114
	Stainless steel	Damon™ 3MX	5	0.484 (0.108)	0.344	0.620	0.500	0.542 to 0.620
		In-Ovation® C	5	0.774 (0.013)	0.755	0.787	0.777	0.785 to 0.787
		Mini Sprint®	5	0.616 (0.022)	0.592	0.650	0.609	0.622 to 0.650
		BioQuick®	5	1.309 (0.146)	1.114	1.434	1.372	1.431 to 1.434
2	NiTi	Damon™ 3MX	5	0.404 (0.061)	0.351	0.497	0.392	0.427 to 0.497
		In-Ovation® C	5	0.583 (0.047)	0.515	0.637	0.596	0.607 to 0.637
		Mini Sprint®	5	0.386 (0.049)	0.327	0.439	0.391	0.426 to 0.439
		BioQuick®	4	0.959 (0.269)	0.685	1.288	0.932	1.060 to 1.288
	Stainless steel	Damon™ 3MX	5	0.661 (0.123)	0.480	0.797	0.682	0.737 to 0.797
		In-Ovation® C	5	0.901 (0.033)	0.865	0.946	0.901	0.919 to 0.946
		Mini Sprint®	5	0.768 (0.055)	0.671	0.805	0.786	0.794 to 0.805
		BioQuick®	5	1.527 (0.296)	1.109	1.864	1.614	1.688 to 1.864
2.5	NiTi	Damon™ 3MX	4	0.511 (0.102)	0.384	0.619	0.493	0.609 to 0.619
		In-Ovation® C	4	0.852 (0.031)	0.819	0.886	0.852	0.870 to 0.886
		Mini Sprint®	4	0.536 (0.118)	0.416	0.673	0.488	0.652 to 0.673
		BioQuick®	5	1.213 (0.203)	0.974	1.480	1.201	1.339 to 1.480
	Stainless steel	Damon™ 3MX	5	0.956 (0.066)	0.864	1.039	0.965	0.985 to 1.039
		In-Ovation® C	5	0.989 (0.029)	0.967	1.029	0.971	1.010 to 1.029
		Mini Sprint®	5	0.956 (0.020)	0.935	0.979	0.948	0.976 to 0.979
		BioQuick®	5	1.913 (0.070)	1.845	2.022	1.883	1.940 to 2.022

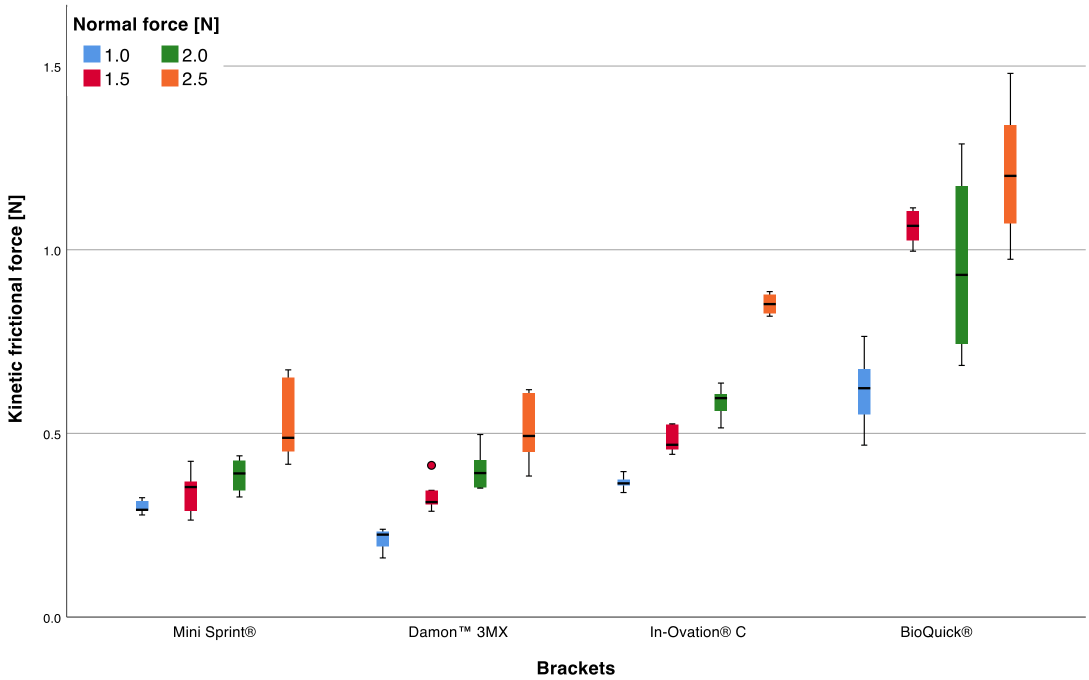

Figure 28: Box-Whisker plots of the kinetic frictional force of different bracket-wire combined with 0.018"x0.025" NiTi wires.

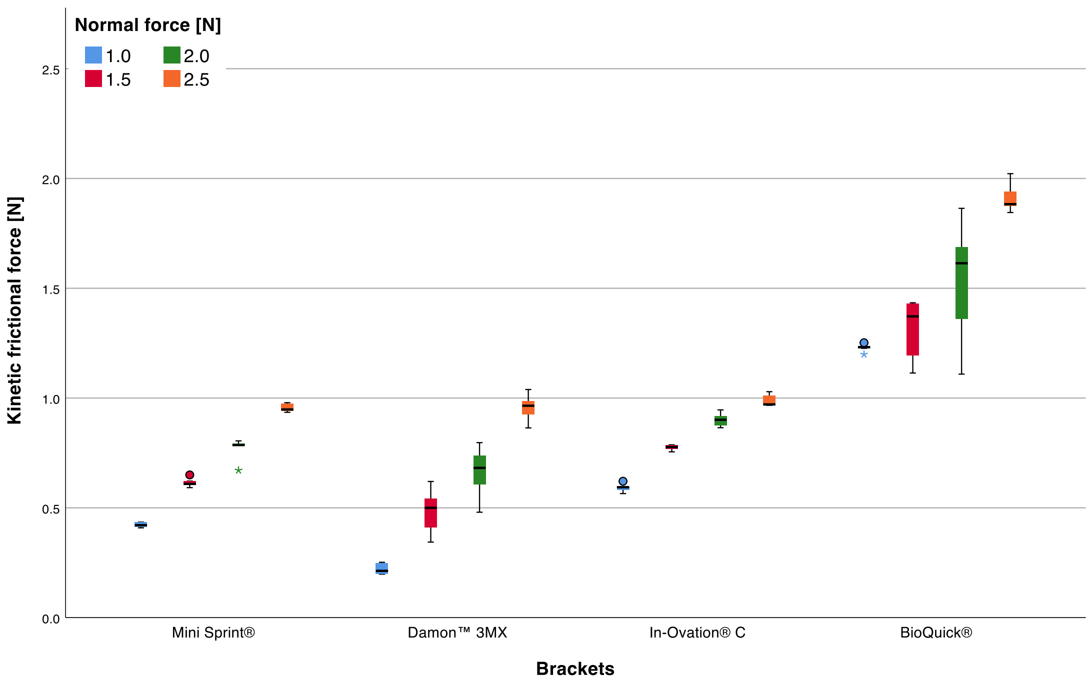

Figure 29: Box-Whisker plots of the kinetic frictional force of different bracket-wire combined with 0.018"x0.025" stainless steel wires.

Table 14: Descriptive statistics for kinetic frictional force of different bracket-wire combined with 0.019"x0.025" NiTi and stainless steel wires at various normal forces. N-count; SD-Standard deviation; Min-Minimum; Max-Maximum; CI-confidence interval for the mean.

Kinetic Frictional Force [N]								
Normal Force [N]	**Archwire Material**	**Bracket**	**N**	**Mean (SD)**	**Min**	**Max**	**Median**	**95% CI**
1	NiTi	Damon™ 3MX	5	0.179 (0.015)	0.164	0.205	0.177	0.179 to 0.205
		In-Ovation® C	5	0.356 (0.030)	0.306	0.379	0.361	0.377 to 0.379
		Mini Sprint®	5	0.195 (0.054)	0.148	0.269	0.181	0.199 to 0.269
		BioQuick®	5	0.786 (0.105)	0.606	0.878	0.811	0.832 to 0.878
	Stainless steel	Damon™ 3MX	5	0.223 (0.065)	0.152	0.317	0.208	0.256 to 0.317
		In-Ovation® C	5	0.435 (0.106)	0.279	0.559	0.448	0.495 to 0.559
		Mini Sprint®	5	0.272 (0.022)	0.238	0.294	0.274	0.288 to 0.294
		BioQuick®	5	1.174 (0.078)	1.061	1.265	1.188	1.217 to 1.265
1.5	NiTi	Damon™ 3MX	5	0.256 (0.026)	0.235	0.293	0.244	0.275 to 0.293
		In-Ovation® C	5	0.463 (0.069)	0.373	0.551	0.451	0.507 to 0.551
		Mini Sprint®	5	0.337 (0.030)	0.300	0.370	0.326	0.365 to 0.370
		BioQuick®	5	0.914 (0.106)	0.792	1.010	0.965	0.997 to 1.010
	Stainless steel	Damon™ 3MX	5	0.483 (0.073)	0.371	0.549	0.477	0.549 to 0.549
		In-Ovation® C	5	0.805 (0.262)	0.475	1.108	0.866	0.974 to 1.108
		Mini Sprint®	5	0.484 (0.033)	0.439	0.510	0.507	0.508 to 0.510
		BioQuick®	5	1.503 (0.018)	1.476	1.526	1.503	1.511 to 1.526
2	NiTi	Damon™ 3MX	5	0.357 (0.104)	0.265	0.517	0.323	0.400 to 0.517
		In-Ovation® C	5	0.550 (0.111)	0.426	0.694	0.529	0.630 to 0.694
		Mini Sprint®	5	0.410 (0.074)	0.343	0.507	0.396	0.428 to 0.507
		BioQuick®	5	0.713 (0.053)	0.667	0.798	0.691	0.730 to 0.798
	Stainless steel	Damon™ 3MX	5	0.645 (0.182)	0.460	0.866	0.677	0.764 to 0.866
		In-Ovation® C	5	1.220 (0.018)	1.189	1.232	1.230	1.231 to 1.232
		Mini Sprint®	5	0.677 (0.017)	0.661	0.704	0.671	0.681 to 0.704
		BioQuick®	5	2.700 (0.131)	2.471	2.792	2.759	2.759 to 2.792
2.5	NiTi	Damon™ 3MX	4	0.493 (0.094)	0.400	0.592	0.483	0.586 to 0.592
		In-Ovation® C	4	0.845 (0.073)	0.781	0.935	0.831	0.871 to 0.935
		Mini Sprint®	4	0.524 (0.135)	0.374	0.685	0.516	0.633 to 0.685
		BioQuick®	5	0.952 (0.053)	0.882	1.002	0.961	1.001 to 1.002
	Stainless steel	Damon™ 3MX	5	0.902 (0.161)	0.666	1.049	0.961	1.023 to 1.049
		In-Ovation® C	5	1.084 (0.239)	0.730	1.352	1.088	1.243 to 1.352
		Mini Sprint®	5	0.956 (0.020)	0.935	0.979	0.948	0.976 to 0.979
		BioQuick®	5	2.945 (0.045)	2.879	2.996	2.949	2.973 to 2.996

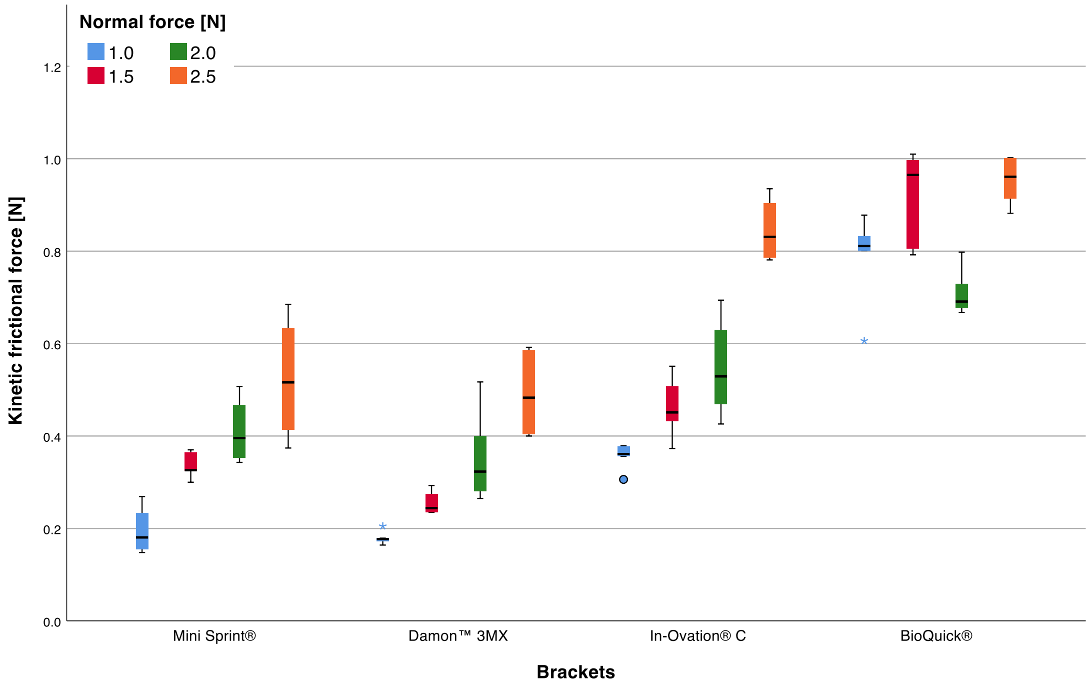

Figure 30: Box-Whisker plots of the kinetic frictional force of different bracket-wire combined with 0.019”x0.025” NiTi wires.

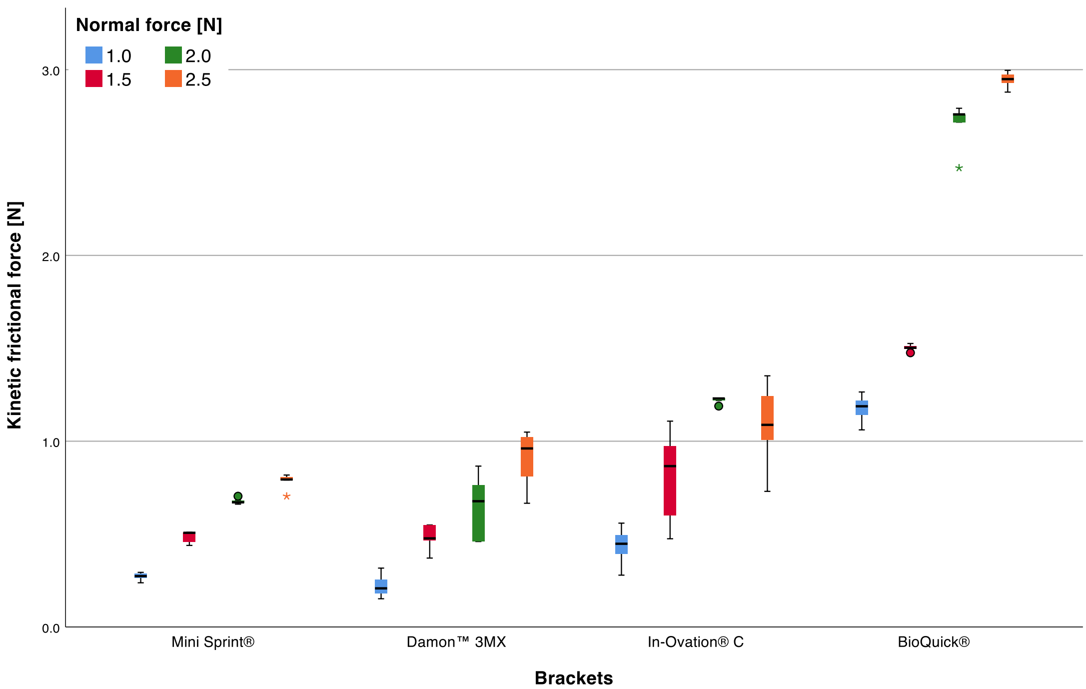

Figure 31: Box-Whisker plots of the kinetic frictional force of different bracket-wire combined with 0.019”x0.025” stainless steel wires.

3.2.3. INFERENTIAL STATISTICS

3.2.3.1. INFLUENCE OF DIFFERENT BRACKET-WIRE COMBINATIONS

The comparison of different bracket-wire combinations is analysed with ANOVA combined with Tukey *post-hoc* test and the findings are presented in Tables 15 to 20.

3.2.3.1.1. STATIC FRICTION

It can be observed from Table 15 that almost all static friction values show no significant difference when combined with 0.016”x0.022” NiTi wires ($P > 0.05$), with the exception of In-Ovation® C and Mini Sprint® ($P < 0.05$*). If the dimension of NiTi wire is increased, almost all brackets show highly significant differences ($P < 0.05$*), the exception is the comparison between Damon™ 3MX and Mini Sprint® brackets in combination with large size wires ($P > 0.05$) (Tables 16 and 17).

However, when combined with 0.016”x0.022” stainless steel wires, almost all brackets show highly significant differences ($P < 0.05$*), except the comparison between Damon™ 3MX and In-Ovation® C, Mini Sprint® and BioQuick® brackets ($P > 0.05$) (Table 15). If the stainless steel wire size increases, almost all brackets show highly significant differences when combined with large size wires, except for the comparison of Damon™ 3MX and Mini Sprint® brackets combined with 0.019”x0.025” ($P > 0.05$) (Tables 16 and 17).

Table 15: Results of two-way ANOVA combined with Tukey post hoc test, comparing static frictional force of different bracket combined with 0.016“x0.022” wires. Mean Difference (I-J) - The absolute difference between the mean values in two different groups; Std. Error - Standard Deviation Error; CI - confidence intervals for the mean. *present $P < 0.05$.

Static Frictional Force [N] (Tukey HSD)						
Material type	**(I) Brackets**	**(J) Brackets**	**Mean Difference (I-J)**	**Std. Error**	***P***	**95% CI**
NiTi	Damon™ 3MX	In-Ovation® C	0.006	0.022	0.994	-0.054 to 0.065
		Mini Sprint®	-0.060	0.023	0.052	-0.120 to 0.0005
		BioQuick®	-0.031	0.022	0.520	-0.090 to 0.028
	In-Ovation® C	Damon™ 3MX	-0.006	0.022	0.994	-0.065 to 0.054
		Mini Sprint®	-0.065*	0.022	0.023	-0.124 to -0.007
		BioQuick®	-0.036	0.022	0.348	-0.094 to 0.021
	Mini Sprint®	Damon™ 3MX	0.060	0.023	0.052	-0.0005 to 0.120
		In-Ovation® C	0.065*	0.022	0.023	0.007 to 0.124
		BioQuick®	0.029	0.022	0.568	-0.030 to 0.087
	BioQuick®	Damon™ 3MX	0.031	0.022	0.520	-0.028 to 0.090
		In-Ovation® C	0.036	0.022	0.348	-0.021 to 0.094
		Mini Sprint®	-0.029	0.022	0.568	-0.087 to 0.030
Stainless steel	Damon™ 3MX	In-Ovation® C	-0.042	0.020	0.149	-0.094 to 0.010
		Mini Sprint®	-0.108*	0.020	<0.001	-0.160 to -0.057
		BioQuick®	-0.159*	0.020	<0.001	-0.211 to -0.108
	In-Ovation® C	Damon™ 3MX	0.042	0.020	0.149	-0.010 to 0.094
		Mini Sprint®	-0.066*	0.020	0.007	-0.118 to -0.014
		BioQuick®	-0.117*	0.020	<0.001	-0.169 to -0.066
	Mini Sprint®	Damon™ 3MX	0.108*	0.020	<0.001	0.057 to 0.160
		In-Ovation® C	0.066*	0.020	0.007	0.014 to 0.118
		BioQuick®	-0.051	0.020	0.053	-0.103 to 0.001
	BioQuick®	Damon™ 3MX	0.159*	0.020	<0.001	0.108 to 0.211
		In-Ovation® C	0.117*	0.020	<0.001	0.066 to 0.169
		Mini Sprint®	0.051	0.020	0.053	-0.001 to 0.103

Table 16: Results of two-way ANOVA combined with Tukey post hoc test, comparing static frictional force of different bracket combined with 0.018”x0.025” wires. Mean Difference (I-J) - The absolute difference between the mean values in two different groups; Std. Error - Standard Deviation Error; CI - confidence intervals for the mean. *present *P* < 0.05.

Static Frictional Force [N] (Tukey HSD)						
Material type	**(I) Brackets**	**(J) Brackets**	**Mean Difference (I-J)**	**Std. Error**	***P***	**95% CI**
NiTi	Damon™ 3MX	In-Ovation® C	-0.162*	0.031	<0.001	-0.244 to -0.081
		Mini Sprint®	0.006	0.031	0.998	-0.075 to 0.086
		BioQuick®	-0.490*	0.031	<0.001	-0.571 to- 0.408
	In-Ovation® C	Damon™ 3MX	0.162*	0.031	<0.001	0.081 to 0.244
		Mini Sprint®	0.168*	0.031	<0.001	0.087 to 0.249
		BioQuick®	-0.327*	0.031	<0.001	-0.409 to -0.246
	Mini Sprint®	Damon™ 3MX	-0.006	0.031	0.998	-0.086 to 0.075
		In-Ovation® C	-0.168*	0.031	<0.001	-0.249 to -0.087
		BioQuick®	-0.495*	0.031	<0.001	-0.576 to -0.415
	BioQuick®	Damon™ 3MX	0.490*	0.031	<0.001	0.408 to 0.571
		In-Ovation® C	0.327*	0.031	<0.001	0.246 to 0.409
		Mini Sprint®	0.495*	0.031	<0.001	0.415 to 0.576
Stainless steel	Damon™ 3MX	In-Ovation® C	-0.222*	0.029	<0.001	-0.299 to -0.146
		Mini Sprint®	-0.144*	0.029	<0.001	-0.220 to -0.068
		BioQuick®	-0.791*	0.029	<0.001	-0.867 to -0.714
	In-Ovation® C	Damon™ 3MX	0.222*	0.029	<0.001	0.146 to 0.299
		Mini Sprint®	0.078*	0.029	0.042	0.002 to 0.155
		BioQuick®	-0.568*	0.029	<0.001	-0.645 to -0.492
	Mini Sprint®	Damon™ 3MX	0.144*	0.029	<0.001	0.068 to 0.220
		In-Ovation® C	-0.078*	0.029	0.042	-0.155 to -0.002
		BioQuick®	-0.647	0.029	<0.001	-0.723 to -0.570
	BioQuick®	Damon™ 3MX	0.791*	0.029	<0.001	0.714 to 0.867
		In-Ovation® C	0.568*	0.029	<0.001	0.492 to 0.645
		Mini Sprint®	0.647	0.029	<0.001	0.570 to 0.723

Table 17: Results of two-way ANOVA combined with Tukey post hoc test, comparing static frictional force of different bracket combined with 0.019”x0.025” wires. Mean Difference (I-J) - The absolute difference between the mean values in two different groups; Std. Error - Standard Deviation Error; CI - confidence intervals for the mean. *present $P < 0.05$.

Static Frictional Force [N] (Tukey HSD)						
Material type	**(I)Brackets**	**(J)Brackets**	**Mean Difference (I-J)**	**Std. Error**	***P***	**95% CI**
NiTi	Damon™ 3MX	In-Ovation® C	-0.184*	0.027	<0.001	-0.257 to -0.112
		Mini Sprint®	-0.003	0.028	0.999	-0.077 to 0.070
		BioQuick®	-0.532*	0.027	<0.001	-0.604 to -0.461
	In-Ovation® C	Damon™ 3MX	0.184*	0.027	<0.001	0.112 to 0.257
		Mini Sprint®	0.181*	0.028	<0.001	0.107 to 0.255
		BioQuick®	-0.348*	0.027	<0.001	-0.420 to -0.275
	Mini Sprint®	Damon™ 3MX	0.003	0.028	0.999	-0.070 to 0.077
		In-Ovation® C	-0.181*	0.028	<0.001	-0.255 to -0.107
		BioQuick®	-0.529*	0.028	<0.001	-0.602 to -0.455
	BioQuick®	Damon™ 3MX	0.532*	0.027	<0.001	0.461 to 0.604
		In-Ovation® C	0.348*	0.027	<0.001	0.275 to 0.420
		Mini Sprint®	0.529*	0.028	<0.001	0.455 to 0.602
Stainless steel	Damon™ 3MX	In-Ovation® C	-0.317*	0.033	<0.001	-0.405 to -0.229
		Mini Sprint®	-0.051	0.033	0.421	-0.139 to 0.037
		BioQuick®	-1.389*	0.033	<0.001	-1.477 to -1.301
	In-Ovation® C	Damon™ 3MX	0.317*	0.033	<0.001	0.229 to 0.405
		Mini Sprint®	0.266*	0.033	<0.001	0.178 to 0.354
		BioQuick®	-1.072*	0.033	<0.001	-1.160 to -0.984
	Mini Sprint®	Damon™ 3MX	0.051	0.033	0.421	-0.037 to 0.139
		In-Ovation® C	-0.266*	0.033	<0.001	-0.354 to -0.178
		BioQuick®	-1.337	0.033	<0.001	-1.426 to -1.249
	BioQuick®	Damon™ 3MX	1.389 *	0.033	<0.001	1.301 to 1.477
		In-Ovation® C	1.072 *	0.033	<0.001	0.984 to 1.160
		Mini Sprint®	1.337	0.033	<0.001	1.249 to 1.426

3.2.3.1.2. KINETIC FRICTION

As detailed in Tables 18-20, the kinetic friction of various bracket-wire dimensions is similar to the static one. When combined with large dimension NiTi and stainless steel wires respectively, the kinetic friction also shows a highly significant difference ($P < 0.05$*) similar to static friction in almost all comparisons of brackets in Tables 19 and 20, except between Damon™ 3MX and Mini Sprint® brackets ($P > 0.05$). At the same time, the kinetic friction shows no significant difference when combined with 0.016”x0.022” NiTi wires ($P > 0.05$), except Mini Sprint® compared with Damon™ 3MX and In-Ovation® C ($P < 0.05$*). However, when combined with 0.016”x0.022” stainless steel wires, almost all brackets present highly significant differences ($P < 0.05$*), except for the comparison between In-Ovation® C and Mini Sprint® ($P > 0.05$) (Table 18). Thus, if smaller sizes are tested, stainless steel archwires present more significant differences than NiTi archwires.

Table 18: Results of two-way ANOVA combined with Tukey post hoc test, comparing kinetic frictional force of different bracket combined with 0.016”x0.022” wires. Mean Difference (I-J) - The absolute difference between the mean values in two different groups; Std. Error - Standard Deviation Error; CI - confidence intervals for the mean. *present *P* < 0.05.

Kinetic Frictional Force [N] (Tukey HSD)						
Material type	**(I) Brackets**	**(J) Brackets**	**Mean Difference (I-J)**	**Std. Error**	***P***	**95% CI**
NiTi	Damon™ 3MX	In-Ovation® C	0.006	0.024	0.995	-0.059 to 0.070
		Mini Sprint®	-0.069*	0.025	0.035	-0.134 to -0.004
		BioQuick®	-0.013	0.024	0.951	-0.077 to 0.051
	In-Ovation® C	Damon™ 3MX	-0.006	0.024	0.995	-0.070 to 0.059
		Mini Sprint®	-0.074*	0.024	0.015	-0.138 to -0.011
		BioQuick®	-0.019	0.024	0.860	-0.081 to 0.044
	Mini Sprint®	Damon™ 3MX	0.069*	0.025	0.035	0.004 to 0.134
		In-Ovation® C	0.074*	0.024	0.015	0.011 to 0.138
		BioQuick®	0.056	0.024	0.104	-0.008 to 0.119
	BioQuick®	Damon™ 3MX	0.013	0.024	0.951	-0.051 to 0.077
		In-Ovation® C	0.019	0.024	0.860	-0.044 to 0.081
		Mini Sprint®	-0.056	0.024	0.104	-0.119 to 0.008
Stainless steel	Damon™ 3MX	In-Ovation® C	-0.058*	0.017	0.005	-0.102 to -0.014
		Mini Sprint®	-0.068*	0.017	0.001	-0.112 to -0.023
		BioQuick®	-0.165*	0.017	<0.001	-0.210 to -0.121
	In-Ovation® C	Damon™ 3MX	0.058*	0.017	0.005	0.014 to 0.102
		Mini Sprint®	-0.009	0.017	0.994	-0.053 to 0.035
		BioQuick®	-0.107*	0.017	<0.001	-0.151 to -0.063
	Mini Sprint®	Damon™ 3MX	0.068*	0.017	0.001	0.023 to 0.112
		In-Ovation® C	0.009	0.017	0.994	-0.035 to 0.053
		BioQuick®	-0.098*	0.017	<0.001	-0.142 to -0.054
	BioQuick®	Damon™ 3MX	0.165*	0.017	<0.001	0.121 to 0.210
		In-Ovation® C	0.107*	0.017	<0.001	0.063 to 0.151
		Mini Sprint®	0.098*	0.017	<0.001	0.054 to 0.142

Table 19: Results of two-way ANOVA combined with Tukey post hoc test, comparing kinetic frictional force of different bracket combined with 0.018”x0.025” wires. Mean Difference (I-J) - The absolute difference between the mean values in two different groups; Std. Error - Standard Deviation Error; CI - confidence intervals for the mean. *present *P* < 0.05.

Kinetic Frictional Force [N] (Tukey HSD)						
Material type	**(I) Brackets**	**(J) Brackets**	**Mean Difference (I-J)**	**Std. Error**	***P***	**95% CI**
NiTi	Damon™ 3MX	In-Ovation® C	-0.184*	0.033	<0.001	-0.270 to -0.097
		Mini Sprint®	-0.017	0.032	0.948	-0.103 to 0.068
		BioQuick®	-0.589*	0.033	<0.001	-0.676 to -0.503
	In-Ovation® C	Damon™ 3MX	0.184*	0.033	<0.001	0.097 to 0.270
		Mini Sprint®	0.166*	0.032	<0.001	0.081 to 0.251
		BioQuick®	-0.406*	0.033	<0.001	-0.492 to -0.320
	Mini Sprint®	Damon™ 3MX	0.017	0.032	0.948	-0.068 to 0.103
		In-Ovation® C	-0.166*	0.032	<0.001	-0.251 to -0.081
		BioQuick®	-0.572*	0.032	<0.001	-0.657 to -0.487
	BioQuick®	Damon™ 3MX	0.589*	0.033	<0.001	0.503 to 0.676
		In-Ovation® C	0.406*	0.033	<0.001	0.320 to 0.492
		Mini Sprint®	0.572*	0.032	<0.001	0.487 to 0.657
Stainless steel	Damon™ 3MX	In-Ovation® C	-0.234*	0. 031	<0.001	-0.315 to -0.152
		Mini Sprint®	-0.110*	0. 031	0.004	-0.192 to -0.029
		BioQuick®	-0.914*	0. 031	<0.001	-0.995 to -0.833
	In-Ovation® C	Damon™ 3MX	0.234*	0. 031	<0.001	0.152 to 0.315
		Mini Sprint®	0.124*	0. 031	0.001	0.042 to 0.205
		BioQuick®	-0.680*	0. 031	<0.001	-0.762 to -0.599
	Mini Sprint®	Damon™ 3MX	0.110*	0. 031	0.004	0.029 to 0.192
		In-Ovation® C	-0.124*	0. 031	0.001	-0.205 to -0.042
		BioQuick®	-0.804	0. 031	<0.001	-0.885 to -0.722
	BioQuick®	Damon™ 3MX	0.914*	0. 031	<0.001	0.833 to 0.995
		In-Ovation® C	0.680*	0. 031	<0.001	0.599 to 0.762
		Mini Sprint®	0.804	0.031	<0.001	0.722 to 0.885

Table 20: Results of two-way ANOVA combined with Tukey *post hoc test*, comparing kinetic frictional force of different bracket combined with 0.019”x0.025” wires. Mean Difference (I-J) - The absolute difference between the mean values in two different groups; Std. Error - Standard Deviation Error; CI - confidence intervals for the mean. *present $P < 0.05$.

Kinetic Frictional Force [N] (Tukey HSD)						
Material type	**(I) Brackets**	**(J) Brackets**	**Mean Difference (I-J)**	**Std. Error**	***P***	**95% CI**
NiTi	Damon™ 3MX	In-Ovation® C	-0.216*	0.025	<0.001	-0.283 to -0.149
		Mini Sprint®	-0.052	0.026	0.188	-0.120 to 0.016
		BioQuick®	-0.520*	0.025	<0.001	-0.586 to -0.453
	In-Ovation® C	Damon™ 3MX	0.216*	0.025	<0.001	0.149 to 0.283
		Mini Sprint®	0.164*	0.026	<0.001	0.095 to 0.233
		BioQuick®	-0.303*	0.025	<0.001	-0.370 to -0.236
	Mini Sprint®	Damon™ 3MX	0.052*	0.026	0.188	-0.016 to 0.120
		In-Ovation® C	-0.164*	0.026	<0.001	-0.233 to -0.095
		BioQuick®	-0.467*	0.026	<0.001	-0.535 to -0.399
	BioQuick®	Damon™ 3MX	0.520*	0.025	<0.001	0.453 to 0.586
		In-Ovation® C	0.303*	0.025	<0.001	0.236 to 0.370
		Mini Sprint®	0.467*	0.026	<0.001	0.399 to 0.535
Stainless steel	Damon™ 3MX	In-Ovation® C	-0.323*	0. 038	<0.001	-0.424 to -0.222
		Mini Sprint®	0.009	0. 038	0.995	-0.092 to 0.110
		BioQuick®	-1.517*	0. 038	<0.001	-1.618 to -1.416
	In-Ovation® C	Damon™ 3MX	0.323*	0. 038	<0.001	0.222 to 0.424
		Mini Sprint®	0.332*	0. 038	<0.001	0.231 to 0.433
		BioQuick®	-1.194*	0. 038	<0.001	-1.295 to -1.093
	Mini Sprint®	Damon™ 3MX	-0.009	0. 038	0.995	-0.110 to 0.092
		In-Ovation® C	-0.332*	0. 038	<0.001	-0.433 to -0.231
		BioQuick®	-1.526*	0. 038	<0.001	-1.628 to -1.425
	BioQuick®	Damon™ 3MX	1.517*	0. 038	<0.001	1.416 to 1.618
		In-Ovation® C	1.194*	0. 038	<0.001	1.093 to 1.295
		Mini Sprint®	1.526*	0.038	<0.001	1.425 to 1.628

3.2.3.2. INFLUENCE OF DIFFERENT NORMAL FORCES

The two-way ANOVA combined with Tukey *post-hoc* test was used to evaluate the significant differences of frictional values among the comparison of different normal forces in various bracket-wire combinations (Tables 21 to 26).

3.2.3.2.1. STATIC FRICTION

As assessed from the Tables 21 to 23, when combined with NiTi archwires all bracket-wire combinations present highly significant differences under various normal forces ($P < 0.05$*), except for the comparison between 1.5N and 2N ($P > 0.05$). When coupled with stainless steel wires, all the differences between the tested samples are highly significant under the comparison of various normal forces ($P < 0.05$*).

Table 21: Results of two-way ANOVA combined with Tukey *post hoc test*, comparing static frictional force of different bracket combined with 0.016”x0.022” wires. Mean Difference (I-J) - The absolute difference between the mean values in two different groups; Std. Error - Standard Deviation Error; CI - confidence intervals for the mean. *present $P < 0.05$.

Static Frictional Force [N] (Tukey HSD)						
Material type	**(I) Normal force (N)**	**(J) Normal force (N)**	**Mean Difference (I-J)**	**Std. Error**	***P***	**95% CI**
NiTi	1.0	1.5	-0.099*	0.022	<0.001	-0.158 to -0.039
		2.0	-0.150*	0.022	<0.001	-0.207 to -0.092
		2.5	-0.332*	0.022	<0.001	-0.390 to -0.274
	1.5	1.0	0.099*	0.022	<0.001	0.039 to 0.158
		2.0	-0.051	0.022	0.116	-0.110 to 0.008
		2.5	-0.233*	0.023	<0.001	-0.293 to -0.173
	2.0	1.0	0.150*	0.022	<0.001	0.092 to 0.207
		1.5	0.051	0.022	0.116	-0.008 to 0.110
		2.5	-0.182*	0.022	<0.001	-0.241 to -0.124
	2.5	1.0	0.332*	0.022	<0.001	0.274 to 0.390
		1.5	0.233*	0.023	<0.001	0.173 to 0.293
		2.0	0.182*	0.022	<0.001	0.124 to 0.241
Stainless steel	1.0	1.5	-0.235*	0.020	<0.001	-0.287 to -0.184
		2.0	-0.440*	0.020	<0.001	-0.491 to -0.388
		2.5	-0.494*	0.020	<0.001	-0.546 to -0.442
	1.5	1.0	0.235*	0.020	<0.001	0.184 to 0.287
		2.0	-0.205*	0.020	<0.001	-0.256 to -0.153
		2.5	-0.259*	0.020	<0.001	-0.310 to -0.207
	2.0	1.0	0.440*	0.020	<0.001	0.388 to 0.491
		1.5	0.205*	0.020	<0.001	0.153 to 0.256
		2.5	-0.054*	0.020	0.036	-0.106 to -0.003
	2.5	1.0	0.494*	0.020	<0.001	0.442 to 0.546
		1.5	0.259*	0.020	<0.001	0.207 to 0.310
		2.0	0.054*	0.020	0.036	0.003 to 0.106

Table 22: Results of two-way ANOVA combined with Tukey *post hoc test*, comparing static frictional force of different bracket combined with 0.018”x0.025” wires. Mean Difference (I-J) - The absolute difference between the mean values in two different groups; Std. Error - Standard Deviation Error; CI - confidence intervals for the mean. *present $P < 0.05$.

Static Frictional Force [N] (Tukey HSD)						
Material type	**(I) Normal force (N)**	**(J) Normal force (N)**	**Mean Difference (I-J)**	**Std. Error**	***P***	**95% CI**
NiTi	1.0	1.5	-0.173*	0.031	<0.001	-0.253 to -0.092
		2.0	-0.187*	0.031	<0.001	-0.269 to -0.105
		2.5	-0.398*	0.031	<0.001	-0.479 to -0.316
	1.5	1.0	0.173*	0.031	<0.001	0.092 to 0.253
		2.0	-0.014	0.031	0.965	-0.095 to 0.066
		2.5	-0.225*	0.031	<0.001	-0.306 to -0.144
	2.0	1.0	0.187*	0.031	<0.001	0.105 to 0.269
		1.5	0.014	0.031	0.965	-0.066 to 0.095
		2.5	-0.211*	0.031	<0.001	-0.292 to -0.129
	2.5	1.0	0.398*	0.031	<0.001	0.316 to 0.479
		1.5	0.225*	0.031	<0.001	0.144 to 0.306
		2.0	0.211*	0.031	<0.001	0.129 to 0.292
Stainless steel	1.0	1.5	-0.160*	0.029	<0.001	-0.236 to -0.083
		2.0	-0.349*	0.029	<0.001	-0.425 to -0.272
		2.5	-0.637*	0.029	<0.001	-0.713 to -0.561
	1.5	1.0	0.160*	0.029	<0.001	0.083 to 0.236
		2.0	-0.189*	0.029	<0.001	-0.265 to -0.113
		2.5	-0.477*	0.029	<0.001	-0.554 to -0.401
	2.0	1.0	0.349*	0.029	<0.001	0.272 to 0.425
		1.5	0.189*	0.029	<0.001	0.113 to 0.265
		2.5	-0.288	0.029	<0.001	-0.365 to -0.212
	2.5	1.0	0.637*	0.029	<0.001	0.561 to 0.713
		1.5	0.477*	0.029	<0.001	0.401 to 0.554
		2.0	0.288	0.029	<0.001	0.212 to 0.365

Table 23: Results of two-way ANOVA combined with Tukey post hoc test, comparing static frictional force of different bracket combined with 0.019”x0.025” wires. Mean Difference (I-J) - The absolute difference between the mean values in two different groups; Std. Error - Standard Deviation Error; CI - confidence intervals for the mean. *present *P* < 0.05.

Static Frictional Force [N] (Tukey HSD)						
Material type	**(I) Normal force (N)**	**(J) Normal force (N)**	**Mean Difference (I-J)**	**Std. Error**	***P***	**95% CI**
NiTi	1.0	1.5	-0.084*	0.027	0.016	-0.157 to -0.012
		2.0	-0.095*	0.028	0.006	-0.168 to -0.021
		2.5	-0.301*	0.028	<0.001	-0.374 to -0.227
	1.5	1.0	0.084*	0.027	0.016	0.012 to 0.157
		2.0	-0.010	0.027	0.982	-0.083 to 0.062
		2.5	-0.216*	0.027	<0.001	-0.289 to -0.144
	2.0	1.0	0.095*	0.028	0.006	0.021 to 0.168
		1.5	0.010	0.027	0.982	-0.062 to 0.083
		2.5	-0.206*	0.028	<0.001	-0.279 to -0.133
	2.5	1.0	0.301*	0.028	<0.001	0.227 to 0.374
		1.5	0.216*	0.027	<0.001	0.144 to 0.289
		2.0	0.206*	0.028	<0.001	0.133 to 0.279
Stainless steel	1.0	1.5	-0.280*	0.033	<0.001	-0.368 to -0.192
		2.0	-0.714*	0.033	<0.001	-0.802 to -0.626
		2.5	-0.848*	0.033	<0.001	-0.936 to -0.760
	1.5	1.0	0.280*	0.033	<0.001	0.192 to 0.368
		2.0	-0.434*	0.033	<0.001	-0.522 to -0.346
		2.5	-0.568*	0.033	<0.001	-0.656 to -0.480
	2.0	1.0	0.714*	0.033	<0.001	0.626 to 0.802
		1.5	0.434*	0.033	<0.001	0.346 to 0.522
		2.5	-0.134*	0.033	0.001	-0.222 to -0.045
	2.5	1.0	0.848*	0.033	<0.001	0.760 to 0.936
		1.5	0.568*	0.033	<0.001	0.480 to 0.656
		2.0	0.134*	0.033	0.001	0.045 to 0.222

3.2.3.2.2. KINETIC FRICTION

As detailed in the following Tables 24 to 26, the kinetic frictional forces are compared pairwise among different normal forces. Similar to the static force values, when combined with large dimension NiTi archwires all bracket-wire combinations present highly significant differences with the testing normal forces ($P < 0.05$*), except for the comparison between 1.5N and 2N ($P > 0.05$). If combined with 0.016”x0.022” NiTi wires, all the tested samples show highly significant differences between the various normal forces ($P < 0.05$*). Additionally, all sizes of stainless steel archwires have highly significant differences in the comparisons of different normal forces ($P < 0.05$*).

Table 24: Results of two-way ANOVA combined with Tukey post hoc test, comparing kinetic frictional force of different bracket combined with 0.016”x0.022” wires. Mean Difference (I-J) - The absolute difference between the mean values in two different groups; Std. Error - Standard Deviation Error; CI - confidence intervals for the mean. *present $P < 0.05$.

Kinetic Frictional Force [N] (Tukey HSD)						
Material type	**(I) Normal force (N)**	**(J) Normal force (N)**	**Mean Difference (I-J)**	**Std. Error**	***P***	**95% CI**
NiTi	1.0	1.5	-0.106*	0.024	<0.001	-0.170 to -0.041
		2.0	-0.189*	0.024	<0.001	-0.251 to -0.126
		2.5	-0.375*	0.024	<0.001	-0.438 to -0.311
	1.5	1.0	0.106*	0.024	<0.001	0.041 to 0.170
		2.0	-0.083*	0.024	0.006	-0.147 to -0.019
		2.5	-0.269*	0.025	<0.001	-0.334 to -0.204
	2.0	1.0	0.189*	0.024	<0.001	0.126 to 0.251
		1.5	0.083*	0.240	0.006	0.019 to 0.147
		2.5	-0.186*	0.024	<0.001	-0.250 to -0.123
	2.5	1.0	0.375*	0.024	<0.001	0.311 to 0.438
		1.5	0.269*	0.025	<0.001	0.204 to 0.334
		2.0	0.186*	0.024	<0.001	0.123 to 0.250
Stainless steel	1.0	1.5	-0.249*	0.017	<0.001	-0.293 to -0.205
		2.0	-0.420*	0.017	<0.001	-0.464 to -0.376
		2.5	-0.479*	0.017	<0.001	-0.523 to -0.435
	1.5	1.0	0.249*	0.017	<0.001	0.205 to 0.293
		2.0	-0.171*	0.017	<0.001	-0.215 to -0.127
		2.5	-0.230*	0.017	<0.001	-0.274 to -0.186
	2.0	1.0	0.420*	0.017	<0.001	0.376 to 0.464
		1.5	0.171*	0.017	<0.001	0.127 to 0.215
		2.5	-0.059*	0.017	0.004	-0.103 to -0.015
	2.5	1.0	0.479*	0.017	<0.001	0.435 to 0.523
		1.5	0.230*	0.017	<0.001	0.186 to 0.274
		2.0	0.059*	0.017	0.004	0.015 to 0.103

Table 25: Results of two-way ANOVA combined with Tukey *post hoc test*, comparing kinetic frictional force of different bracket combined with 0.018”x0.025” wires. Mean Difference (I-J) - The absolute difference between the mean values in two different groups; Std. Error - Standard Deviation Error; CI - confidence intervals for the mean. *present P < 0.05.

Kinetic Frictional Force [N] (Tukey HSD)						
Material type	**(I) Normal force (N)**	**(J) Normal force (N)**	**Mean Difference (I-J)**	**Std. Error**	***P***	**95% CI**
NiTi	1.0	1.5	-0.172*	0.032	<0.001	-0.257 to -0.087
		2.0	-0.181*	0.033	<0.001	-0.267 to -0.095
		2.5	-0.392*	0.033	<0.001	-0.478 to -0.306
	1.5	1.0	0.172*	0.032	<0.001	0.087 to 0.257
		2.0	-0.009	0.032	0.993	-0.094 to 0.077
		2.5	-0.220*	0.032	<0.001	-0.305 to -0.134
	2.0	1.0	0.181*	0.033	<0.001	0.095 to 0.267
		1.5	0.009	0.032	0.993	-0.077 to 0.094
		2.5	-0.211*	0.033	<0.001	-0.297 to -0.125
	2.5	1.0	0.392*	0.033	<0.001	0.306 to 0.478
		1.5	0.220*	0.032	<0.001	0.134 to 0.305
		2.0	0.211*	0.033	<0.001	0.125 to 0.297
Stainless steel	1.0	1.5	-0.180*	0.031	<0.001	-0.261 to -0.098
		2.0	-0.348*	0.031	<0.001	-0.429 to -0.267
		2.5	-0.587*	0.031	<0.001	-0.668 to -0.506
	1.5	1.0	0.180*	0.031	<0.001	0.098 to 0.261
		2.0	-0.169*	0.031	<0.001	-0.250 to -0.087
		2.5	-0.408*	0.031	<0.001	-0.489 to -0.326
	2.0	1.0	0.348*	0.031	<0.001	0.267 to 0.429
		1.5	0.169*	0.031	<0.001	0.087 to 0.250
		2.5	-0.239*	0.031	<0.001	-0.320 to -0.158
	2.5	1.0	0.587*	0.031	<0.001	0.506 to 0.668
		1.5	0.408*	0.031	<0.001	0.326 to 0.489
		2.0	0.239*	0.031	<0.001	0.158 to 0.320

Table 26: Results of two-way ANOVA combined with Tukey post hoc test, comparing kinetic frictional force of different bracket combined with 0.019”x0.025” wires. Mean Difference (I-J) - The absolute difference between the mean values in two different groups; Std. Error - Standard Deviation Error; CI - confidence intervals for the mean. *present $P < 0.05$.

Kinetic Frictional Force [N] (Tukey HSD)						
Material type	**(I) Normal force (N)**	**(J) Normal force (N)**	**Mean Difference (I-J)**	**Std. Error**	***P***	**95% CI**
NiTi	1.0	1.5	-0.104*	0.025	0.001	-0.171 to -0.037
		2.0	-0.124*	0.026	<0.001	-0.192 to -0.056
		2.5	-0.308*	0.026	<0.001	-0.375 to -0.240
	1.5	1.0	0.104*	0.025	0.001	0.037 to 0.171
		2.0	-0.020	0.025	0.862	-0.087 to 0.047
		2.5	-0.203*	0.025	<0.001	-0.270 to -0.136
	2.0	1.0	0.124*	0.026	<0.001	0.056 to 0.192
		1.5	0.020	0.025	0.862	-0.047 to 0.087
		2.5	-0.184*	0.026	<0.001	-0.251 to -0.116
	2.5	1.0	0.308*	0.026	<0.001	0.240 to 0.375
		1.5	0.203*	0.025	<0.001	0.136 to 0.270
		2.0	0.184*	0.026	<0.001	0.116 to 0.251
Stainless steel	1.0	1.5	-0.293*	0.038	<0.001	-0.394 to -0.191
		2.0	-0.785*	0.038	<0.001	-0.886 to -0.683
		2.5	-0.902*	0.038	<0.001	-1.004 to -0.801
	1.5	1.0	0.293*	0.038	<0.001	0.191 to 0.394
		2.0	-0.492*	0.038	<0.001	-0.593 to -0.391
		2.5	-0.610*	0.038	<0.001	-0.711 to -0.509
	2.0	1.0	0.785*	0.038	<0.001	0.683 to 0.886
		1.5	0.492*	0.038	<0.001	0.391 to 0.593
		2.5	-0.118	0.038	0.016	-0.219 to -0.017
	2.5	1.0	0.902*	0.038	<0.001	0.801 to 1.004
		1.5	0.610*	0.038	<0.001	0.509 to 0.711
		2.0	0.118	0.038	0.016	0.017 to 0.219

4. DISCUSSION

It is an important objective of this research to understand the influence of variables such as orthodontic material, different environmental media and varying normal forces on the frictional force. Considering the fact, that a proper and moderate force will have an optimal response on the tooth movement in orthodontic treatment, the importance of the detailed knowledge about frictional forces becomes obvious. Therefore, the effect of the single factors like archwire dimension and material, as well as ligation method, environmental media and normal forces are examined in detail. To prevent additional inadvertent influences on the measurements, factors like the brand of the artificial saliva, human saliva donator, temperature and the sliding speed are kept constant.

4.1. MATERIAL STUDY

4.1.1. THE INFLUENCE OF FLUID TESTING MEDIA

In an oral environment, brackets and archwires are immersed in saliva. Thus, frictional research referenced in orthodontics needs to consider not only bracket-wire combinations but also the oral environment (Chang et al. 2013).

The present investigations are conducted under controlled temperature of 36±1℃in wet as well as dry conditions. Aforementioned research concluded that both, dry and wet conditions, exist in the oral cavity. The authors concluded that “dry” surfaces form if the contact between the archwire and the bracket are able to squeeze out the saliva layers. Thus, the “wet” surfaces are present if the appliance is immersed in saliva of the orthodontic patient (Kusy and Whitley 1997). Furthermore, when an orthodontic patient suffering from a systemic disease such as the Sjoegren syndrome, this patient has to use artificial saliva to relieve discomfort and lubricate the oral cavity. Therefore, artificial saliva may in some cases even be present during an orthodontic treatment. Apart from that, water, as the main component of saliva, makes the present in-vitro investigation comparable to other fluid media.

The effect of saliva on friction is discussed controversially: Saliva could either act as lubricant (Baker et al. 1987; Fidalgo et al. 2011; Tselepis et al. 1994), as an adhesive (Kusy and Schafer 1995; Pimentel et al. 2013; Pratten et al. 1990; Stannard et al. 1986) or some literature even indicates that it has a negligible effect on friction (Andreasen and Quevedo 1970). A previous research reported the effect of saliva substitute leads to a statistically significant reduction of frictional force of as much as 15% to 19% (Baker et al. 1987). Consistent with the opinion above, some studies claim that artificial saliva works as a lubricant and is able to decrease the frictional force (Fidalgo et al. 2011; Tselepis et al. 1994), while some other authors find that artificial saliva acts like an adhesive and increases the frictional force (Pimentel et al. 2013; Pratten et al. 1990; Stannard et al. 1986). Another study also confirms that saliva has the effect of increasing frictional coefficients (Kusy and Schafer 1995). However, a conclusion of another research mentions that saliva had no significant effect on lubricating the contact surface of bracket-wire combinations (Andreasen and Quevedo 1970).

In addition, some researchers compare wet and dry conditions and observe contradictory findings, too. Some of them claim that the friction obtained with artificial saliva is greater than that of human saliva, water, and dry conditions (Kusy and Whitley 2003). Others observe that friction shows no difference in the presence of artificial saliva and human saliva, while higher friction is found with the use of distilled water or under dry condition (Leal et al. 2014).

In the present study, both artificial saliva and human saliva are observed to be acting as adhesive in most of the cases having the effect of increasing static and kinetic frictional force in all bracket-wire combinations, which is supported by previous studies (Kusy and Schafer 1995; Pimentel et al. 2013; Pratten et al. 1990; Stannard et al. 1986). From the observation of the boxplot diagrams, the friction of In-Ovation® C bracket produced under whole human saliva is higher than that of artificial saliva, especially combined with archwires of bigger cross sections. However, the friction of metal brackets (BioQuick® and Mini Sprint®) under the influence of artificial saliva is higher than that of whole human saliva (Figure 14 to 19). This performance may be due to a varying interaction of human and artificial saliva with the different materials of the brackets. Artificial saliva appears to have a greater impact on the friction of metal brackets, while the influence of whole human saliva on the friction of ceramic brackets was higher, which may be attributed to variations in surface roughness of ceramics versus metal brackets. While sintered metals can be surface polished quite easily, this is not the case for sintered alumina ceramics which have about the same hardness as the polishing media, usually also made from the same material. Therefore, the discrepancy in performance of friction may result from the differences in surface composition and surface roughness in combination with artificial saliva and human saliva as well as the presence of mucins in the latter (Vissink et al. 1984; Winkeljann et al. 2018).

Considering the controversy above, aforementioned research gave the reason that the discrepancies in results may also be due to different loading forces that are applied to the bracket-wire combinations and may result in saliva either acting as lubricant or as adhesive. In some cases, saliva is forced out of the contact area of bracket and wire in the higher load situations and thus increase the friction, while at lower loads it acts as a lubricant (Pratten et al. 1990). In addition, the subtle difference of the components of artificial saliva and the technique used on the experimental models may also lead to different amounts of frictional force and coefficients (Kusy and Whitley 2003; Tselepis et al. 1994).

In conclusion, saliva composition, viscosity, surface roughness and surface energy of the involved frictional surfaces and even operation techniques, are extremely complex and may explain divergences in the frictional force and coefficients found in the present work as well as in previous studies.

4.1.2. THE INFLUENCE OF TESTING TEMPERATURE

Apart from the fluid states, the temperature condition is also a factor potentially affecting the frictional force. As preceding research assumed, the friction force could be increased as the oral temperature goes up, because an increasing temperature raises the plateau stress of the NiTi wire, which results in higher stiffness of the archwire. This higher stiffness may lead to a distinct binding and therefore higher frictional forces. (Chang et al. 2013). In fact, the short-term temperature changes affect not just the stiffness of the NiTi wire, but also the treatment efficiency due to shifting clinical forces and therefore prolong the duration of therapy (Meling and Odegaard 2001; Tonner and Waters 1994). While the increase of temperature leads to an increase of the plateau stress of the NiTi wire, the surface hardness as of the involved frictional partners has a direct effect on the frictional forces (Henao and Kusy 2004; Matarese et al. 2008). However, during the stress-induced martensitic transformation from the austenite phase to the martensite phase, which comes along with the well-known stress-strain plateau, the hardness of the NiTi alloy effectively reduces, as the martensite is much softer than the austenite. In other words, this means that the further the material is strained the softer it becomes and the higher is the friction exerted between NiTi wire and bracket surface, because harder materials are in general less prone to friction as compared to softer material of the same material class.

For the purpose of simulating normal oral temperature, all tests were operated under the condition of 36℃in the present study. Except the situation that people eating cold and hot food, the temperature of 35-36℃is maintained in a human's oral environment. This also makes the test more significant for guiding the clinical treatment and explains why the variation of temperature isn't chosen as a parameter in the present work for the tribological system.

4.1.3. THE INFLUENCE OF MATERIAL BRACKETS

Based on the results of the present research, In-Ovation® C (ceramic self-ligating) brackets showed higher frictional values than Mini Sprint® (conventional stainless steel) brackets especially combined with stainless steel wires of bigger cross sections in whole human saliva (Tables 3 and 4, Figures 14 to 19). This finding is also supported by previous studies, which stated that ceramic brackets exhibit higher frictional coefficients than stainless steel brackets when combined with 0.019”x0.025” archwires in the oral environment (Fidalgo et al. 2011; Nishio et al. 2004). As observed in figure 14 to19, comparing Mini Sprint®, In-Ovation® and BioQuick® with 0.016”x0.022” wires under dry state, the median and variances were similar and performed much lower as compared to other environments. However, when combined with larger wires, In-Ovation® C showed higher frictional force values than Mini Sprint® especially in whole human saliva, while, BioQuick® produced the highest friction under all four environments. In addition to the materials of brackets, it could be seen that the clip mechanism of self-ligating brackets is also an important factor affecting friction. As active self-ligating brackets, the clip stiffness of BioQuick® is stronger than that of In-Ovation® C, resulting in an active pressure force pressing on the wire. However, a previous investigation came to the conclusion that In-Ovation® C brackets produce lower frictional forces if compared to conventionally ligated metal brackets (Voudouris et al. 2010).

These inconsistent findings about the performance of different bracket materials regarding frictional forces may be explained by the material properties, surface roughness and the kind of clip mechanism of the respective self-ligating brackets. As the commonly accepted concept, the rougher surface of ceramic brackets compared to metal brackets is the main reason for higher friction values (Pratten et al. 1990; Reicheneder et al. 2007). Moreover, the sliding of the wires within the slots of brackets could damage the wire surfaces, due to the higher frictional coefficient and surface hardness of ceramic materials (Tanne et al. 1991). However, other study that supported In-Ovation® C brackets producing lower friction attributed the reason of decreasing friction of In-Ovation® C to the Chromium-Copper (Cr-Co) clip and the new ceramic-injection moulding technique (Voudouris et al. 2010). They considered that the Cr-Co clip of the In-Ovation® C bracket showed more freedom, and the curved shape of the clip also produced lower seating forces, which may attribute to lower friction. Additionally, depending on the evaluation of Voudouris et al., the lower friction of ceramic material also issued from the smoother and glass-like slot, which is a result of the new ceramic-injection moulding technique (Voudouris et al. 2010).

Conclusively, conventional and ceramic brackets showed very different patterns of forces explained by the specific bracket material composition. This situation should be considered during planning of clinical treatment when choosing the appropriate type of mechanics for each case (Francisconi et al. 2016).

4.1.4. THE INFLUENCE OF SLIDING VELOCITY AND THE SIGNIFICANCE OF STATIC AND KINETIC FRICTION

The debates about static and kinetic friction in orthodontics is controversial in many investigations (Downing et al. 1994; Khambay et al. 2004). From the clinical perspective, overcoming the static frictional force at the interface of bracket and wire is more important and is considered a necessary precondition for tooth movement. This is because static friction is the force that determines the magnitude of the force system acting on the tooth and its amount is usually greater than kinetic friction (Monteiro et al. 2014; Redlich et al. 2003).

As reported by previous studies the velocity of orthodontic tooth movement is as slow as 0.023 µm/min and the tooth sliding movement is not continuous at this extremely low velocity for all situation that occur in clinical treatment (Braun et al. 1999; Burrow 2009). In fact, from an engineering point of view this slow movement may well be considered being quasi-static or even static. Therefore, as the main point of view, kinetic friction is considered almost irrelevant for the discontinuous orthodontic tooth movement (Burrow 2009).

In any case, it is very hard to obtain this slow speed in a laboratory test. Taking previous studies into account, various velocity setups are applied in laboratory researches, such as 0.5mm/min, 2mm/min, 5mm/min, 10mm/min, 12.7mm/min and 18.8mm/min (Bednar et al. 1991; Drescher et al. 1989; Kapur et al. 1999; Kusy and Whitley 2000; Loftus et al. 1999; Park et al. 2004; Pizzoni et al. 1998; Prososki et al. 1991; Thorstenson and Kusy 2002; Tidy 1989; Zufall and Kusy 2000). Additionally, these experimental speeds are also consistent with the statement of Feynman et al. (2006). They mentioned that the frictional law is only valid for moderate drawing speeds, because of the generation of excessive heat if the speed gets too high (Feynman et al. 2006). Therefore, in the present study, the linear velocity is chosen at 10mm/min, which is the most commonly used value found in literature.

As a previous study shows, the variety of velocities also has an influence on the performance of the frictional coefficient (Kusy and Whitley 1989). According to the statements of the before mentioned authors, the coefficients for the stainless steel and NiTi archwire were unaffected by decreasing sliding velocity from 10 to 0.0005mm/min. However, for cobalt-chromium and beta-titanium archwires, the coefficients increased and decreased respectively under the same sliding conditions (Kusy and Whitley 1989). In conclusion, the literature about the effect of drawing speed on the frictional forces is inconsistent, but needs further research as the experimental setup needs to reflect as good as possible the quasi-static situation found in clinical appliances.

4.2. SIMULATION OF THE CLINCIAL SITUATION

4.2.1. THE INFLUENCE OF ARCHWIRE MATERIAL

The wire material is one of the most important factors affecting the frictional force. According to the results of some investigations, NiTi wires produced higher frictional force than stainless steel wires (Drescher et al. 1989; Ireland et al. 1991; Kapila et al. 1990; Nishio et al. 2004; Saunders and Kusy 1994; Thomas et al. 1998; Tidy 1989). Other researchers observed that there is no significant difference between stainless steel and NiTi wires (Cacciafesta et al. 2003; Downing et al. 1994; Loftus et al. 1999; Peterson et al. 1982). Therefore, considering the different results above, a study concluded that the force of ligation applied in various investigations and the archwires used being provided by different manufactures and combined with different bracket materials could be the main reasons of the discrepancies (Thorstenson and Kusy 2003).

However, the results of the present investigation show, that the significantly lower friction provided by NiTi wire is most likely a result of their lower stiffness and rigidness compared to stainless steel wires especially when using larger wire cross sections (Tables 9 to 14). This finding in the present research is consistent with previous studies (Frank and Nikolai 1980; Prososki et al. 1991; Tselepis et al. 1994). Several of them compared the frictional values produced by these two kinds of wires under certain contact angles between wire and bracket's slot, and had the results of higher frictional forces with stainless steel wires. They attributed the reason of this phenomenon to the binding angulation, which can make the normal force between wire and bracket increasing with higher stiffness (Frank and Nikolai 1980; Tselepis et al. 1994). Although the angulation and torque have been offset in the current investigation, the different material characteristics between stainless steel and NiTi wire may also result in such discrepancy. Another reason for the lower frictional forces of NiTi may result from the fact that NiTi is transforming from austenite to martensite under pressure, reducing the local stresses between the contact points of the surfaces in the frictional system (Pepper et al. 2009). Due to its exceptional frictional performance, NiTi is used industrially in extremely demanding applications.

Compared to NiTi, stainless steel is less flexible due to its higher elastic modulus and yields higher normal forces under complete surface contact between wire and bottom of the bracket slot. Therefore, it can be concluded that the frictional force values are most likely influenced by the material composition, texture, contact angles and Young's Moduli of orthodontic archwire materials.

4.2.2. THE INFLUENCE OF NORMAL FORCE EXERTED ON TOOTH

Forces perpendicular to a surface are defined as normal forces in physics. In orthodontics, the force of the ligation acts perpendicular to the brackets or tooth's surface, respectively and is therefore considered a normal force. To understand the frictional mechanics, the normal force is an important aspect to consider when evaluating frictional forces. In most studies, the frictional force decreases as the normal force produced by ligation is reduced, which is verified in the present study. Both, the static as well as the kinetic frictional force increase proportionally if the normal force is raised (Henao and Kusy 2004; Tecco et al. 2007; Thorstenson and Kusy 2001). Furthermore, different methods of ligation investigated have resulted in varying normal forces and their corresponding frictional forces. Therefore, only moderately tied stainless steel ligature forces generate relatively low frictional forces during sliding therapy. In the descriptive results of the simulation of the clinical situation tests, the static and kinetic frictional force increase in every subgroup as the normal force increases (Tables 9 to 14). As viewed from the Tables 21 to 26, all the testing samples showed highly significant difference under the comparisons of various normal forces when coupled with stainless steel wires ($P < 0.05$*). While when coupled with NiTi archwires all bracket-wire combinations presented highly significant difference under various normal forces ($P < 0.05$*), except for the comparison between 1.5N and 2N ($P > 0.05$). Thus, the stainless steel wires seemed more sensitive to variation of normal forces than NiTi wires, which may be due to the increased resistance to bending and the high elastic stiffness of stainless steel.

4.2.3. THE INFLUENCE OF ARCHWIRE SIZE

In this investigation, 0.016”x0.022”, 0.018”x0.025”, 0.019”x0.025” rectangular stainless steel and NiTi wires were used, since they are very common for use in orthodontic treatment. Additionally, the evaluation related to frictional values produced by multiple orthodontic bracket-wire combinations under varying testing conditions are not considered in other researches. The current research shows that nearly all bracket-wire couples exhibited a higher static and kinetic friction when using wires with larger cross sections. Namely 0.018”x0.025” and 0.019”x0.025 archwires produced higher friction than that of 0.016”x0.022” archwires (Tables 9 to 14).

The influence of the wire size on friction is various; most studies conclude that friction increases as wire size increases (Angolkar et al. 1990; Cacciafesta et al. 2003; Frank and Nikolai 1980). This seems to be an obvious conclusion, as the play between slot and wire is reduced which in general should cause an increase in frictional force. However, another study found that smaller wires result in an increased friction and attributes this to increasing distortion of the smaller wire within the bracket (Ireland et al. 1991). Also, other investigators don’t find a significant relationship between archwire size and friction, and attributed the disputatious results to the different experimental conditions (Tidy 1989).

Based on the results of a previous study, the wire dimension has a strong influence on the friction of self-ligating brackets. With conventional brackets, wire size shows a much lower influence, which is also consistent with the present study (Reicheneder et al. 2008). Mini Sprint® brackets had a lower influence on friction combined with different wire sizes, while for the BioQuick® and In-Ovation® C bracket (Tables 9 to 14), the variation of friction force is more obvious depending on the wire dimension. Hence, it is important to take the dimension of an orthodontic archwire into account when selecting a bracket system in order to generate as low as possible frictional forces.

4.2.4. INFLUENCE OF THE LIGATION MECHANISM

When conventional twin brackets, in this study Mini Sprint® brackets, are tied with stainless steel ligature wires one has to keep in mind that the applied ligature twist cycles have an effect on the frictional force (Thorstenson and Kusy 2003). When the stainless steel ligature wires are slack, conventionally ligated twin bracket-wire combinations could act similar to a passive self-ligating bracket-wire interrelationship. In addition, loosening the ligature by a quarter turn as described above will result in a decreased perpendicular force applied to the slot of conventionally ligated brackets. This decrease is contributing to a reduction of the frictional force. Therefore, the force produced by a stainless steel ligature is subjective and most likely inconstant, as it is strongly dependent on the orthodontist's standard routine during manual ligation (Thorstenson and Kusy 2003).

When coupled with the larger cross section NiTi and stainless steel archwires, the active self-ligating brackets (In-Ovation® C and BioQuick®) show higher static and kinetic frictional values than the passive self-ligating brackets (Damon™ 3MX) and the conventional brackets (Mini Sprint®). Additionally, the metal active self-ligating brackets (BioQuick®) produced higher friction than that of ceramic ones (In-Ovation® C) (Figure 22 to 25, 28 to 31).

In fact, the higher friction force of active self-ligating brackets may be caused by the excessive stiffness of the spring clip which produces an (additional) force acting on the wire (Thomas et al. 1998). The BioQuick® and In-Ovation® C brackets own a spring clip, which could exert additional pressure onto the wire when it is closed, while the Damon® 3MX bracket is different from that of the active self-ligating bracket. The cover of Damon® 3MX bracket slides vertically, creating a passive tube in the bracket slot, which thus does not produce active pressure on the archwire. Furthermore, the Chromium-Copper (Cr-Co) clip and the new ceramic-injected moulding technique of In-Ovation® C bracket may be the reason that it produces lower friction than BioQuick® brackets (Voudouris et al. 2010)

In the analysis of different bracket-wire combinations, the friction of passive self-ligating and conventional brackets showed no significant difference in combination with archwires of larger dimensions, ($P > 0.05$), except with 0.018"x0.025" stainless steel wires ($P < 0.05$*) (Tables 16 to 20). This could be due to the slide of passive self-ligating bracket acting similar to the ligature wire of the conventional brackets. Even when combined with large size wires it will not exert an additional pressure like the clip of active self-ligating bracket.

Additionally, the properties of 0.018"x0.025" stainless steel wires may result in a certain deformation in the process of moving along the slot of bracket, which is leading to the difference between the passive self-ligating and the conventional brackets.

Whereas, when coupled with 0.016"x0.022" NiTi archwires, the differences of friction between various brackets were almost not visible (Figure 20, 21, 26, 27). It can be also observed from Tables 15 and 18 that the friction of passive and metal active self-ligating brackets showed no significant difference when compared with almost all testing brackets respectively ($P > 0.05$). Moreover, when combined with 0.016”x0.022” stainless steel wires, the friction of active self-ligating brackets shows no significant difference with passive self-ligating and conventional brackets ($P > 0.05$). Thus, the differences of friction produced by smaller archwires are not obvious. This could be due to the clearance existing between the smaller wire and the slot of the brackets, which may reduce the contact surfaces in the bracket-wire frictional system.

Therefore, a small clearance between wire and slot of the bracket has a great influence on the frictional force level (Drescher et al. 1989; Omana et al. 1992). If the archwire fills the slot of a bracket and contacts the spring clip or slide without any clearance, active self-ligating brackets can exert an extra perpendicular force on the slot of the bracket produced by the spring clip. In contrast, the cover of passive self-ligating brackets has no active force applied to the wire and finally transmitted to the slot. Not only the “cover” mechanism, but also the size or the geometric position of the archwire in the bracket slot can affect the frictional value. Based on the reasons above, the frictional force of passive self-ligating brackets is lower than that of active self-ligating brackets even if there is no clearance between wire and slot. (Budd et al. 2008; Henao and Kusy 2004; Huang et al. 2012; Kim et al. 2008; Krishnan et al. 2009; Matarese et al. 2008; Stefanos et al. 2010). On the other hand, these findings are in discordance with other authors, who found no significant difference or even observed greater friction in the self-ligating brackets (Henao and Kusy 2004, 2005; Pliska et al. 2011; Pliska et al. 2014; Redlich et al. 2003; Tecco et al. 2007). These discrepancies can be attributed to differences such as, but not limited to varying experimental setups, as well as varying prescriptions, geometries and dimensions of self-ligating brackets. In addition, the materials, which caps or clips are consisting of, and the brackets’ manufacturers have to be taken into consideration. Further studies with reduced number of variables in order to isolate the measured effects from each other are recommended.

4.2.5. THE SIGNIFICANCE OF THE PRESENT RESEARCH FOR THE CLINICAL TREATMENT

As stated in previous studies, the data observed from in vitro research can contribute to a better understanding of the clinical effects related to frictional forces between various bracket-wire combinations. However, it cannot reproduce or correspond to the complete situation that occurs in clinical orthodontic treatment (Stefanos et al. 2010; Thomas et al. 1998). Frictional force is caused in vivo by a variety of factors during clinical tooth movement, which can also influence and produce unpredictable consequences in the frictional force values. Moreover, in consideration of the various experimental methodologies used in different studies, it is also difficult to directly compare amongst respective studies (Nishio et al. 2004). Therefore, the comparative frictional values obtained from research works should be used as mean values for comparing the tendencies of different appliances and guiding the selection of bracket-wire combinations for sliding mechanics (Stefanos et al. 2010).

4.3. OUTLOOK

Based on the results observed in the present study, further and new investigations are needed to focus on following factors:

1. The studies referenced on orthodontic material characteristics in dry and wet states with other commercial brands of artificial saliva. Through the researches, the investigators should compare which component in saliva has the highest influence on friction and which one provides a better performance in decreasing friction at compatible cost.

2. Another aspect is to simulate some clinical conditions during orthodontic malocclusion treatment, such as, angulation, binding or tilt phenomena. Such studies would thereby help relate the current results to a more clinical level.

3. It is also important to focus on the influence of the various length and inter-bracket span of a wire used during sliding mechanism.

4.4. OTHER FACTORS AFFECTING THE FRICTIONAL FORCE

Beside the factors discussed above, there are also some other factors which may occur and have an effect on friction during treatment process:

1. The ligation forces attenuation and indeterminacy: elastomeric ligatures lose elasticity after applying during the orthodontic treatment and the frictional force can be altered. b) The subjective ligating of stainless steel ligature wires: twist cycles of ligature wires and the corresponding forces are varying dependent on the treating orthodontists.

2. Besides saliva and the character of orthodontic materials, other intraoral variables such as, plaque, food residue, acquired pellicle, chewing, tooth number, status of the periodontal tissue, and occlusion should also be considered during the research of frictional force.

Further in vivo investigations are suggested to evaluate how these oral components act on friction in treatment process.

5. CONCLUSION

Based on the condition of the present in-vitro study, it can be concluded that:

1. The frictional force was higher in the wet state than in the dry state. Saliva acts as adhesive and increases the frictional values. The frictional values performed lowest in the dry condition.
2. Passive self-ligating bracket showed significantly lower frictional force compared to the metal active self-ligating brackets bracket for almost all size of testing wires. While, the difference showed not obviously when used with smaller NiTi archwires. Thus, the former bracket might be preferred to be used for the purpose of decreasing friction during tooth movement but difficult to fully express the torque or details especially for the smaller archwires. Likewise, active self-ligating bracket might be more favourably to express torque but should be judiciously used for the sliding mechanics with large dimension archwires.
3. The wire dimension influenced the friction values of both self-ligating and conventional brackets. The larger the wire size, the higher the generated friction. However, the effect on the active self-ligating brackets was greater than that on the passive self-ligating and conventional ones. Thus, the friction of active self-ligating brackets depend mainly on the different wire dimensions.
4. The static and kinetic frictional force increased as the normal force increases, especially combined with stainless steel archwires, which performed more sensitive to normal forces. Thus, different methods of ligation and orthodontic materials have resulted in varying normal forces and their corresponding frictional forces. Only moderately normal forces generated relatively appropriate friction forces during sliding therapy.
5. The friction produced by NiTi wire was lower than that of stainless steel wires, the significantly lower friction provided by NiTi wire is most likely a result of their lower stiffness and rigidness compared to stainless steel wires especially when using large wire dimensions.

REFERENCES

Alfonso MV, Espinar E, Llamas JM, Ruperez E, Manero JM, Barrera JM, Solano E, Gil FJ (2013). Friction coefficients and wear rates of different orthodontic archwires in artificial saliva. J Mater Sci Mater Med; 24(5):1327-32.

Andreasen GF, Quevedo FR (1970). Evaluation of friction forces in the 0.022 x 0.028 edgewise bracket in vitro. J Biomech; 3(2):151-60.

Angolkar PV, Kapila S, Duncanson MG, Jr., Nanda RS (1990). Evaluation of friction between ceramic brackets and orthodontic wires of four alloys. Am J Orthod Dentofacial Orthop; 98(6):499-506.

Arash V, Rabiee M, Rakhshan V, Khorasani S, Sobouti F (2015). In vitro evaluation of frictional forces of two ceramic orthodontic brackets versus a stainless steel bracket in combination with two types of archwires. J Orthod Sci; 4(2):42-6.

Baker KL, Nieberg LG, Weimer AD, Hanna M (1987). Frictional changes in force values caused by saliva substitution. Am J Orthod Dentofacial Orthop; 91(4):316-20.

Bednar JR, Gruendeman GW, Sandrik JL (1991). A comparative study of frictional forces between orthodontic brackets and arch wires. Am J Orthod Dentofacial Orthop; 100(6):513-22.

Begg PR, Kesling PC (1977). The differential force method of orthodontic treatment. Am J Orthod; 71(1):1-39.

Brauchli LM, Senn C, Wichelhaus A (2011). Active and passive self-ligation-a myth? Angle Orthod; 81(2):312-8.

Brauchli LM, Steineck M, Wichelhaus A (2012). Active and passive self-ligation: a myth? Part 1: torque control. Angle Orthod; 82(4):663-9.

Braun S, Bluestein M, Moore BK, Benson G (1999). Friction in perspective. Am J Orthod Dentofacial Orthop; 115(6):619-27.

Budd S, Daskalogiannakis J, Tompson BD (2008). A study of the frictional characteristics of four commercially available self-ligating bracket systems. Eur J Orthod; 30(6):645-53.

Burrow SJ (2009). Friction and resistance to sliding in orthodontics: a critical review. Am J Orthod Dentofacial Orthop; 135(4):442-7.

Cacciafesta V, Sfondrini MF, Ricciardi A, Scribante A, Klersy C, Auricchio F (2003). Evaluation of friction of stainless steel and esthetic self-ligating brackets in various bracket-archwire combinations. Am J Orthod Dentofacial Orthop; 124(4):395-402.

Chang CJ, Lee TM, Liu JK (2013). Effect of bracket bevel design and oral environmental factors on frictional resistance. Angle Orthod; 83(6):956-65.

Christersson CE, Lindh L, Arnebrant T (2000). Film-forming properties and viscosities of saliva substitutes and human whole saliva. Eur J Oral Sci; 108(5):418-25.

Downing A, McCabe J, Gordon P (1994). A study of frictional forces between orthodontic brackets and archwires. Br J Orthod; 21(4):349-57.

Drescher D, Bourauel C, Schumacher HA (1989). Frictional forces between bracket and arch wire. Am J Orthod Dentofacial Orthop; 96(5):397-404.

Ehsani S, Mandich MA, El-Bialy TH, Flores-Mir C (2009). Frictional resistance in self-ligating orthodontic brackets and conventionally ligated brackets. A systematic review. Angle Orthod; 79(3):592-601.

Fann WE, Shannon IL (1978). A treatment for dry mouth in psychiatric patients. Am J Psychiatry; 135(2):251-2.

Feynman RP, Leighton RB, Sands ML (2006). Characteristics of force. In: ed. D (Ed.). The Feynman Lectures on Physics.] San Francisco [u.a.]: Pearson, Addison Wesley.

Fidalgo TK, Pithon MM, Maciel JV, Bolognese AM (2011). Friction between different wire bracket combinations in artificial saliva--an in vitro evaluation. J Appl Oral Sci; 19(1):57-62.

Francisconi MF, Janson G, Henriques JF, Freitas KM (2016). Evaluation of the force generated by gradual deflection of orthodontic wires in conventional metallic, esthetic, and self-ligating brackets. J Appl Oral Sci; 24(5):496-502.

Frank CA, Nikolai RJ (1980). A comparative study of frictional resistances between orthodontic bracket and arch wire. Am J Orthod; 78(6):593-609.

Hain M, Dhopatkar A, Rock P (2006). A comparison of different ligation methods on friction. Am J Orthod Dentofacial Orthop; 130(5):666-70.

Harradine N (2017). Self-ligating Bracket Biomechanics. In: Graber LW, Vanarsdall RL, Jr., Vig KWL, Huang GJ (Eds.). Orthodontics : Current Principles and Techniques.] 6th Ed. St. Louis, Missouri: Elsevier; pp. 729-760.

Harradine NW (2003). Self-ligating brackets: where are we now? J Orthod; 30(3):262-73.

Henao SP, Kusy RP (2004). Evaluation of the frictional resistance of conventional and self-ligating bracket designs using standardized archwires and dental typodonts. Angle Orthod; 74(2):202-11.

Henao SP, Kusy RP (2005). Frictional evaluations of dental typodont models using four self-ligating designs and a conventional design. Angle Orthod; 75(1):75-85.

Huang TH, Luk HS, Hsu YC, Kao CT (2012). An in vitro comparison of the frictional forces between archwires and self-ligating brackets of passive and active types. Eur J Orthod; 34(5):625-32.

Huffman DJ, Way DC (1983). A clinical evaluation of tooth movement along arch wires of two different sizes. Am J Orthod; 83(6):453-9.

Humphrey SP, Williamson RT (2001). A review of saliva: normal composition, flow, and function. J Prosthet Dent; 85(2):162-9.

Ireland AJ, Sherriff M, McDonald F (1991). Effect of bracket and wire composition on frictional forces. Eur J Orthod; 13(4):322-8.

Kapila S, Angolkar PV, Duncanson MG, Jr., Nanda RS (1990). Evaluation of friction between edgewise stainless steel brackets and orthodontic wires of four alloys. Am J Orthod Dentofacial Orthop; 98(2):117-26.

Kapur R, Sinha PK, Nanda RS (1999). Comparison of frictional resistance in titanium and stainless steel brackets. Am J Orthod Dentofacial Orthop; 116(3):271-4.

Khambay B, Millett D, McHugh S (2004). Evaluation of methods of archwire ligation on frictional resistance. Eur J Orthod; 26(3):327-32.

Kim TK, Kim KD, Baek SH (2008). Comparison of frictional forces during the initial leveling stage in various combinations of self-ligating brackets and archwires with a custom-designed typodont system. Am J Orthod Dentofacial Orthop; 133(2):187 e15-24.

Krishnan M, Kalathil S, Abraham KM (2009). Comparative evaluation of frictional forces in active and passive self-ligating brackets with various archwire alloys. Am J Orthod Dentofacial Orthop; 136(5):675-82.

Kusy PR, Schafer DL (1995). Effect of salivary viscosity on frictional coefficients of orthodontic archwire/bracket couples. J. Mater. Sci.: Mater. Med; 6:390-395.

Kusy RP, Whitley JQ (1989). Effects of sliding velocity on the coefficients of friction in a model orthodontic system. Dent Mater; 5(4):235-40.

Kusy RP, Whitley JQ (1997). Friction between different wire-bracket configurations and materials. Semin Orthod; 3(3):166-77.

Kusy RP, Whitley JQ (1999). Influence of archwire and bracket dimensions on sliding mechanics: derivations and determinations of the critical contact angles for binding. Eur J Orthod; 21(2):199-208.

Kusy RP, Whitley JQ (2000). Resistance to sliding of orthodontic appliances in the dry and wet states: influence of archwire alloy, interbracket distance, and bracket engagement. J Biomed Mater Res; 52(4):797-811.

Kusy RP, Whitley JQ (2003). Influence of fluid media on the frictional coefficients in orthodontic sliding. Semin Orthod; 9(4):281-289.

Leal RC, Amaral FL, Franca FM, Basting RT, Turssi CP (2014). Role of lubricants on friction between self-ligating brackets and archwires. Angle Orthod; 84(6):1049-53.

Loftus BP, Artun J, Nicholls JI, Alonzo TA, Stoner JA (1999). Evaluation of friction during sliding tooth movement in various bracket-arch wire combinations. Am J Orthod Dentofacial Orthop; 116(3):336-45.

Lombardo L, Ficara P, Maltoni I, Moser L, Guarneri MP, Siciliani G (2012). Comparison of the anterior limit of the dentition in patients treated with self-ligating straight-wire, conventional straight-wire and standard edgewise appliances. ISRN Dent; 2012:748758.

Matarese G, Nucera R, Militi A, Mazza M, Portelli M, Festa F, Cordasco G (2008). Evaluation of frictional forces during dental alignment: an experimental model with 3 nonleveled brackets. Am J Orthod Dentofacial Orthop; 133(5):708-15.

Mezeg U, Primozic J (2017). Influence of long-term in vivo exposure, debris accumulation and archwire material on friction force among different types of brackets and archwires couples. Eur J Orthod; 39(6):673-679.

Monteiro MR, Silva LE, Elias CN, Vilella Ode V (2014). Frictional resistance of self-ligating versus conventional brackets in different bracket-archwire-angle combinations. J Appl Oral Sci; 22(3):228-34.

Nishio C, da Motta AF, Elias CN, Mucha JN (2004). In vitro evaluation of frictional forces between archwires and ceramic brackets. Am J Orthod Dentofacial Orthop; 125(1):56-64.

Omana HM, Moore RN, Bagby MD (1992). Frictional properties of metal and ceramic brackets. J Clin Orthod; 26(7):425-32.

Park JH, Lee YK, Lim BS, Kim CW (2004). Frictional forces between lingual brackets and archwires measured by a friction tester. Angle Orthod; 74(6):816-24.

Pepper S, DellaCorte C, Noebe R, Hull D, Glennon G (2009). Nitinol 60 as a material for spacecraft triboelements. European Space Agency, (Special Publication) ESA SP; 670.

Peterson L, Spencer R, Andreasen G (1982). A comparison of friction resistance for Nitinol and stainless steel wire in edgewise brackets. Quintessence Int Dent Dig; 13(5):563-71.

Pimentel RF, de Oliveira RS, Chaves M, Elias CN, Gravina MA (2013). Evaluation of the friction force generated by monocristalyne and policristalyne ceramic brackets in sliding mechanics. Dental Press J Orthod; 18(1):121-7.

Pizzoni L, Ravnholt G, Melsen B (1998). Frictional forces related to self-ligating brackets. Eur J Orthod; 20(3):283-91.

Pliska BT, Beyer JP, Larson BE (2011). A comparison of resistance to sliding of self-ligating brackets under an increasing applied moment. Angle Orthod; 81(5):794-9.

Pliska BT, Fuchs RW, Beyer JP, Larson BE (2014). Effect of applied moment on resistance to sliding among esthetic self-ligating brackets. Angle Orthod; 84(1):134-9.

Pratten DH, Popli K, Germane N, Gunsolley JC (1990). Frictional resistance of ceramic and stainless steel orthodontic brackets. Am J Orthod Dentofacial Orthop; 98(5):398-403.

Prososki RR, Bagby MD, Erickson LC (1991). Static frictional force and surface roughness of nickel-titanium arch wires. Am J Orthod Dentofacial Orthop; 100(4):341-8.

Redlich M, Mayer Y, Harari D, Lewinstein I (2003). In vitro study of frictional forces during sliding mechanics of "reduced-friction" brackets. Am J Orthod Dentofacial Orthop; 124(1):69-73.

Reicheneder CA, Baumert U, Gedrange T, Proff P, Faltermeier A, Muessig D (2007). Frictional properties of aesthetic brackets. Eur J Orthod; 29(4):359-65.

Reicheneder CA, Gedrange T, Berrisch S, Proff P, Baumert U, Faltermeier A, Muessig D (2008). Conventionally ligated versus self-ligating metal brackets--a comparative study. Eur J Orthod; 30(6):654-60.

Saunders CR, Kusy RP (1994). Surface topography and frictional characteristics of ceramic brackets. Am J Orthod Dentofacial Orthop; 106(1):76-87.

Stannard JG, Gau JM, Hanna MA (1986). Comparative friction of orthodontic wires under dry and wet conditions. Am J Orthod; 89(6):485-91.

Stefanos S, Secchi AG, Coby G, Tanna N, Mante FK (2010). Friction between various self-ligating brackets and archwire couples during sliding mechanics. Am J Orthod Dentofacial Orthop; 138(4):463-467.

Stolzenberg J (1935). The Russell attachment and its improved advantages. Int J Orthod Dent Child; 21:837-40.

Szczupakowski A, Reimann S, Dirk C, Keilig L, Weber A, Jager A, Bourauel C (2016). Friction behavior of self-ligating and conventional brackets with different ligature systems. J Orofac Orthop; 77(4):287-95.

Tanne K, Matsubara S, Shibaguchi T, Sakuda M (1991). Wire friction from ceramic brackets during simulated canine retraction. Angle Orthod; 61(4):285-90; discussion 291-2.

Tecco S, Di Iorio D, Cordasco G, Verrocchi I, Festa F (2007). An in vitro investigation of the influence of self-ligating brackets, low friction ligatures, and archwire on frictional resistance. Eur J Orthod; 29(4):390-7.

Tecco S, Tete S, Festa F (2009). Friction between archwires of different sizes, cross-section and alloy and brackets ligated with low-friction or conventional ligatures. Angle Orthod; 79(1):111-6.

Thomas S, Sherriff M, Birnie D (1998). A comparative in vitro study of the frictional characteristics of two types of self-ligating brackets and two types of pre-adjusted edgewise brackets tied with elastomeric ligatures. Eur J Orthod; 20(5):589-96.

Thorstenson GA, Kusy RP (2001). Resistance to sliding of self-ligating brackets versus conventional stainless steel twin brackets with second-order angulation in the dry and wet (saliva) states. Am J Orthod Dentofacial Orthop; 120(4):361-70.

Thorstenson GA, Kusy RP (2002). Comparison of resistance to sliding between different self-ligating brackets with second-order angulation in the dry and saliva states. Am J Orthod Dentofacial Orthop; 121(5):472-82.

Thorstenson GA, Kusy RP (2003). Effects of ligation type and method on the resistance to sliding of novel orthodontic brackets with second-order angulation in the dry and wet states. Angle Orthod; 73(4):418-30.

Tidy DC (1989). Frictional forces in fixed appliances. Am J Orthod Dentofacial Orthop; 96(3):249-54.

Tselepis M, Brockhurst P, West VC (1994). The dynamic frictional resistance between orthodontic brackets and arch wires. Am J Orthod Dentofacial Orthop; 106(2):131-8.

Vissink A, Waterman HA, s-Gravenmade EJ, Panders AK, Vermey A (1984). Rheological properties of saliva substitutes containing mucin, carboxymethylcellulose or polyethylenoxide. J Oral Pathol (Journal of Oral Pathology & Medicine); 13(1):22-8.

Voudouris JC, Schismenos C, Lackovic K, Kuftinec MM (2010). Self-ligation esthetic brackets with low frictional resistance. Angle Orthod; 80(1):188-94.

Wichelhaus A, Eichenberg T, Günter A (2017). Farbatlanten der Zahnmedizin Kieferorthopädie - Therapie Band 1. 1. Stuttgart: Thieme.

William RP, Henry WF, David MS (2007). In: ed. (Ed.). Contemporary orthodontics.] St. Louis, Mo.: Mosby Elsevier; pp. 2-23.

Williams CL, Khalaf K (2013). Frictional resistance of three types of ceramic brackets. J Oral Maxillofac Res; 4(4):e3.

Winkeljann B, Bussmann AB, Bauer MG, Lieleg O (2018). Oscillatory Tribology Performed With a Commercial Shear Rheometer. Biotribology; 14:11-18.

Zufall SW, Kusy RP (2000). Sliding mechanics of coated composite wires and the development of an engineering model for binding. Angle Orthod; 70(1):34-47.

ACKNOWLEDGEMENTS

I would like to express my sincerest thanks and appreciation to my supervisor Prof. Dr. Andrea Wichelhaus for providing me the opportunity to do my study and finish doctoral study in Munich University. Her fully support and creative guidance encouraged me a lot and inspired me in science.

I am particularly grateful to Mr. Thomas Stocker, the head of the biomechanics laboratory, for his thoughtful and thorough guidance, especially experiment design, experimental technical guidance, result analysis, thesis correction and so on. And also thank to the predecessor Dr. Sebastian Stapfner, who was able to help me and played a major role at the initial stage of my experimental research. I am totally impressed with their knowledge, experience and professional spirit.

I would also like to thank to Dr. Uwe Baumert and Mr. Matthias Mertmann for their expert advices and guidance during my research and dissertation writing.

And also thanks to my colleagues and my friends, Mr. Philip Gruber, Ms. Teodora Popova, Ms. Jianwei Shi, Ms. Mila Janjic, Ms. Changyun Sun, Ms. Wanchen Ning, Ms. Jieqi Jin, Ms. Marina Khitynova and all my other friends. During my life and study, they give me a great deal of support and courage, let me march ahead.

Lastly, I deeply appreciate my parents and my family. Because of their silent support and the deepest love, I can beat it all.

Eidesstattliche Versicherung

Li, Haoyan

Name, Vorname

Ich erkläre hiermit an Eides statt,

dass ich die vorliegende Dissertation mit dem Titel

In-vitro investigation of frictional behavior and influence of normal forces on orthodontic materials in wet and dry states

selbständig verfasst, mich außer der angegebenen keiner weiteren Hilfsmittel bedient und alle Erkenntnisse, die aus dem Schrifttum ganz oder annähernd übernommen sind, als solche kenntlich gemacht und nach ihrer Herkunft unter Bezeichnung der Fundstelle einzeln nachgewiesen habe.

Ich erkläre des Weiteren, dass die hier vorgelegte Dissertation nicht in gleicher oder in ähnlicher Form bei einer anderen Stelle zur Erlangung eines akademischen Grades eingereicht wurde.

München, 14.08.2021

Ort, Datum

Haoyan Li

Unterschrift Doktorandin bzw. Doktorand